OPTIMIZATION THE PROCESS PARAMETERS AND THERMAL PROCESSING FOR TOMATO JUICE WITH NANOFLUID IN DOUBLE PIPE HEAT EXCHANGER AND EVALUATING ITS QUALITATIVE PROPERTIES

Thesis

Submitted to the

G. B. Pant University of Agriculture & Technology
Pantnagar- 263145, Uttarakhand, India

By

ESHANT CHAUDHARY
Id. No. 57968

IN PARTIAL FULFILLMENT OF THE REQUIREMENTS FOR THE DEGREE OF

Master of Technology
In
Agricultural Engineering
(Process and Food Engineering)

September, 2023

ACKNOWLEDGMENT

First and foremost, thanks to the God almighty, for providing me the opportunity to accomplish my education after all the joy and sorrow during the process and for providing me the strength and courage to complete this research successfully. No matter how long my journey has been, but what eventually matters in the end is the outcome of my hard work, sacrifice, failure, doubts, suffering, criticism and persistence.

With all sense of elation and honesty, I would like to express my sincere gratitude towards my advisor Er. Sachin Kumar, Assistant Professor of Post Harvest Process and Food Engineering, College of Technology, G. B. Pant University of Agriculture and Technology, for providing his invaluable guidance, appreciation and constant help throughout the thesis work. It helped me to move forward in the successful culmination of the project work. I express deep sense of obligation to him as he made it possible for me to submit the thesis in the present form.

I also express my gratitude and indebtedness to the esteemed members of my advisory committee, Dr. P.K. Omre, Professor of Department of Post Harvest Process and Food Engineering, Dr. S.S Bhandari, Assistant Professor of Department of Mechanical Engineering for their valuable support, suggestions, encouragement and help at several stages of present investigation.

I would like to thank all the respected teachers of the Department of Post Harvest Process and Food Engineering Dr. N.C. Shahi, professor and Head, Department of Post Harvest Process and Food Engineering and Dr. Manish Dak, for their cooperation and warm affection during journey. I also express my deepest sense of reverence and indebtedness to Dr. Alakananda Ashok, Dean, College of Technology and Dr. K.P. Raverkar, Dean, College of Post Graduate Studies, G. B. Pant University

of Agriculture and Technology, for extending all the necessary help and providing facilities for the study.

I express my sincere thanks to the office staff especially Er. Rahul Kumar Sir, Sangeeta Ma'am for the necessary help regarding the procedures required in completion of the thesis. Among the laboratory staff, I am thankful to Narendra Sir, Aslam Sir and Geeta Ma'am who were extremely supportive during the various laboratory tasks that helped throughout my study.

My heartfelt thanks to all the members of PHP&FE family who have been with me in Pantnagar during my study program. I avail this opportunity to express my profound thanks to all my seniors, Bilal Sir, Sheeba Ma'am, Shikhangi Ma'am, Shreejaya Ma'am, Anu Ma'am, Priya Ma'am Aarshi Ma'am and Hariom Sir for their help & constant inspiration during my research work. I am grateful to all of my friends, batch mates and express my deepest thanks to Aviral, Bareera, Avantika and others for their extreme support, encouragement and cooperation during hard times. I would like to thank my junior's as well for their unreserved support during the journey.

I am truly blessed to have such a wonderful family, I would like to thank my Grandfather Mr. Udaiveer Singh Rawat, my Father Mr. Dinesh Chaudhary, my Mother Mrs. Suneeta Chaudhary, my Sister Miss Bhawna Singh, who have made me capable of pursuing this degree course. Their selfless love, affection, endless support, and encouragement gave me courage to fight against all odds.

At last, I would like to thank my Late Grandmother who is a symbol of strength, courage and wisdom Late Smt. Omwati Chaudhary' for all the love and affection.

Pantnagar **(Eshant Chaudhary)**
September, 2023 **Author**

CERTIFICATE - I

This is to certify that the thesis entitled **"OPTIMIZATION THE PROCESS PARAMETERS AND THERMAL PROCESSING FOR TOMATO JUICE WITH NANOFLUID IN DOUBLE PIPE HEAT EXCHANGER AND EVALUATING ITS QUALITATIVE PROPERTIES"** submitted in partial fulfillment of the requirements for the degree of **Master of Technology in Agricultural Engineering** with major in **Process and Food Engineering** of the College of Post Graduate Studies, G.B. Pant University of Agriculture and Technology. Pantnagar, is a record of bonafide research carried out by **Mr. Eshant Chaudhary**, Id. No. **57968**, under my supervision and no part of the thesis has been submitted for any other degree or diploma.

The assistance and help received during the investigation and source of literature have been duly acknowledged.

Pantnagar
September, 2023

(Sachin Kumar)
Chairman
Advisory Committee

CERTIFICATE - II

We, the undersigned, members of Advisory Committee of **Eshant Chaudhary**, Id. No**. 57968**, a candidate for the degree of **Master of Technology in Agricultural Engineering** with major in **Process and Food Engineering**, agree that the thesis entitled **" OPTIMIZATION THE PROCESS PARAMETERS AND THERMAL PROCESSING FOR TOMATO JUICE WITH NANOFLUID IN DOUBLE PIPE HEAT EXCHANGER AND EVALUATING ITS QUALITATIVE PROPERTIES"** may be submitted in partial fulfillment of the requirements for the degree.

(Sachin Kumar)
Chairman
(Advisory Committee)

(P.K Omre)
Member

(S.S Bhandari)
Member

CONTENTS

LIST OF TABLES

LIST OF FIGURES

LIST OF PLATES

LIST OF ABBREVIATION

ANOVA	Analysis of Variance
e.g.	for example
et al.	and others
etc.	et cetera
F	F-Value
Fig.	Figure
g	Gram (s)
h	hour (s)
i.e,	that is
mg	Milligram
min	Minute
MS	Mean square
No.	Number
N	Newton
RSM	Response surface methodology
R^2	Coefficient of Determinations
s	second
SS	Sum of square
LOF	lack of fit
w/v	weight by volume
/	per
%	percent
U	unit
℃	Degree of Centigrade
µgm	microgram(s)
ΔE	Color difference

Introduction

Chapter 1 INTRODUCTION

Tomatoes (*Lycopersicon esculentum*) hold significant global agricultural importance, being cultivated in nearly every nation. The red hue of tomatoes is attributed to the carotenoid compound called lycopene, constituting roughly 83% of the total pigments found in tomatoes. The lycopene levels found in tomatoes vary significantly among different types of tomatoes, their stages of ripeness, and the conditions in which they are grown. Scientific research has indicated that regular consumption of tomatoes or their processed products is linked to a reduced likelihood of developing certain types of cancer. Tomatoes hold a distinct nutritional value and are sometimes referred to as the "poor man's orange." A fully ripe tomato contains a high moisture content of 94%, approximately 3-5% natural sugars, 15-30 mg of ascorbic acid breper 100 g, 7.5-10.5 mg of titratable acidity per 100 g, and 25-30 mg of lycopene per 100 g. **(Shi *et al*., 1999)**. In 2018, the global output of both fresh and processed tomatoes reached approximately 182 million tons. China stands as the leading tomato producer, trailed by the United States and India. Among U.S. states, Florida holds the second position in fresh tomato production. Over the past ten years, tomato consumption has consistently risen, as demonstrated by a notable 54% growth in worldwide tomato production between 2000 and 2014 **(Koltun *et al*., 2021).** This pigment, which imparts the red color, features a polyene structure characterized by a lengthy carbon chain with alternating single and double bonds. These double bonds selectively absorb and radiate light within the red spectrum, resulting in the characteristic red appearance of tomatoes **(Hobson and Davies, 1976).** Of paramount significance in tomatoes, lycopene is an antioxidant that possesses the ability to counteract free radicals within the body. These unstable molecules can inflict cellular damage, contributing to a range of health issues such as cancer, premature aging, heart ailments, osteoporosis, diabetes, and various other conditions. The level of antioxidant effectiveness in tomatoes can significantly differ based on factors such as genetic strains, the stage of ripeness, and the environment they are cultivated in. Tomatoes are recognized for their potent antioxidant properties within the body **(Stahl and Sies, 1996).**

Vitamin C, scientifically referred to as ascorbic acid, is a vital nutrient crucial for various essential functions within the body. Among its key roles is supporting the

immune system by aiding in the generation of white blood cells, which are critical for addressing infections and ailments. Moreover, vitamin C plays a pivotal part in the healing of wounds, as it's necessary for producing collagen, a protein pivotal for mending damaged tissues. Additionally, this nutrient contributes to maintaining strong bones by aiding in the absorption of iron, a mineral indispensable for robust bone health.

Vitamin C also has a significant role in enhancing eye health, participating in the production of collagen, a vital component of the eye's transparent outer layer, known as the cornea. Lastly, vitamin C plays a role in stress alleviation by facilitating the synthesis of cortisol, a hormone that helps the body manage and adapt to stress. All in all, ascorbic acid, commonly known as vitamin C, is an essential nutrient with a wide array of functions critical for the overall well-being and proper functioning of the human body **(Akanbi and Oludemi, 2004).**

A cup of tomato juice offers approximately 20% of the recommended daily intake (RDI) of vitamin C. The actual vitamin C content in tomato juice can differ due to factors like the tomato variety used, processing methods, and storage duration. The act of cooking or heating tomato juice has the potential to diminish a portion of its vitamin C content**.**

Heat treatment holds significant importance within the food sector, particularly in improving the excellence and lifespan of diverse food items like milk, fruit juices, concentrates, and mixtures. Among the prevalent uses of thermal processing is pasteurization, a method that entails swiftly heating food products to a minimum of 78°C. Although this approach proficiently eradicates detrimental microorganisms and enzymes, it could potentially impact the sensory qualities of fruit juices. The application of heat to tomatoes through thermal processing can bring about alterations in their nutritional characteristics. This procedure involves factors like temperature, shifts in pH levels, and interaction with oxygen, all of which can influence the makeup of tomatoes **(Akanbi and Oludemi, 2004)**. Notably, a significant change occurs in the reduction of vitamin C content, as this nutrient is sensitive to heat and can degrade during thermal processing. Moreover, the processing may lead to a decrease in the antioxidant capabilities of tomatoes, which are attributed to substances like lycopene. Additionally, water-soluble nutrients including vitamins

B and C, alongside specific minerals, have the potential to leach out during the thermal processing phase. Conversely, thermal processing has the capacity to improve the accessibility of certain nutrients by disintegrating cell structures. Nevertheless, this method can also modify the flavor and consistency of tomatoes. The application of heat to food items brings about notable transformations in their structural makeup, giving rise to a range of physical, chemical, and biochemical shifts. If thermal processing is not swiftly executed or done at suitable lower temperatures, the structures of fruit juices experience detrimental changes that lead to the division of the juice into separate phases. This partition is predominantly linked to the degradation of pectin, a constituent accountable for upholding the stability and texture of fruit juices **(Hsu *et al*., 2008).**

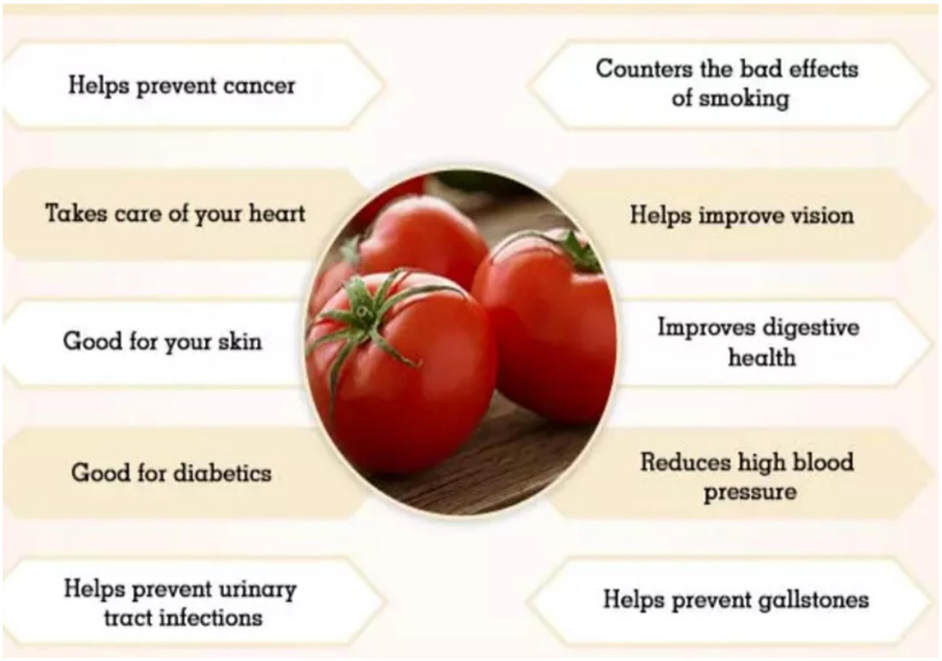

Fig 1.1: Health benefits of tomato juice

Currently, a prominent subject of conversation in heat processing pertains to the requirement for a substantial increase in heat flow, alongside the goal of reducing the reliance on heat transfer machinery within the realm of the food industry. In response to the challenges mentioned earlier, multiple strategies have been investigated to amplify the effectiveness of heat transfer. Nevertheless, these approaches have been restricted by the suboptimal functioning of conventional heat transfer liquids like water. In contrast, when assessed against bulk fluids, especially at

the micro level, fluids at the nanoscale exhibit a noteworthy enhancement in thermal conductivity. Even at minimal nanoparticle concentrations (1-5% weight/volume), the thermal conductivity can be elevated by over 20% **(Xuan and Li, 2003)**. In recent times, nanofluids have attracted considerable interest owing to their exceptional stability, resulting in a multitude of research investigations being undertaken in this domain. The remarkable stability demonstrated by nanofluids has generated substantial curiosity among researchers. The food processing industry is exploring nanofluids as a prospective and innovative substitute for conventional heat transfer fluids. Applications like refrigeration, freezing, thawing, pasteurization, sterilization, drying, and evaporation in the realm of food-related procedures are instances where nanofluids have the potential to be utilized for transferring heat from a heating or cooling source to the food item **(Salari and Jafari, 2020).**

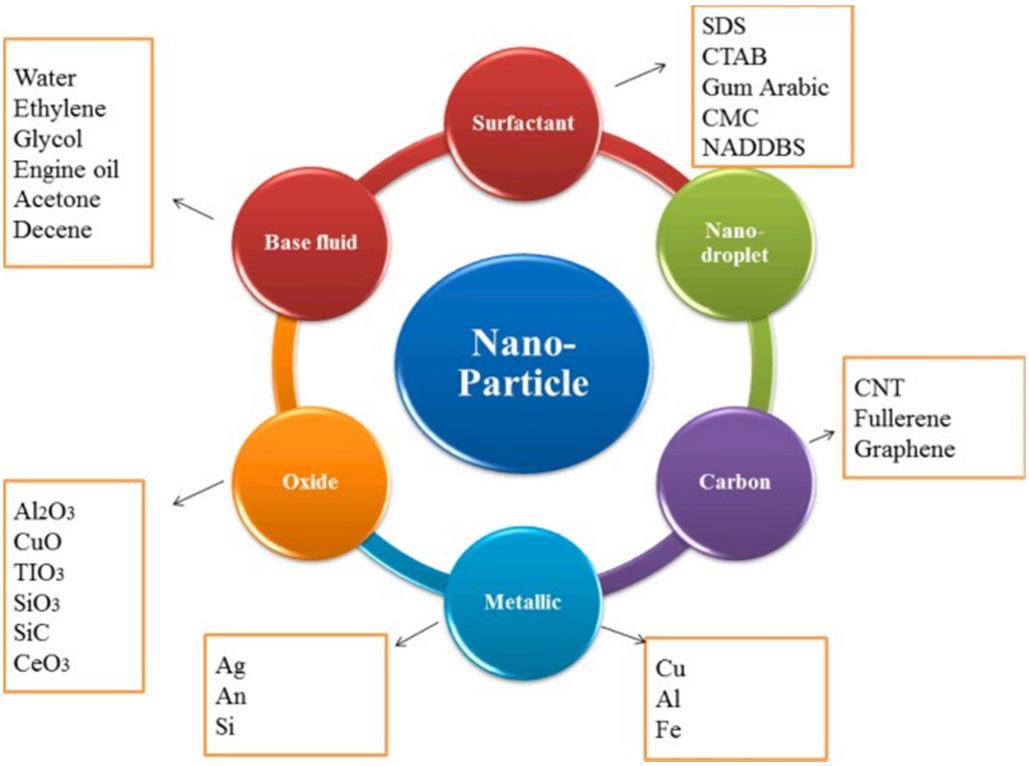

Fig 1.2: NPs, Surfactants & NFs types

Nanofluids have gained significant attention recently due to their remarkable stability, leading to numerous research studies being conducted in this area. The high stability exhibited by nanofluids has captured considerable interest from researchers. Innovative research was conducted on utilizing nanofluids for thermal processing of

fruit juices, marking the initial application of this technology in the food industry. The findings highlighted the potential of alumina nanoparticles as highly effective agents for heat transfer in various industries beyond the conventional ones, including food processing. This study, conducted by **(Jafari *et al*., 2017)**, shed light on the promising role of alumina nanoparticles (Al_2O_3) in enhancing heat transfer processes for a wide range of applications. **(Jabbari *et al*., 2018),** also demonstrates the potential of nanofluid-based thermal processing in enhancing the quality of tomato juice. The utilization of appropriate nanoparticle concentrations, lower temperatures, and shorter processing times can result in improved lycopene retention, reduced color degradation, and favorable pH/acidity levels. These findings contribute to the development of optimized thermal processing techniques for tomato juice, promoting its nutritional value and consumer acceptance in the market. Further research is warranted to explore additional quality parameters and optimize the nanofluid- based processing conditions for other food products.

1.1 Research Objectives

Currently, the crucial requirement is to optimize the thermal treatment process to ensure the better amount of retention of quality of tomato juice. To summarize, the primary objective of our research is to enhance the heat transfer rate in a double pipe heat exchanger. Furthermore, integrating nanoparticles into this system has the capability to enhance the heat transfer process even further. This approach involving nanoparticles is expected to result in a substantial improvement in heat transfer efficiency. Additionally, it aims to effectively preserve crucial quality parameters throughout the heat transfer process.

The main objectives of this research are:

1. To examine the heat transfer enhancement by (Al_2O_3/water) nanofluid in the thermalprocessing of tomato juice using a double pipe heat exchanger.
2. To study the influence of nanofluid on the retention of quality parameters during the thermal treatment of tomato juice.
3. To optimize the process parameters of treated tomato juice.

Review of Literature

Chapter 2 REVIEW OF LITERATURE

The tomato holds a special place among preferred vegetables due to its abundance of essential nutrients, functional components, and antioxidants. These include lycopene, b-carotene, acarotene, cryptoxanthin, lutein, along with various flavonoids, phenolic acids, and ascorbic acid **(Odriozola-Serrano *et al*., 2009).** Tomato juice stands as a popular and nourishing drink, undergoing heat-based processing for safety assurance, prolonged shelf life, and sustained quality standards. However, conventional thermal methods can lead to undesired outcomes like diminished color, alterations in nutritional composition, and changes in sensory characteristics. The incorporation of (Al_2O_3/water) nanofluid in tomato juice processing presents a promising avenue, with potential advantages in elevating heat transfer efficiency while preserving quality. This review paper aims to critically assess existing research concerning the impact of employing (Al_2O_3/water) nanofluid during thermal processing on various quality aspects of tomato juice. By scrutinizing the scientific literature, this review seeks to offer insights into progress made, challenges faced, and potential gains associated with this innovative approach. Grasping the effects of (Al_2O_3/water) nanofluid thermal processing on elements such as color, nutritional content, texture, sensory attributes, and overall quality of tomato juice will aid in refining thermal processing techniques, leading to superior product quality and enhanced consumer satisfaction. The review will succinctly summarize key discoveries, methodologies utilized, and constraints encountered in prior investigations. It will also identify research gaps and propose areas warranting further exploration. Through amalgamating existing information, this review strives to provide a comprehensive comprehension of how (Al_2O_3/water) nanofluid thermal processing influences the quality of tomato juice. Ultimately, this knowledge will push forward food processing technologies, enabling the production of high-caliber tomato juice that aligns with consumer expectations and remains competitive in the market.

2.1 Tomato (Lycopersicon esculentum)

In the present day, tomatoes are available not only in their fresh form but are also transformed into various processed products like paste, soup, juice, sauce,

powder, concentrate, or preserved whole. Among the vegetables consumed globally, tomatoes hold a significant position, following potatoes, and they might just be the most favored produce from home gardens. In terms of worldwide cultivation, the year 2011 witnessed a production of nearly 160 million tons of tomatoes, positioning them as the seventh most crucial crop type. This ranking place tomatoes after maize, rice, wheat, potatoes, soybeans and cassava **(Bergougnoux, 2014).**

Over the past two decades, both the production of tomatoes and the land area devoted to their cultivation have experienced a twofold increase. Interestingly, while Europe and the Americas held the leading positions in tomato production two decades ago, the current landscape is marked by Asia's dominance in the tomato market. China now holds the top position, succeeded in descending order by India, the USA, Turkey, Egypt, Iran, Italy, Brazil, Spain, and Uzbekistan **(Bergougnoux, 2014).** Among all vegetables, the tomato (Lycopersicon esculentum) holds a notable position as a significant component of the Mediterranean Diet, both in terms of quality and quantity.

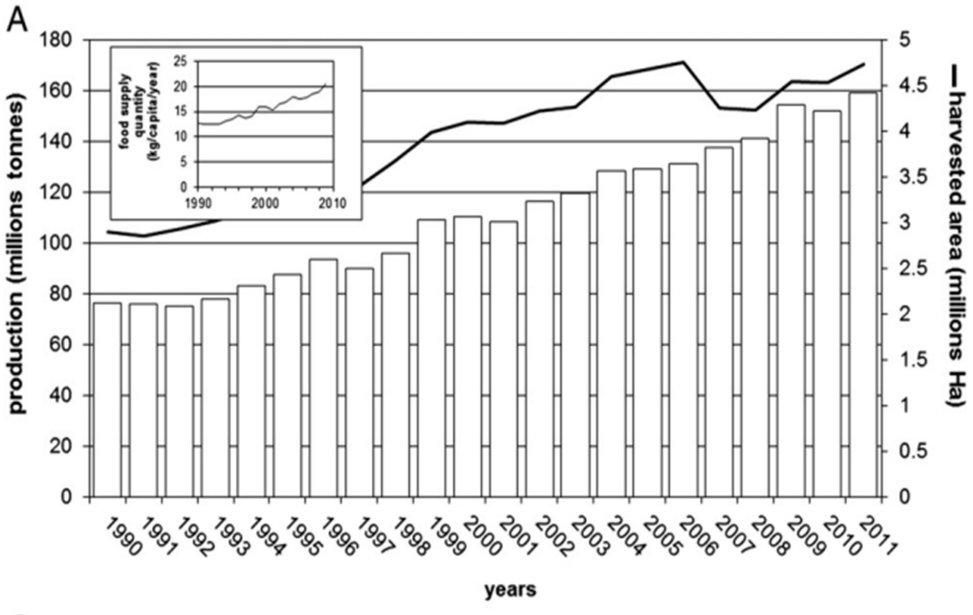

Fig 2.1: Tomato production increasing per year (Bergougnoux, 2014)

Tomatoes exhibit variations in terms of their weight, color, firmness, juice and pulp content, thickness of the outer layer, and the quantity of seeds they contain. In a study by **Shi and Maguer, (2000)**, it was noted that across eight distinct tomato

varieties, the average firmness levels ranged between 4.0 and 8.4 pounds per square inch. Among all, Pusa Ruby exhibited the least fruit firmness, while Lerica showcased the highest.

Viuda-Martos *et al.* (2014) indicated that the history of tomatoes, a vegetable widely accessible in the present day, stretches back extensively. Tomatoes have been grown for consumption in Europe since the 16th century; however, they were once regarded as toxic in certain regions and were solely employed for ornamental purposes.

According to **Kaur *et al.* (2008)**, tomatoes are primarily enjoyed as a fresh staple food owing to their favorable nutritional attributes; however, they are also becoming increasingly prevalent in numerous well-liked tomato-based items. Over 80% of cultivated tomatoes are utilized in processed forms, including juice, soup, concentrate, dry-concentrate, sauce, salsa, puree, dried tomatoes, ketchup, and paste.

As outlined by **Sogi *et al.* (2003)**, the by-products generated during the processing of tomatoes (as depicted in Figure 1) primarily originate from tomato pomace. Wet pomace is composed of approximately 33% seeds, 27% skin, and 40% pulp. On the other hand, dried pomace consists of around 44% seeds and 56% pulp and skin.

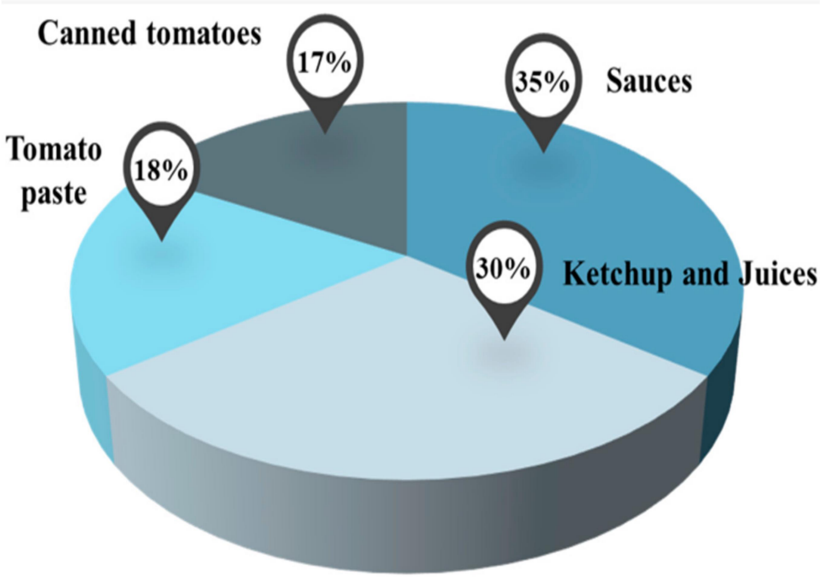

Fig 2.2: Graphic representation of estimated percentages of tomato processed by-products **(Raiola *et al.*, 2015)**

As mentioned by **Khachik *et al*. (1995)**, within the realm of plant carotenoids, a mere 14 are present in human tissues. Among these, tomato and its derivatives provide a substantial contribution to nine of the mentioned carotenoids. They hold a prominent status as the primary source of lycopene, neurosporene, gamma-carotene, phytoene, and phytofluene.

Table 2.1: Chemical composition of tomato

Components	Percentage Range
Water	94-95%
Carbohydrates	3-4%
Sugars (glucose, fructose)	2-3%
Dietary Fiber	1-2%
Protein	0.9-1.2%
Fat	0.2-0.4%
Ash (Minerals)	0.6-0.9%
Vitamin C	20-30 mg/100g
Vitamin A	500-700 IU/100g
Lycopene	1-8 mg/100g
Beta-Carotene	0.1-0.6 mg/100g

Source: Nutritional Composition and Bioactive Compounds in Tomatoes and Their Impact on Human Health and Disease **(Ali *et al*., 2020).**

2.1.1 Nutritional properties of tomato

Tomato fruits boast a wealth of vitamins, minerals, and organic acids, making them widely recognized as a nourishing food. Additionally, these fruits harbor a diverse range of flavor-enhancing compounds that enhance the taste and aroma of vegetable-based dishes created using them. In terms of primary fruit vegetables, tomatoes are ranked 16th in terms of vitamin A content and 13th as a source of vitamin C **(Ali *et al*., 2020).**

2.1.1.1 Lycopene

Lycopene, the red-hued pigment, is notably prevalent in red fruits and vegetables, with tomatoes and their derivatives being prominent sources. Despite its

long-standing use as a natural food coloring agent, lycopene has gained significant interest as a pharmaceutical element more recently **(Cadoni *et al*., 1999).** Lycopene stands as a frequently employed pigment, enjoying strong endorsement from the food sector both as a food additive and due to its health-related advantages. The demand for lycopene remains on an upward trajectory, driven by its roles as a red coloring agent and antioxidant. The global consumption of lycopene surged to 15,000 metric tons in 2004, a threefold increase from the 5,000 metric tons recorded in 1995 **(Kong *et al*., 2010).**

Anguelova and Warthesen (2000) has indicated that levels of lycopene in the bloodstream and the intake of lycopene through tomatoes were linked in an opposite manner to the likelihood of specific cancer forms. These cancers include prostate cancer, digestive-tract cancers, and lung cancer.

According to **Lovrić *et al.* (1970)**, within processed tomato products, the transformation of lycopene is brought about by isomerization and autoxidation. This leads to a reduction in the overall lycopene content, a decline in the share of all-trans lycopene, loss of color, and the emergence of undesirable grassy flavors.

Table 2.2 Lycopene content in different tomatoes and tomato products

S. No.	Product	Lycopene content (mg/100 g)	Reference
1	Tomato peel	55.70	Calvo *et al.,* (2008)
2	Tomato pomace	28.64	Huang *et al.*, (2008)
3	Tomato puree	27.39	Yildiz and Baysal, (2007)
4	Tomato paste	26.18	Østerlie and Lerfall (2005)
5	Ketchup	1.9-26.2	Lugasi *et al.*, (2003)
6	Tomato powder	1.44	Liu *et al.*, (2010)
7	Tomato juice	7.13	Liu *et al.*, (2010)

The degradation of lycopene due to processing and storage of tomato products has been examined in a review by **(Bergougnoux, 2014).**

Bramley (2000) states that humans are incapable of synthesizing lycopene internally, it becomes imperative to acquire sufficient amounts from dietary sources in order to harness its health-enhancing properties. Tomatoes and tomato-derived products stand as primary providers of lycopene in Western diets. Notably, juice, ketchup, soups, and sauces are key contributors to lycopene intake. During the production of these products, a common operational step involves thermal processing. While it's recognized that thermal treatment can lead to nutrient loss, past research has indicated that lycopene tends to exhibit stability in tomato-based food systems when subjected to mild thermal processes.

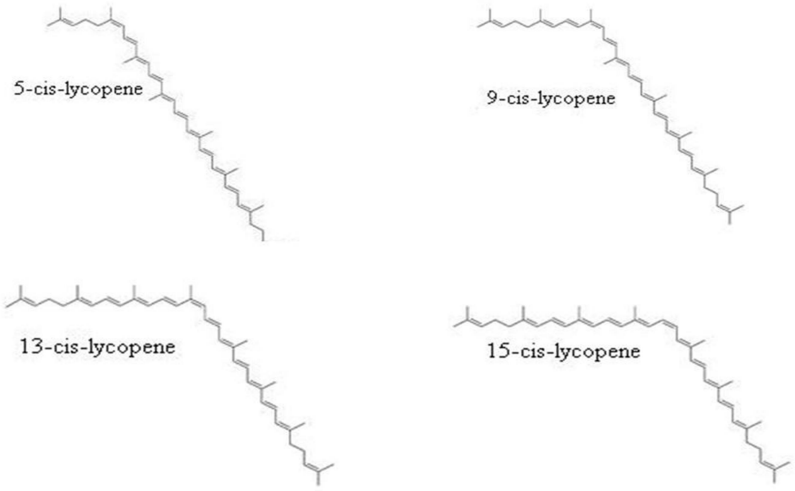

Fig 2.3: The most common isomeric lycopene forms **(Calvo *et al*., 2008)**

Goula and Adamopoulos (2005) extensively researched the preservation of lycopene in various tomato products through thermal processing, which involves procedures like cooking, concentration, and dehydration for the production of items such as tomato paste, tomato ketchup, and tomato juice. Their studies consistently revealed that lycopene degradation occurs during these processes, with the degree of loss contingent upon factors such as the specific treatment method employed, the temperature applied, the duration of processing, and the influence of oxygen and light**.**

Colle *et al*. (2010) stated that the impact of heat processing on the nutritional quality of food items is well-established. This quality is determined not only by the

nutrient content but also by the extent to which nutrients are made accessible to the body (bioaccessibility). This study was conducted to comprehensively understand how thermal processing affects the degradation, isomerization, and bioaccessibility of lycopene isomers in tomato pulp, without incorporating any additional substances. The bioaccessibility, representing the proportion of the nutrient that can be released from the food's structure, was gauged through a lab-based method. The findings revealed the robust resistance of lycopene to thermal stress. Although exposure to 140°C led to isomerization, the contribution of cis-lycopene to the overall lycopene content remained minimal. The study also affirmed that thermal processing could heighten the in vitro bio accessibility of lycopene in tomato pulp, with notable enhancements seen at temperatures of 130°C and 140°C. However, it's important to note that such intense processing conditions might negatively affect other aspects of quality and nutrient content. Therefore, while thermal processing holds potential to enhance the nutritional value of tomato pulp (without external additions), its feasibility seems somewhat limited.

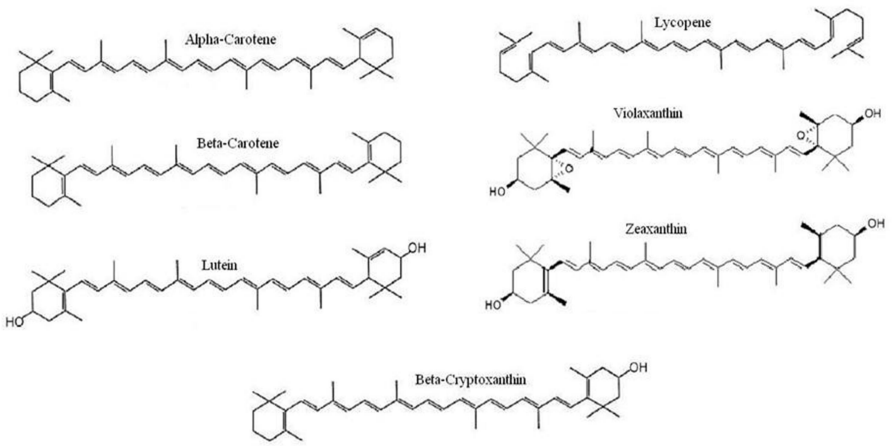

Fig 2.4: Structure of some major dietary carotenoids (Calvo *et al.*, 2008)

2.1.1.2 Ascorbic acid (Vitamin C)

Vitamin C, also known as ascorbic acid, is crucial for human health due to its diverse roles in various bodily functions. It serves as an essential antioxidant, which means it helps protect cells from damage caused by harmful molecules called free radicals. This antioxidant property contributes to the overall well-being and longevity of cells, tissues, and organs. Furthermore, vitamin C plays a pivotal role in collagen synthesis, a protein necessary for the formation and maintenance of skin, blood

vessels, bones, and other connective tissues. It aids wound healing, promotes healthy skin, and ensures the integrity of blood vessels **(Jacob, 1990)**.

In addition, vitamin C is involved in the production of neurotransmitters, such as serotonin and norepinephrine, which regulate mood and stress responses. It has been associated with reducing the risk of chronic diseases like cardiovascular diseases and certain cancers.

Hobson and Davies (1976) stated that the concentration of ascorbic acid is influenced by the type of variety and the technological processes used. On average, the ascorbic acid levels in diverse varieties vary between 150 and 230 mg/kg.

Charles, N. (2014) examined how the levels of vitamin C and beta-carotene are affected in tomatoes when they are subjected to various cooking methods: raw, boiled, and fried. As the boiling or frying time increased (ranging from 2 to 30 minutes), there was a notable decline in the quantities of beta-carotene and vitamin C. For instance, boiling the tomatoes for 30 minutes resulted in a substantial reduction of 61.4% in beta-carotene content and 49.4% in vitamin C content. Similarly, when the tomatoes were fried for 30 minutes, there was a significant decrease of 63.6% in beta-carotene and 50.0% in vitamin C. This suggests that subjecting tomatoes to extended heat exposure can lead to a degradation of their vitamin C content.

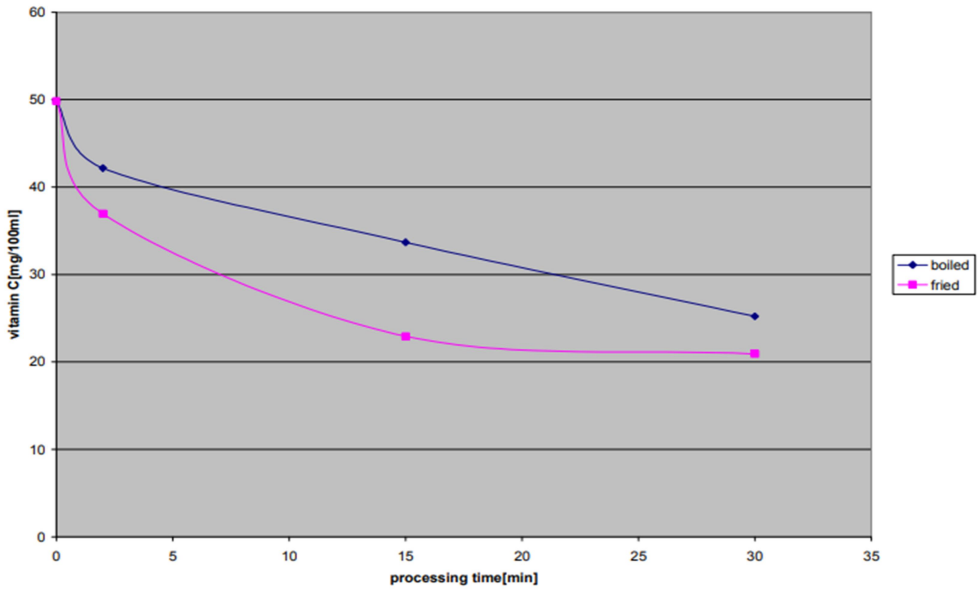

Fig 2.5: Effect of Period of Processing on Vitamin C content of Tomato (Charles N, 2014)

Ordóñez-Santos and Martínez-Girón (2019) examined the impact of various temperatures (70°C, 80°C, and 90°C) on the degradation of vitamin C within tomato juice. As the juice underwent heating, there was a notable reduction in the amount of vitamin C present. This reduction was particularly rapid when higher temperatures were applied.

WINSTON and MILLER (2006) examined how vitamin C levels change over time in various fresh fruits: Pineapple, Orange, Watermelon, and Tomato. They collected juice from these fruits and tested their vitamin C content at different conditions—room temperature, 40°C, and after 7 days of storage. Pineapple juice contained the highest vitamin C content, followed by Orange, Watermelon, and Tomato juices. Heating the juices at 40°C led to a decrease in vitamin C. After storing the juices for 7 days at room temperature, vitamin C content dropped in all the juices, although the decrease was less compared to the boiled juices. The rate of vitamin C loss during storage varied depending on the storage methods employed.

Table 2.3: Health benefits of vitamin C (Jacob, 1990).

S. No.	Health benefits	Description
1	Antioxidant Protection	Vitamin C acts as an antioxidant, helping to protect cells from damage by free radicals.
2	Immune System Support	It boosts the immune system, aiding in the defense against infections and illnesses.
3	Collagen Production	Vitamin C is vital for collagen synthesis, which is essential for healthy skin, bones, and gums
4	Wound Healing	It assists in wound healing by supporting tissue repair and aiding in the formation of scars
5	Cardiovascular Health	It may contribute to heart health by improving blood vessel function and reducing inflammation.
6	Skin Health	Vitamin C promotes healthy skin by aiding in the production of collagen and fighting oxidative stress.
7	Eye Health	Vitamin C is linked to a reduced risk of age-related macular degeneration and cataracts.
8	Allergy Management	It can have a mild antihistamine effect, which may help alleviate symptoms of allergies.

Ladi *et al.* (2017) examined how the composition of both raw tomatoes and their juice changes over time and during storage. The study also investigated the impact of storing tomato juice for 18 months on its properties. The study discovered that certain healthy components in the juice showed a minor decrease after being stored for 18 months, including vitamin C which ranged from 24.50 to 20.18 mg per 100 grams, and lycopene which decreased from 85.41 to 79.22 mg per kilogram.

2.1.1.3 Total soluble solid (TSS)

Total soluble solids (TSS), often referred to as soluble sugars, is a measurement used to quantify the amount of dissolved sugars and other soluble components in a liquid, such as tomato juice. In the context of tomatoes, TSS reflects the concentration of sugars, organic acids, and other dissolved substances that contribute to the taste and sweetness of the fruit. The TSS value is an important factor in determining the flavor, texture, and overall quality of tomato products like juices, sauces, and processed foods **(Charles N, 2014).**

Gould (1992) examined that tomato sauce heated through conventional methods, showed that at temperatures of 70°C, 80°C, 90°C, and 100°C, the highest levels of total soluble solids were observed at 100°C. Moreover, the total soluble solids exhibited a continuous rise with longer durations of heating.

Makroo *et al.* (2017) examined the impact of ohmic heating on the total soluble solids in tomato juice. The study concluded that changes in heating temperature and time didn't cause substantial differences in total soluble solids. The results also demonstrated a direct relationship between higher temperature, longer heating duration, and increased total dissolved solids in the juice. The average total soluble solids content ranged from about 3.2 to 3.6 °Brix.

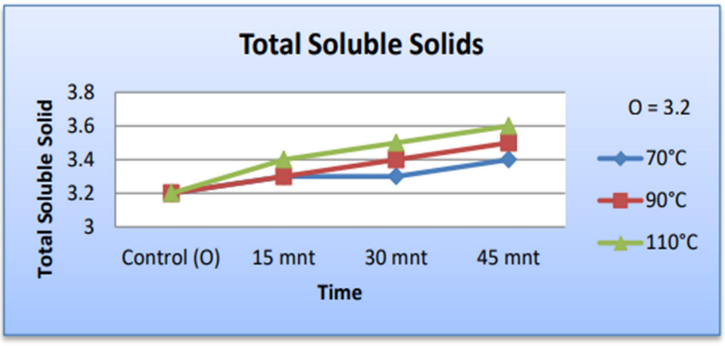

Fig 2.6: Effect of Temperature (°C) and Heating Time (minutes) on Total Soluble Solid Content. (Makroo *et al.*, 2017)

2.1.1.4 Total phenolic content (TPC)

The total phenolic content indicates the combined quantity of phenolic compounds found in tomato juice. The existence of phenolic compounds, encompassing flavonoids and other antioxidants, contributes to the health-promoting aspects of tomato juice, including its potential to combat oxidative stress and inflammation **(Colle *et al.*, 2010).**

Bramley (2000) examined that pasteurization of tomato juice potentially lead to a decrease in the total phenolic content due to the heat sensitivity of certain phenolic compounds. The degree of change would depend on several factors related to the pasteurization process and the original phenolic composition of the juice.

2.1.2 PHYSICO-CHEMICAL CHARACTERISTICS OF TOMATOES

Tomatoes are a nourishing vegetable, and their physical and chemical attributes vary based on factors such as the type, ripeness stage, region, and season. Differences in the physical properties of tomato fruits, including weight, color, number of compartments, amount of pulp and juice, firmness, thickness of the outer layer, and seed count, have been well-established **(Bhattacharyya *et al.*, 1979).**

2.1.2.1 pH

Colle *et al.* (2010) stated that pH value of tomato juice is a measure of its acidity. Heating the juice can potentially cause a slight increase in pH, making it less acidic, but the change is usually minimal and intended to maintain the juice's quality.

Makroo *et al.* (2017) study revealed noteworthy differences in heating temperatures and durations' effects on tomato juice pH. Higher temperatures corresponded to higher pH values, while longer heating durations correlated with lower pH values for the juice. The pH of the tomato juice ranged from 4.05 to 4.64 on average.

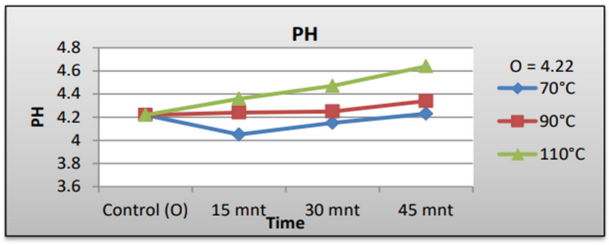

Fig 2.7: Effect of Temperature (°C) and Heating Time (minutes) on pH. (Makroo *et al.*, 2017)

Jafari *et al.* (2017b) investigated how the use of nanofluids could reduce the duration of traditional thermal processing and its influence on the quality of tomato juice. Although the influence of time on pH and acidity indicators was not found to be significant, temperature notably affected these factors. Considering the variables studied, optimizing the outcome would involve selecting a temperature of 70°C, a concentration of 4%, and a processing time of 30 seconds.

Sánchez-Moreno *et al.* (2006) stated that the freshly prepared tomato juice had a pH of 2.73, while the thermally treated ones exhibited higher pH values. This indicates that the pH tends to slightly increase after thermal treatment, with a rise of about 3.4 in pH value.

Adekunte *et al*. (2010) stated that, tomato juice was exposed to varying levels of sonication amplitudes, spanning from 24.4 to 61.0 μm, all maintained at a consistent frequency of 20 kHz. The treatment durations ranged from 2 to 10 minutes, employing a pulsing pattern with 5 seconds on followed by 5 seconds off. Unexpectedly, there were no noteworthy distinctions ($p < 0.05$) detected regarding pH, Brix content, or treatable acidity levels.

2.1.2.2 Color

Gupta *et al.* (2010) studied that during a 52-week storage period at temperatures of 4°C, 25°C, and 37°C, alterations in color values (ΔE) were observed in both processed and control samples. Comparing to the initial state of the control sample, all processed samples exhibited color changes influenced by both storage temperature and duration. In most cases, the changes in color values (ΔE) due to the degradation of lycopene followed a relatively linear pattern, as indicated by regression coefficient values exceeding 0.85 ($R^2 > 0.85$).

Badin *et al.* (2023) used a multiphysics model to assess the pasteurization of crushed tomato in glass bottles. Simulations at different temperatures (80°C, 90°C, and 100°C) showed that the 100°C process retained the best quality, with 92.25% color retention, 74.76% lycopene retention, and 83.68% ascorbic acid retention. Contrastingly, the 80°C treatment had lower retentions: 65.60% color, 18.35% lycopene, and 36.13% ascorbic acid.

Calligaris *et al.* (2002) examined alterations in color for frozen tomato purees stored at temperatures of -7°C and -18°C. Both unblanched and blanched samples displayed color changes with sigmoidal patterns due to radical reactions. Greater color

transformations were observed in unblanched purees than in blanched ones, ascribed to carotenoid fading stemming from chemical and enzyme-driven oxidation reactions. The influence of storage temperature was noticeable exclusively in the case of unblanched tomato samples.

ZHAO *et al.* (2013) demonstrated that alterations in tomato color are frequently quantified using the a*/b* ratio. Another commonly utilized indicator for expressing changes in tomato color is the hue angle. This measure is preferred due to its ease of detection compared to variations in chroma or lightness.

Barreiro *et al.* (1997) stated that color is typically defined using three coordinates, and there exist different color scales for characterizing it: CIE-X,Y,Z; the 'L', 'a', 'b'; and the Rd, a, b scales. Color indexes and differences can also be calculated based on these values. The 'L', 'a', 'b' scale is known for its ability to effectively distinguish subtle color variations in the darker portion of the color space, making it suitable for saturated colors like those found in tomato products. This scale is widely used for food products due to these advantages.

Gould (1992) explained that after thermal treatment, the color of tomatoes can undergo changes. These changes are commonly observed as alterations in the a*/b* ratio or variations in the 'L', 'a', 'b' colour scale. The hue angle, another indicator of color, might also be used to express these changes. Thermal treatment can lead to shifts in color due to various chemical and physical reactions, impacting factors like pigments and structural changes in the tomatoes. The extent and nature of color changes depend on the specific conditions of the thermal treatment and the properties of the tomatoes being processed.

2.2 Nanofluid

Traditionally, water serves as the base fluid for heat transfer; however, its low thermal conductivity can impede efficient and swift heating processes. This characteristic is particularly limiting when rapid heating is crucial **(Chintamani and Ghuge, 2015)**. According to **Qazi, (2017)**, effective heat transfer fluids (HTFs) should possess high thermal conductivity, substantial volumetric heat capacity, and minimal viscosity. It's widely acknowledged that the thermal conductivity of solids like copper and aluminum oxide significantly exceeds that of conventional liquids. Hence, introducing these solids in particle form to HTFs has the potential to significantly augment the overall thermal conductivity of the fluid. In 1995, the

Argonne National Laboratory's Choi and Eastman pioneered the creation of solid-impregnated fluids with elevated thermal conductivity. They coined these fluids 'nanofluids' (NFs) due to the inclusion of metallic nanoparticles (solid) in industrial HTFs **(Khan and Arasu, 2019).**

Ali *et al.* (2018) stated that several factors impact the thermal conductivity of nanofluids (NFs), including attributes like acidity, clustering, additives, base fluid type, and nanoparticle characteristics (such as concentration, size, shape, temperature, and material).

Han *et al.* (2017) studied a double tube heat exchanger with nanofluids on the cold side, operating under turbulent conditions with Reynolds numbers between 20,000 and 60,000. The findings demonstrate that heat transfer improves as the temperature and volume concentrationof nanoparticles increase. The results indicate a substantial enhancement compared to water, with a maximum increase of 24.5% in the Nusselt number observed at an inlet temperature of 50℃.

Tiwari *et al.* (2013) compared experimentally the heat transfer performances of different nanofluids (CeO_2, Al_2O_3, TiO_2, and SiO_2) in a plate heat exchanger. The results revealed that CeO_2/water exhibited the best performance, achieving a maximum performance index enhancement of 16%. Moreover, this nanofluid required a comparatively lower optimum concentration of 0.75 vol.% among the studied nanofluids.

Sözen *et al.* (2016) studied the heat transfer performance of fly ash nanofluid was evaluated while flowing through either a PFCTHE (Parallel Flow Counter Flow Tube Heat Exchanger) or a CFCTHE (Cross Flow Counter Flow Tube Heat Exchanger). They observed a significant performance improvement of 31.2% in PFCTHE (Parallel Flow Counter Flow Tube Heat Exchanger) and 6.9% in CFCTHE (Cross Flow Counter Flow Tube Heat Exchanger). The optimum overall heat transfer coefficient ratio (Un/Uw) was determined as 1.6 for PFCTHE and 1.3 for CFCTHE. Additionally, the optimal values for the heat transfer coefficient ratios (hi,n-fly/hi,w) and (ho,n-fly/ho,w) were 1.93 and 1.2, respectively, for PFCTHE, while both ratios were found to be 1.1 for CFCTHE**.**

Jafari *et al.* (2017a) studied that the use of alumina can effectively reduce the heating process duration, particularly at higher nanoparticle concentrations. This leads to lower energy consumption and better preservation of product quality and

nutritional properties. Substituting 4% nanofluids for water can maintain higher levels of vitamin C and lycopene by approximately 6% and 10%, respectively. The ΔE* indices for fruit juices processed with water, 2% nanofluids, and 4% nanofluids were 3.26, 2.21, and 1.14, respectively. Alumina nanofluid thermal processing of watermelon juices did not significantly alter pH and TSS values compared to pasteurization and PEF processes. This study demonstrates the potential of nanofluid thermal technology to significantly enhance the nutritional content of food products.

Arya *et al.* (2019) studied the application of MgO-ethylene glycol nanofluid in a double pipe heat exchanger. The study revealed that the heat transfer coefficient in the heat exchanger can be improved by 27% when using MgO-ethylene glycol nanofluid with a concentration of 0.3 wt.% compared to the base fluid (ethylene glycol). Additionally, the presence of MgO nanoparticles led to a 35% increase in pressure drop at the same concentration.

Anoop *et al.* (2013) examined the thermal performance of nanofluids in industrial heat exchangers. They formulated silicon dioxide-water (SiO2-water) nanofluids with three different mass particle concentrations: 2%, 4%, and 6%. The nanofluids were created by dispersing 20 nm diameter nanoparticles in distilled water. Experimental comparisons were made between the overall heat transfer coefficient and pressure drop for water and nanofluids. The study concluded that heat transfer was enhanced due to the improved thermal conductivity of the nanofluids. However, the nanofluids exhibited increased pressure drop due to the higher viscosity**.**

Salari and Jafari (2020) concluded that nanofluids exhibit increased thermal conductivity and viscosity compared to base fluids. However, higher viscosity leads to drawbacks such as increased pressure drop and pumping power. To mitigate viscosity effects, an optimal concentration for each nanofluid is necessary. In the food industry, nanofluids have shown promising results in reducing processing time and preserving food quality and bioactive compounds during thermal processing operations like pasteurization.

Barzegarian *et al.* (2016) showed that substituting water with TiO_2/water nanofluid resulted in a notable increase in convective heat transfer coefficient (HTC) ranging from 2.5%-23.7%. Additionally, the overall heat transfer coefficient (OHTC) experienced an increase ranging from 1.2%-8.5% at nanoparticle concentrations of 0.3% -1.5%.

Said *et al*. (2019) demonstrated that the utilization of CuO/water nanofluids in a shell and tube heat exchanger improved its effectiveness while reducing energy consumption and overall costs. They observed an 11% increase in convective heat transfer coefficient (HTC) and a 7% increase in overall heat transfer coefficient (OHTC) when nanofluids were employed. Additionally, they concluded that the stability of nanofluids deteriorated as the volume fraction of nanoparticles increased.

Shahrul *et al*. (2016) investigated the impact of different water-based nanofluids on the performance of a shell and tube heat exchanger. They found that using ZnO/water (with PVP surfactant), Al_2O_3/water, and SiO_2/water nanofluids at volume concentrations of 0.3%, 0.5%, and 0.5% respectively, resulted in improvements of 35%, 26%, and 12% in overall heat transfer coefficient (OHTC). The study also highlighted the significant influence of fluid flow rate on heat transfer. With a constant shell-side volumetric flow rate (4 L/m), the highest enhancement in heat transfer was achieved at tube-side volumetric flow rates of 6 L/m for ZnO/water, 7 L/m for Al_2O_3/water, and 7 L/m for SiO_2/water nanofluids.

Leela Vinodhan *et al*. (2016) aimed to enhance the heat transfer performance of a double pipe heat exchanger by incorporating baffles and CuO/water nanofluids. They observed an 8% increase in the Nusselt number and a 25% increase in heat transfer coefficient (HTC) when using CuO/water nanofluids with a nanoparticle concentration of 0.2%. With the addition of baffles, the Nusselt number and HTC further improved to 12% and 30%, respectively.

Wang *et al*. (2019) examined the impact of using CNT nanofluids stabilized by gum Arabic on heat transfer within a concentric tube heat exchanger under turbulent flow conditions. The investigation showcased a remarkable enhancement in thermal conductivity, ranging from 67% to 250%, with the use of CNT nanofluids compared to water. This enhancement was observed at nanoparticle concentrations of 0.051% to 0.085% and temperatures spanning 25°C to 55°C. The research underscored the significant influence of both temperature and nanoparticle concentration on thermal conductivity. Additionally, a noteworthy increase of 7% to 202% in the convective heat transfer coefficient (HTC) was recorded when CNT nanofluids were employed within the same concentration and temperature range. The study demonstrated that nanofluids possessed higher viscosity and density than water yet concluded that their impact on deteriorating heat transfer performance through

pressure drop escalation could be disregarded due to their more pronounced positive influence on HTC. Moreover, the findings indicated that at elevated temperatures, viscosity tended to decrease, possibly attributed to reduced intramolecular forces between nanoparticles and the base fluid molecules.

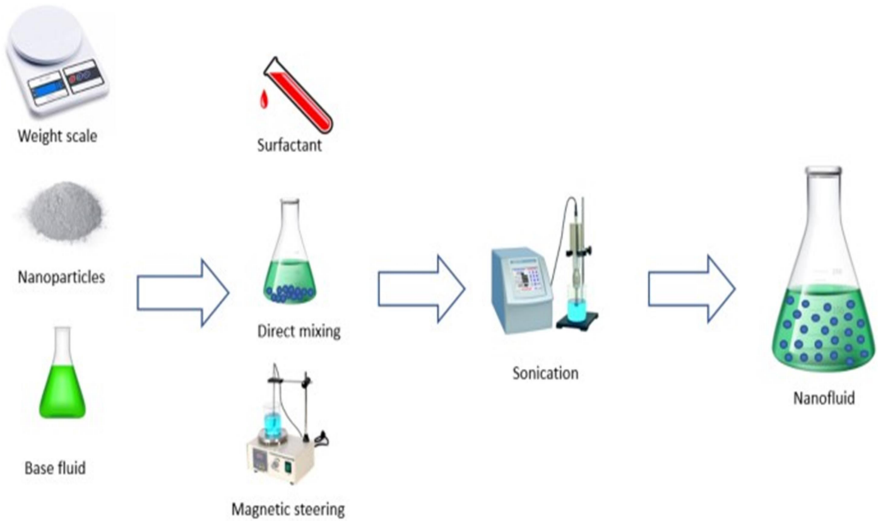

Fig 2.8: Flow diagram of nanofluid (Chintamani and Ghuge, 2015)

2.2.1 Preparation of nanofluid

The technique employed for creating nanofluids plays a crucial role in enhancing thermal conductivity through the addition of nanoparticles. Nanofluid preparation methods are typically divided into one-step and two-step approaches. In the one-step method, nanoparticles are directly produced and distributed within the fluid using methods like physical vapor deposition (PVD) or liquid chemical techniques. On the other hand, the two-step approach involves initially synthesizing nanoparticles, nanofibers, or nanotubes as nanopowders through techniques like inert gas condensation, chemical vapor deposition, or mechanical alloying. Subsequently, nanofluids are formed by dispersing these nanopowders into the base fluid **(Salari and Jafari, 2020).**

Babita *et al.* (2016) stated that commercially, the two-step technique is predominantly employed for crafting nanofluids. This approach offers advantages like the ability to achieve extensive production and the flexibility to utilize various fluids for nanofluid creation. Nonetheless, a significant drawback of the two-step method is the tendency for nanoparticles to aggregate or clump together.

Yu and Xie (2012) examined that the one-step approach offers several benefits, including the elimination of stages like drying, storage, transportation, and dispersion of nanopowders. This approach also helps in reducing the tendency of nanoparticles to form clusters. Nanofluid preparation using the one-step method can be achieved either through physical or chemical means, each with its drawbacks. Physical techniques are not suitable for large-scale nanofluid production due to high costs.

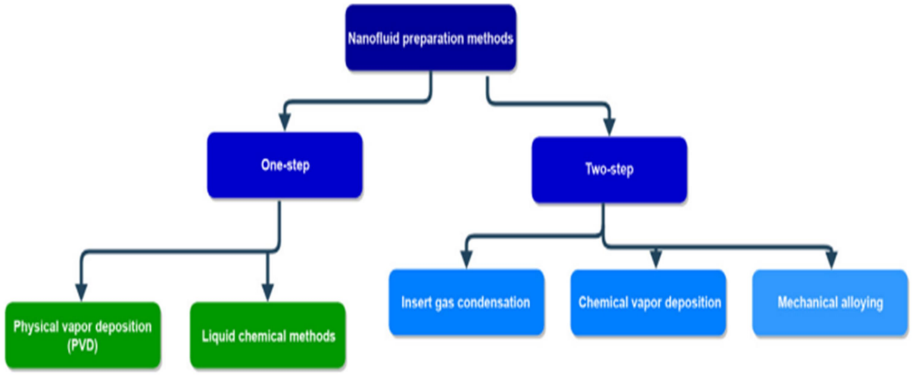

Fig 2.9: Nanofluid preparation methods. (Salari and Jafari, 2020)

2.2.2 Thermophysical properties of nanofluid

Thermophysical properties encompass attributes or qualities that determine how a material conducts heat. These properties play a critical role in calculating important parameters like heat transfer coefficients (HTC), pressure drop, and energy efficiency. The performance of industrial heat transfer equipment relies heavily on these parameters **(Salari and Jafari, 2020).**

2.2.2.1 Thermal conductivity of nanofluids

Ahmadi *et al.* (2018) stated that thermal conductivity, together with viscosity, is a significant thermophysical property that impacts the heat transfer characteristics of a fluid. Research indicates that the incorporation of nanoparticles results in an elevation of thermal conductivity. This implies that enhancing thermal conductivity leads to an improvement in heat transfer efficiency.

Murshed *et al.* (2005) conducted a study revealing that the most significant increase in thermal conductivity of TiO2/water nanofluid occurred when the nanoparticle volume fraction was set at 5%. This enhancement was measured at 29.70% for nanoparticle sizes of 15 nm and 32.80% for sizes of 10 nm to 40 nm.

Li and Peterson (2006) investigated the thermal conductivity of Cu/water nanofluids prepared using a chemical reduction technique. They noted a 23.8% increase in water's thermal conductivity upon the addition of 0.1 vol.% Cu nanoparticles. Additionally, they found that at a temperature of 70°C, the incorporation of 0.3 vol.% and 0.9 vol.% of silver nanoparticles into water resulted in thermal conductivity enhancements of 27% and 80%, respectively**.**

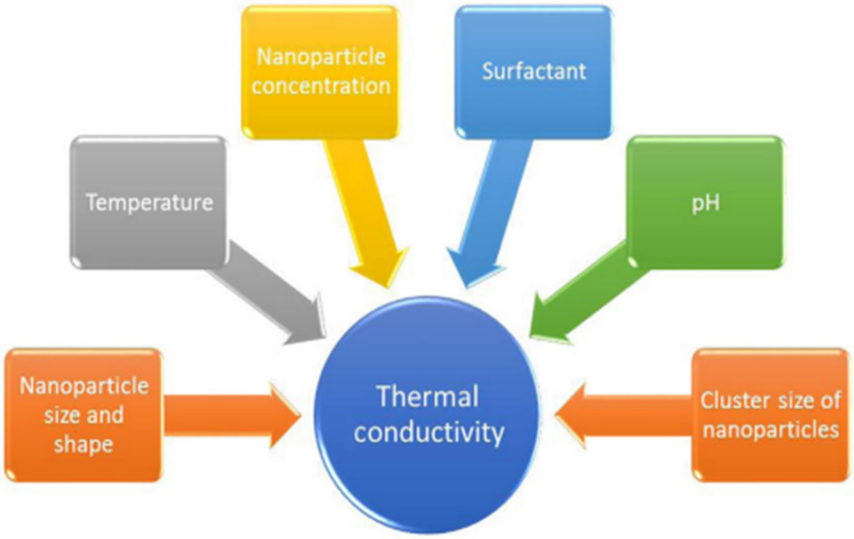

Fig 2.10: Influential factors on nanofluid thermal conductivity (Salari and Jafari, 2020)

Sadri *et al.* (2014) documented a 10.47% increase in the thermal conductivity of methanol by introducing 0.5 vol.% of Al_2O_3 nanoparticles, while a 14.29% enhancement was observed with 0.5 vol.% SiO2 nanoparticles. They also noted a 22.31% rise in the thermal conductivity of water when 0.5 wt.% of multiwalled carbon nanotubes (MWCNTs) and 0.25 wt.% of gum Arabic were added, with sonication conducted at 45°C for 40 minutes.

Han *et al.* (2017) examined the thermal conductivity of gold (Au) nanoparticles. Their research indicated that the inclusion of spherical gold nanoparticles resulted in a rise of 12.58% to 21.43% in the thermal conductivity of Argon liquid, while rod-shaped gold nanoparticles led to an increase of 15.3% to 29.6%. These improvements were observed with a volume fraction of nanoparticles ranging from 0.5% to 3%.

2.2.2.2 Viscosity of nanofluids

Mishra *et al.* (2014) demonstrated that viscosity holds a comparable level of importance as thermal conductivity among nanofluid properties. Its influence directly affects convective heat transfer, pressure drop, and pumping power. The inclusion of nanoparticles contributes to elevated viscosity in base fluids, a factor often viewed unfavorably due to its contradictory impact on the beneficial enhancement of heat transfer performance through increased thermal conductivity.

According to **Qazi (2017)**, an increase in the volume concentration of Fe_2O_3 from 0.5% to 5% led to a 22.5% increase in nanofluid viscosity at 293 K. They also demonstrated that the viscosity of Fe_2O_3/water nanofluid with 0.5 vol.% nanoparticles decreased by 52.94% as the temperature rose from 293 to 333 K. Additionally, they found that the viscosity of Al_2O_3/water nanofluid containing 5 vol.% nanoparticles was 2.36 times higher than that of the base fluid.

According to **Nikkhah (2015)**, the introduction of 6.12 vol.% CuO into a mixture of ethylene glycol and water (60:40) led to a viscosity increase of approximately fourfold.

Fig 2.11: Influential factors on viscosity of nanofluids (Salari and Jafari, 2020)

Qazi (2017), stated that the impact of temperature on the viscosity of nanofluids appears to be more significant than the influence of nanoparticle size.

2.2.2.3 Density of nanofluids

Density is another crucial thermophysical property of nanofluids due to its similar impact as viscosity on characteristics like Reynolds number, friction factor, pressure drop, and pumping power.

In accordance with **Sözen *et al.* (2016)**, density is defined as the ratio of an object's mass to its volume. The density of fluids is influenced by various factors, including chemical composition, soluble components, temperature, and pressure.

Pastoriza-Gallego *et al.* (2009) demonstrated that the density of nanofluids is notably influenced by nanoparticle concentration, while temperature has no significant impact on density. Furthermore, the size of nanoparticles has been found to play a crucial role in determining nanofluid density, with smaller particles leading to increased density.

Sen Gupta *et al.* (2011) examined the necessity of incorporating the nanolayer when creating an accurate numerical model for predicting nanofluid density. The nanolayer refers to a slim region situated at the boundary between the suspended particles and the molecules of the base fluid.

2.2.2.4 Specific heat capacity of nanofluids

The specific heat capacity indicates the quantity of thermal energy required for a material to experience a temperature alteration. To determine parameters such as thermal diffusivity, dynamic thermal conductivity, and the Prandtl number, accurate measurement of the material's specific heat capacity is crucial. It appears that elevating the volume fraction of nanoparticles within a nanofluid generally leads to a reduction in its specific heat capacity **Fan and Wang (2011)**

Namburu *et al.* (2007) investigated the viscosity and specific heat of silicon dioxide (SiO2) nanoparticles with different diameters (20, 50, and 100 nm) suspended in a 60:40 mixture of ethylene glycol and water by weight. Nanofluids containing particle volume percentages ranging from 0% to 10% were examined, and viscosity experiments were conducted across a broad temperature range (from 23°C to 50°C) to assess their suitability in cold environments. The impact of nanoparticle diameter on the rheology of SiO2 nanofluids was studied, revealing non-Newtonian behaviour at sub-zero temperatures for certain particle volume concentrations. A new correlation was developed based on experimental data to relate viscosity with particle volume

percentage and nanofluid temperature. Additionally, the specific heats of SiO2 nanofluids with varying particle volume concentrations were presented.

Fan and Wang (2011) stated that nanofluids, comprising nanoparticle-laden fluids, are a rapidly evolving technology with broad applications in nanotechnology and biotechnology. Their potential to reshape heat transfer practices is profound. This review delves into the advancements in understanding the thermal properties of nanofluids, with a specific focus on their thermal conductivity. It explores experimental data, mechanisms behind conductivity enhancement, and predictive models. Despite ongoing research to unravel the intricate microstructure-conductivity relationship, significant progress has been made. The influence of factors like Brownian motion, convection, liquid layering, and nanoparticle clusters on enhanced conductivity is examined. Among these factors, the presence of nanoparticle clusters is widely accepted as a key contributor. Although current predictive models often rely on empirical parameters, a novel first-principles theory based on thermal waves presents a promising approach that offers both macroscopic insights and a microstructure-conductivity relationship devoid of empirical elements.

2.2.3 Application of nanofluids in thermal processing of food product

There has been a growing interest and significant advancements in improving heat transfer in the food industry through thermal processes. A new and emerging approach involves using nanofluids as substitutes for traditional heat transfer fluids to address heat transfer challenges in food processing. This review focuses on the latest techniques for producing and applying these nanofluids, particularly for liquid food decontamination. The study also examines how factors like temperature and nanoparticle concentration affect the thermal and viscous properties of these nanofluids. Furthermore, the impact of these nanofluids on the quality of food materials is explored. The review identifies several gaps in nanofluid research, including the need for controlled and systematic experiments, stability assessment over thermal cycles, enhancing compatibility between base fluids and nanomaterials, and evaluating toxicity and environmental consequences **(Tarafdar *et al.*, 2021)**.

Jabbari *et al.* (2018) this study demonstrates the potential of nanofluid-based thermal processing in enhancing the quality of tomato juice. The utilization of appropriate nanoparticle concentrations, lower temperatures, and shorter processing

times can result in improved lycopene retention, reduced color degradation, and favorable pH/acidity levels. These findings contribute to the development of optimized thermal processing techniques for tomato juice, promoting its nutritional value and consumer acceptance in the market. Further research is warranted to explore additional quality parameters and optimize the nanofluid- based processing conditions for other food products.

Salari and Jafari (2020) concluded that nanofluids have a higher thermal conductivity and viscosity in comparison to the base fluids. Higher viscosity deteriorates the process efficiency by increasing the pressure drop and pumping power. In order to minimize the effect of viscosity, an optimum concentration for each nanofluid should be obtained. Regarding the food industry, a significant reduction in processing time and better retention of food quality and bioactive compounds have been reported by using nanofluids in thermal processing operations such as pasteurization.

Fan and Wang (2011) results showed that qualitative and nutritional properties of watermelon juices processed with nano-fluids in terms of lycopene and vitamin C retention, and color were, respectively, 9.89, 6.18 and 50.38% better than the samples processed with water.

Jafari *et al.* (2017a) findings indicate that the application of nanofluids in enhancing heat exchanger performance within food processing facilities offers advantages both in terms of technical optimization and the potential impact on food product quality.

According to **Taghizadeh-Tabari *et al.* (2016)**, their findings revealed that incorporating TiO2 nanoparticles into distilled water and increasing nanoparticle concentration led to a slight increase in pressure drop, but the magnitude of the increase was not substantial. Specifically, at a TiO2 concentration of 0.8%, the pressure drop increased by 8% compared to water. The utilization of nanofluids has implications for crucial technical factors like energy consumption, processing time, and the efficiency of food processing equipment. Studies have indicated that substituting conventional heat transfer fluids with nanofluids results in noteworthy reductions in energy consumption and processing time, while simultaneously enhancing the overall effectiveness of the food processing equipment.

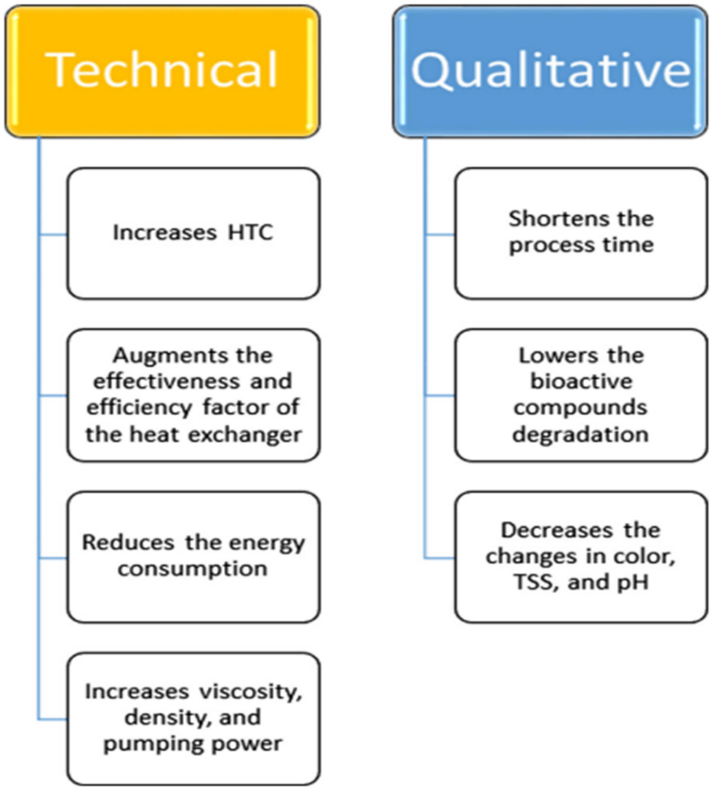

Fig 2.12: The effects of nanofluids on heat exchanger performance in the food industry (Salari and Jafari, 2020)

Numerous endeavors have been undertaken to enhance the efficiency of heat exchange systems across diverse industries. Among the recent techniques introduced, nanofluids have garnered attention. The rationale behind adopting nanofluids stems from the recognition that conventional heat transfer fluids like water and ethylene glycol exhibit suboptimal performance, posing a limitation to heat exchanger effectiveness. Nanofluids, comprised of nanoparticles dispersed within conventional fluids, represent a novel fluid generation that holds promise for significantly enhancing thermal conductivity. Thermal conductivity stands as one of the pivotal factors impacting the overall heat transfer efficiency of heat exchange apparatuses. However, nanofluids are not devoid of challenges that impede their practical implementation. Chief among these is nanoparticle clustering, leading to sedimentation and suspension destabilization. Consequently, various methods have been proposed to enhance particle stability, encompassing techniques like sonication, surfactant utilization, and pH adjustment. Another hurdle in applying nanofluids industrially lies in achieving stable and uniform nanofluids on a large scale and at an

economical cost. Moreover, the increase in fluid viscosity upon nanoparticle addition is viewed unfavourably due to its detrimental impact on pressure drop and pumping power **(Allahyar *et al*., 2016).**

Salari and Jafari (2020) suggested that in the realm of the food industry, nanofluids possess significant potential to enhance thermal processes from both technical and qualitative standpoints. Evidence indicates that the utilization of nanofluids can expedite thermal procedures by necessitating lower temperatures and shorter durations, thereby promoting the preservation of attributes like color, total soluble solids, pH, and bioactive components such as vitamin C, phenolics, and lycopene. To gain a more comprehensive understanding, further exploration is warranted, encompassing diverse products, applicable heat exchangers in the food sector, and a range of processes like concentration, sterilization, and pasteurization, all tested under varying operational conditions. Given the impact of fouling on heat transfer equipment and its operational challenges, delving into the influence of nanofluids on fouling is also crucial for a deeper comprehension.

2.3 Al_2O_3 Nanofluid

Kumar *et al.* (2018) the investigation of Al_2O_3 nanofluids based on water, paraffin, and ethylene glycol in a shell and tube heat exchanger revealed a significant enhancement in the heat transfer coefficient and thermal conductivity compared to the base fluids. Increasing the concentration of nanoparticles resulted in a marginal improvement in the heat transfer coefficient. The improvement in heat transfer coefficient was more pronounced at higher turbulence levels, attributed to the homogeneous distribution of nanoparticles achieved at higher temperatures. Factors such as sonication time, temperature, pressure difference, and the choice of base fluid were considered in characterizing the nanofluid heat transfer coefficients. In the turbulent regime, the nanofluids exhibited higher pressure drop compared to the base fluids, while no significant change was observed in the laminar region. Overall, these findings contribute to a better understanding of nanofluid heat transfer characteristics and have implications for the design and optimization of heat transfer systems involving nanofluids.

Chavda *et al.* (2014) investigated the impact of different concentrations of Al_2O_3 nanofluid mixed with water as the base fluid on the heat transfer characteristics of a double pipe heat exchanger, considering both parallel and counter flow

arrangements. The volume concentrations of the prepared Al_2O_3 nanofluid ranged from 0.001% to 0.01%. The study concluded that the overall heat transfer coefficient increases as the volume concentration of Al_2O_3 nano-dispersion rises, compared to water, up to a concentration of 0.008%. After reaching this point, the overall heat transfer coefficient starts to decrease.

Albadr *et al.* (2013) conducted an experimental study on a counter-flow horizontal shell and tube heat exchanger using an Al_2O_3-water nanofluid. They observed that the thermal conductivity and viscosity of the nanofluid increased with higher particle concentrations. At a particle volume concentration of 2%, the Al_2O_3 nanofluid exhibited significantly higher heat transfer characteristics, with an overall heat transfer coefficient of 700.242 W/m2K compared to 399.15 W/m2K for water. This resulted in an enhancement ratio of 1.754, indicating that the nanofluid's overall heat transfer coefficient was 57% greater than that of distilled water.

Raei *et al.* (2016) found that using γ- Al_2O_3/water nanofluids with a nanoparticle volume fraction of 0.15% resulted in a significant 19.3% increase in overall heat transfer coefficient (OHTC). When the inlet temperature of the nanofluids was raised from 45°C to 65°C, the average heat transfer rate improved by up to 53%. While the OHTC decreased with increasing flow rate compared to water, the researchers noted that based on their experimental results, increasing the nanofluid flow rate had a positive impact on OHTC and heat transfer rate.

Akyürek *et al.* (2018) conducted experiments on a concentric tube heat exchanger to study the impact of Al_2O_3/water nanofluids, with or without wire coil turbulators, on heat transfer and pressure drop. They found that adding nanoparticles at volume fractions ranging from 0.4% to 1.6% in water resulted in a substantial increase in the Nusselt number, ranging from 35.66% to 168.26%. The researchers concluded that nanofluids are more suitable for use without turbulators because their findings indicated that the use of turbulators led to a significant increase in pressure drop.

Allahyar *et al.* (2016) conducted a comparative study to examine the impact of Al_2O_3/water nanofluids and Al_2O_3-Ag/water hybrid nanofluids on the thermal performance of a coiled heat exchanger. The results showed that at a Reynolds number of 4687 and a nanoparticle concentration of 0.4%, both the hybrid and

Al_2O_3/water nanofluids yielded significant enhancements in the Nusselt number, with approximately 31.58% and 28.42% improvements, respectively.

Jabbari *et al.* (2018) demonstrated from a technical standpoint, incorporating Al_2O_3 nanoparticles into water and elevating the particle concentration yields significant enhancements in thermal conductivity, viscosity, and density, while concurrently leading to a notable reduction in specific heat capacity. Regarding heat transfer attributes, an investigation focusing on the thermal processing of tomato juice showcased that utilizing Al_2O_3/water nanofluids with 2% and 4% nanoparticle concentrations led to an increase of 5.42% and 11.94% in heat transfer coefficient (HTC), respectively. Similarly, a separate study demonstrated that employing Al_2O_3/water nanofluids with nanoparticle concentrations of 1%, 2%, and 4% during the thermal processing of watermelon juice resulted in overall heat transfer enhancements of 5%, 8%, and 13%, respectively.

Ghanbarpour *et al.* (2014) presents both an empirical investigation and a theoretical analysis of the thermal conductivity and viscosity of Al_2O_3/water nanofluids. Diverse Al_2O_3 nanoparticle suspensions with concentrations ranging from 3% to 50% by mass and temperatures spanning 293 K to 323 K were examined. The outcomes indicate that as temperature and particle concentration increase, the thermal conductivity and viscosity of the nanofluids also increase, with viscosity experiencing a more substantial rise than thermal conductivity. The enhancements in thermal conductivity and viscosity vary from 1.1% to 87% and 18.1% to 300%, respectively. Furthermore, the findings highlight that thermal conductivity exhibits a nonlinear relationship with concentration but a linear correlation with temperature. The experimental results are compared with existing correlations in the literature, leading to suggested modifications. Lastly, the study explores the average heat transfer coefficient using different bases of comparison, such as equal Reynolds number, fluid velocity, and pumping power, within fully developed laminar and turbulent flow regimes. Notably, it concludes that equal Reynolds number as a basis can be misleading, and equal pumping power might be a more appropriate criterion for evaluating the benefits of using nanofluids over base fluids.

Materials & Methods

Chapter 3 MATERIALS AND METHODS

This chapter presents an in-depth account of the materials and methods employed during the course of the research investigation. The primary objective of this research is to retain the quality of tomato juice during nanofluid aided thermal processing. All the practical aspects of the study were conducted within the premises of two departments: the Department of Post Harvest Process and Food Engineering in the College of Technology, as well as the Department of Food Science and Technology in the College of Agriculture, located at G. B. Pant University of Agriculture and Technology in Pantnagar, Uttarakhand, India.

This chapter comprehensively covers various aspects including the sourcing of raw materials, the meticulous selection of process parameters which encompass independent, dependent, and constant variables, the formulation of the experimental design, and the step-by-step account of the actual experimental procedures conducted.

3.1 Experimental Materials

3.1.1 Tomato

A significant quantity of Pant T-3 variety tomatoes was obtained from the nearby market in Pantnagar. This selection aimed to maintain consistent quality throughout the experiment. The gathered tomato fruits underwent a thorough cleaning and sorting process to eliminate any extraneous elements, dust, or impurities.

3.1.2 Nanofluid

High-purity aluminium oxide nanoparticles (99% purity) was obtained from Shilpent, Shilpa Enterprises located in Delhi. The alumina nanoparticles was utilized in the heat exchanger as part of the heating medium, without any direct contact between the nanofluids and the product.

3.1.3 Chemicals, glassware and equipment

Analysis was conducted using chemicals of analytical grade, procured from established suppliers. All borosil made glassware was appropriately cleansed, washed, and subjected to sterilization procedures.

3.1.4 Experimental equipments

A range of tools is utilized for both the processing and assessment of quality parameters in tomato juice.

A comprehensive listing of these equipment items, along with their corresponding specifications, are given in **Table 3.1.**

Table 3.1 Equipment used and their specifications

Equipments/Apparatus	**Specification**	**Make**
Filter paper	Whatman No. 1, dia-125mm	AXIVA, Sichem Biotech
Stop watch	Range 15 min, least count 0.01 sec	Timex
Refrigerator	310 liters	Kelvinator
Test tube	Capacity: 25, 50 ml	Borosil
Pipette	Capacity: 1, 5, 10ml	Borosil
Beaker	Capacity:100, 250, 500, 1000ml	Borosil
Conical flask	Capacity:25, 50, 100, 250 ml	Borosil
Measuring cylinder	50 mm diameter	Borosil
Volumetric flask	Capacity: 100, 250ml	Borosil
Balance electronic	Capacity-300g Least count-0.01g	Winsor
Spectrophotometer	UV-Vis, double beam, LI-2904 (LASANY)	Lasany
Digital pH meter	Citizen ID50-01	Citizen
Magnetic Stirrer	Citizen Scale,1500rpm	Citizen

3.2 Experimental setup

The double pipe heat exchanger is a fundamental type of heat transfer device used to efficiently exchange thermal energy between two fluids. This heat exchanger design consists of two concentric pipes, with one smaller pipe enclosed within a larger outer pipe. The two fluids, typically with different temperatures, flow in separate pipes, allowing heat to transfer between them.

Table 3.2 Double pipe heat exchanger specifications

Serial No.	Equipment/Apparatus	Specification	Make
1.	Outer Stainless Steel Pipe (SS 304)	Length: 3200mmDiameter: 50mm Thickness: 3mm	Jindal Steel
2.	Inner Stainless Steel Pipe (SS 304)	Length: 3500mmDiameter: 20mm, Thickness: 1.5mm	Jindal Steel
3.	Industrial Immersion Rod Heater	Power: 2000 watts	Generic
4.	Reservoir	No. of Reservoirs: 3 Capacity of 2 Reservoirs: 40ltrs Capacity of 1 Reservoir: 45ltrs	Generic
5.	Flow meter	No. of Flowmeters used: 2 Accuracy: up to 10^{-4} Unit: Kilolitres	Crescent
6.	Pressure Gauge	No. of Pressure Gauge used: 4Range: 1-10 psi , Unit: psi	Waaree
7.	Thermocouple	No. of Thermocouples used: 6J Type: 4 , K Type: 2	Thermonic
8.	Insulation	Nitrile Rubber	Generic
9.	Pump	No. of Pumps used: 2 Power: 0.5HP Max Flow rate: up to 0.6 kg/sec	KOEL electric (Kirloskar)
10.	Data Logger	Can be used for all type of thermocouples No.of Channels:8	Ambetronics
11.	Gate Valve (SS 304)	No. of Valves: 12	
12.	Ball Valve (SS 304)	No. of Valves: 2	

The double pipe heat exchanger utilized in this study is situated within the Research and Development laboratory of the Department of Post-Harvest Process and Food Engineering at GBPUAT in Pantnagar, Uttarakhand. The design of this heat exchanger follows a U-shaped arrangement and possesses an overall length of 3.50 meters. The specifications of double pipe heat exchanger is given in **Table 3.2**.

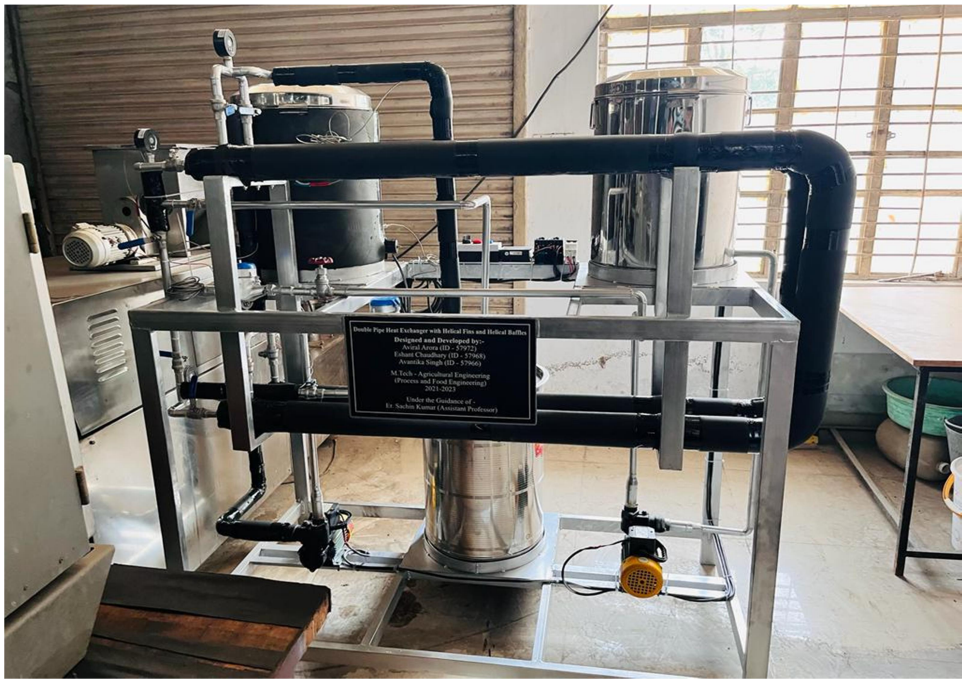

Fig 3.1: Front view of Double pipe heat exchanger

Fig 3.2: Back view of double pipe heat exchanger

3.3 Preliminary trials to select process parameters for final experiments

A preliminary experiment was conducted after reviewing previous studies on the thermal processing of tomato juice using nanofluid. The purpose of this experiment was to determine the independent and constant parameters necessary for analyzing the quality parameters of tomato juice. The experiment took place in the Research and Development Laboratory of the Department of Post-Harvest Process and Food Engineering, College of Technology, Pantnagar.

Experiments were carried out to determine the approximate ranges of independent variables that would lead to the desired outcomes of retaining tomato juice quality and enhancing heat transfer through nanofluids. In this research, the independent factors taken into account were the temperature of the heated fluid, time, and the concentration of the nanofluid. The ranges of these independent variables were established through preliminary trials.

The initial round of experiments encompassed a variety of temperatures (75, 80, 85,90 and 95 °C), durations (20, 30,40 and 50 sec), and nanofluid concentrations (ranging from 0 to 6%). The work by **Jafari *et al.* (2017a)**, underscores the potential of nanofluid-based thermal processing in augmenting the quality of tomato juice. By selecting optimal nanoparticle concentrations, lower temperatures, and shorter processing times, enhancements in lycopene preservation, mitigated color deterioration, and favorable pH/acidity levels were attainable. These findings are instrumental in refining thermal processing techniques for tomato juice, thereby elevating its nutritional value and market acceptance.

Jafari *et al.* (2017a) previously explored a spectrum of temperatures (ranging between 70 and 90°C), nanoparticle concentrations (ranging from 0 to 4%), and durations (ranging from 30 to 90 sec) for thermal processing of tomato juice. Their findings demonstrated that employing 4% nanofluid at 70°C for 30 sec yielded the highest lycopene preservation (96%) in tomato juice, while employing hot water treatment (0% nanoparticle concentration) at 90°C for 90 sec resulted in the lowest lycopene retention (67%).

In a separate investigation**, Jafari *et al.* (2017b)** examined the enhancement of heat transfer through the use of alumina nanoparticles. They focused on three distinct variables: temperature (70, 80, and 90 °C), concentration of alumina nanoparticles (0,

2, and 4 %), and time (30, 60, and 90sec). Their study revealed that a nanofluid comprising four percent Al_2O_3 in water exhibited the highest overall heat transfer coefficients across all Reynolds numbers, surpassing the performance of both a 2% nanofluid and pure water (0% nanofluid). The incorporation of nanoparticles into the underlying heating fluid, water, resulted in a substantial 49% enhancement in the efficiency of the heat exchanger.

After reviewing and preliminary trials, the outcomes highlighted that optimal results for quality preservation were achieved at hot fluid temperatures of 75, 85, and 95°C. Similarly, time intervals of 20, 30, and 40 sec, along with nanofluid concentrations of 0, 2.5, and 5%, were identified as yielding the most favourable results.

3.4 Experimental Plan

Based on preliminary trials the current research work identified the independent, dependent parameters, and constant along with their respective levels that held significance for the process. These selections are outlined in Tables 3.4, 3.5, and 3.6 respectively. The study encompassed diverse combinations of hot fluid temperatures, varying time intervals, and nano fluid concentrations. This comprehensive experimental design encompassed all potential factors germane to the thermal processing of tomato juice.

Table 3.3: List of independent parameters

Independent Variables	**Levels**	**Coded and actual values**		
		-1	0	1
Hot fluid temperature (X1)	3	75	85	95
Processing Time(X2)	3	20	30	40
Nanoparticle concentration (X3)	3	0%	2.5%	5%

Table 3.4: List of constant parameters

Serial No.	**Constant parameters**	**Values**
1.	Flow rate of inner pipe (lpm)	10
2.	Flow rate of outer pipe (lpm)	15
3.	Tomato juice inlet temperature(°C)	30
4.	Length of the Heat Exchanger	3.5m

Table 3.5: List of dependent parameters

Dependent Variables	**References**
Lycopene content	**(Davis *et al*., 2003)**
Vitamin C	**(Jafari *et al*., 2017b)**
pH	**(Chavda *et al*., 2014)**
TSS	**(Chavda *et al*., 2014)**
Total Phenol content	**(Jafari *et al*., 2017b)**
Colour difference	**(Jafari *et al*., 2017b)**
LMTD	**(Kumar *et al*., 2021)**
Overall heat transfer coefficient	**(Salari and Jafari, 2020)**
Rate of heat transfer (Q)	**Han *et al*., (2017)**
Nusselt number (Inner pipe Nu_i)	**Tiwari *et al*., (2013)**
Nusselt number (Outer pipe Nu_o)	**Anoop *et al*., (2013)**
Effectiveness (E)	**Said *et al*., (2019)**

3.5 Experimental Design

The present research study, the Box-Behnken design (BBD) was employed, leveraging insights from preliminary trials to establish the experimental framework. BBD falls under the category of second-order designs that are either rotatable or nearly rotatable, and it is rooted in three-level incomplete factorial designs. This approach aids in identifying strategic points for arranging three-level factorial combinations, thereby facilitating efficient estimation of the mathematical model's first and second-order coefficients. BBD is a type of Response surface methodoly (RSM). The total number of experiments conducted was 17 with 5 centre points, as outlined in **Table 3.6**. The **Eq 3.1** defines the required number of experiments (N) for developing the BBD.

$$N= 2k(k-1)+Co \quad \textbf{…(3.1)}$$

Where,

- N= Total numbers of experiments
- k= Number of Factors
- Co= Number of central points

The optimization process of this methodology involves investigating the outcomes of systematically planned combinations, estimating the coefficients through fitting them into the most suitable mathematical model given the experimental conditions, predicting the outcomes based on the fitted model, and subsequently assessing the adequacy of the model. The Box-Behnken design (BBD) stands as the prevalent approach within Response Surface Methodology (RSM) for various experimental setups **(Thakur *et al*., 2017)**. In this current investigation, the BBD was employed to design and analyze all experiments, encompassing three independent variables each with three levels indicated as -1, 0, and +1. This design facilitates the prediction of responses at intermediate levels not specifically experimented upon. Within this study, a three-level Box-Behnken design was utilized, allowing for the determination of optimal conditions through a minimal number of experiments in comparison to alternative designs.

Each Box-Behnken design (BBD) model in this study comprised a total of 17 experiments, with five experimental runs carried out at the central point, as outlined in **Table 3.6**. An analysis of variance was executed to evaluate the absence of fit and to ascertain the significance of the linear, interaction, and quadratic impacts of the independent variables on the dependent variable. Subsequently, a second-order regression model, represented by **Eq 3.2**, was formulated for each response to delineate the connection between the dependent and independent variables. The adequacy of each model's fit was assessed to ensure its appropriateness.

$$Y = \beta 0 + \sum_{i=1}^{n} \beta_i X_{i+} \sum_{i=1}^{n-1} \sum_{j=i+1}^{n} \beta_{ii} X_i X_{j+} \sum_{i=1}^{n} \beta_{ii} X_i^2 \quad \textbf{... (3.2)}$$

Where,

- Y is response variable, is model intercept;
- X_i and X_j are the independent variables, and
- n is the number of tested variable

Table 3.6: Experimental design using Response Surface Methodology (Box-Behnken design)

Experiment No.	Coded value			Actual value		
	X1	X2	X3	Hot fluid temperature (X1,°C)	Time(X_2, sec)	Nanoparticle concentration (X3, %)
1	-1	-1	0	75	20	2.5
2	1	-1	0	95	20	2.5
3	-1	1	0	75	40	2.5
4	1	1	0	95	40	2.5
5	-1	0	-1	75	30	0
6	1	0	-1	95	30	0
7	-1	0	1	75	30	5
8	1	0	1	95	30	5
9	0	-1	-1	85	20	0
10	0	1	-1	85	40	0
11	0	-1	1	85	20	5
12	0	1	1	85	40	5
13	0	0	0	85	30	2.5
14	0	0	0	85	30	2.5
15	0	0	0	85	30	2.5
16	0	0	0	85	30	2.5
17	0	0	0	85	30	2.5

3.6 Experimental Methodology

The project was conducted in five distinct phases. The initial phase involved preparation of tomato juice and nanofluid followed by the thermal processing of the tomato juice. The subsequent phase encompassed, examining the thermophysical properties of tomato juice and nanofluid followed by the third phase which entailed the evaluation of quality parameters for the tomato juice. The final phase was dedicated to the thermal analysis of these parameters. The comprehensive procedure

to execute the experiments is detailed below. The complete methodology of the experimental work is shown in **Fig 3.3.**

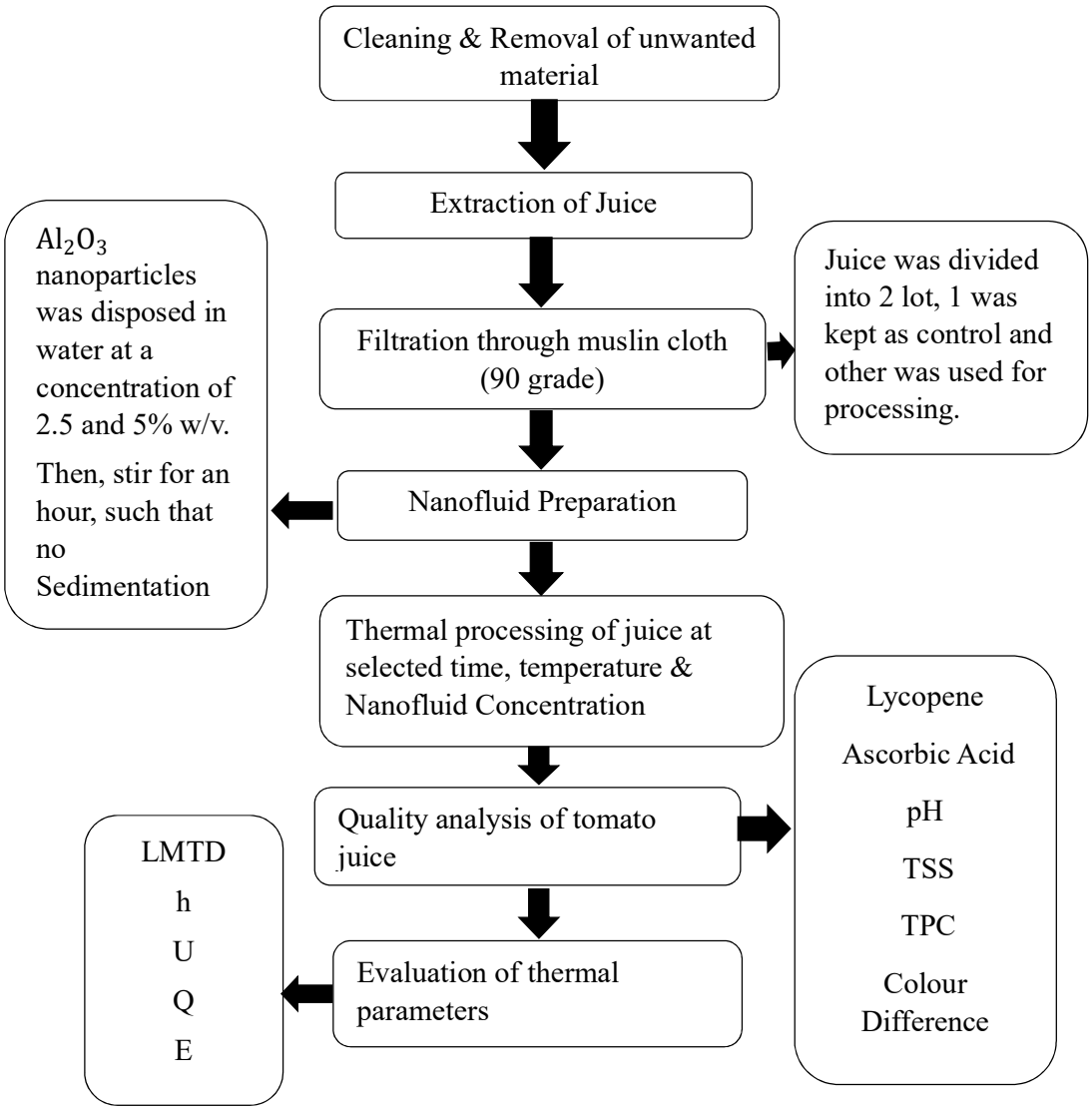

Fig: 3.3: Flow chart describing the experimental plan

3.6.1 Preparation of tomato juice

To perform heat treatment on tomato juice, a substantial quantity of Pant T-3 variety tomatoes was procured from the local market near Pantnagar. This selection was made to ensure uniform quality throughout the experimentation. The harvested tomatoes underwent a meticulous cleaning and sorting procedure to remove any foreign particles, dust, or impurities. Following this, the juice was extracted from the tomatoes using a Panasonic electric juicer mixer. To maintain uniform particle size,

the extracted juice was filtered through a muslin cloth with a fineness grading of 90. The obtained tomato juice was separated into two portions. The first batch served as the control group, designated for quality assessment and thermal analysis. Simultaneously, the second batch underwent thermal processing based on the predetermined independent parameters.

3.6.2 Nanofluid preparation

High-purity aluminium oxide nanoparticles (99% purity) was obtained from Shilpent, Shilpa Enterprises located in Delhi. These nanoparticles was dispersed in deionized distilled water at different volume concentrations of 0, 2.5, and 5% w/v. The dispersion process involves thorough stirring for one hour using a heater-stirrer set at 1500 rpm. This stirring is essential to ensure the stability of the nanofluids, as mentioned by **(Jafari *et al.*, 2017b)**. After an hour there was no sedimentation observed. The alumina nanoparticles was utilized in the heat exchanger as part of the heating medium, without any direct contact between the nanofluids and the product

Table 3.7: Thermophysical properties of Alumina nanoparticle that was used in this research (Jafari *et al.*, 2017a)

Properties	**Description**
Average particle diameter (nm)	20
Density (kg m-3)	3890
Heat capacity (J kg-1 K -1)	880
Thermal conductivity (W m-1 K -1)	36
Base fluid	Water

3.6.3 Thermal processing of tomato juice

Following the preparation of both tomato juice and nanofluid, the process of thermally treating the tomato juice commenced within a double pipe heat exchanger. This thermal processing occurred in a counter flow direction and encompassed varying temperature settings of 75, 85, and 95 °C, as well as distinct time durations of 20, 30, and 40 sec, coupled with different nanofluid concentrations of 0, 2.5, and 5%. The rationale behind selecting the counter flow direction was to enhance heat transfer efficacy compared to the parallel flow configuration.

The procedure involved introducing the tomato juice into the cold fluid tank, while the nanofluid was placed within the hot fluid tank at different concentrations determined by weight-to-volume ratios. Subsequently, the hot water reservoir was heated using a 2-kW heater integrated within it. Insulation with nitrile sheets was employed to counteract heat loss within the double pipe heat exchanger. In this arrangement, the hot fluid circulated through the outer annulus pipe, while the cold fluid flowed within the inner pipe. Once the desired temperature was achieved, the thermal processing commenced. Measurements were taken at various parameter combinations derived from the design expert software. Throughout the procedure, temperature measurements were captured utilizing J and K type thermocouples, while time measurements were acquired through the use of a stopwatch. Upon the completion of the thermal process, the treated juice from different experiments was securely sealed in glass bottles, paving the way for subsequent quality analyses**.** After thermal treatment of tomato juice the pictures has been taken and shown in **Fig 3.4.**

Fig 3.4: Processed tomato juice

3.6.4 Thermophysical properties of tomato

3.6.4.1 Thermal conductivity (k)

Thermal conductivity is a physical property that measures how effectively a material can conduct heat. It quantifies the rate at which heat is transferred through a material due to a temperature difference across it. It indicates how easily heat can flow through a substance. Materials with higher thermal conductivity values are better

conductors of heat, allowing heat to move more quickly through them. Metals, for example, typically have high thermal conductivity, while materials like insulators have lower thermal conductivity values, meaning they are less efficient at conducting heat.

The thermal conductivity of tomatoes typically ranges from approximately 0.3 W/(m·K) at 25°C and 0.5 W/(m·K)at 50°C **(Bhattacharyya *et al*., 1979)**. The other values of thermal conductivity are calculated using interpolation methods. This value indicates how well tomatoes can conduct heat.

3.6.4.2 Specific heat (C_p)

Specific heat, also known as specific heat capacity, is a physical property that quantifies the amount of heat energy required to raise the temperature of a unit mass of a substance by a certain amount (usually by one degree Celsius or one Kelvin). The specific heat of tomato is approximately 0.92 to 1.05 J/g°C within a temperature range of 20 to 30°C **(Bhattacharyya *et al*., 1979).**

3.6.4.3 Density (ρ)

Density is a physical property that quantifies how much mass is contained within a given volume of a substance. In other words, it measures how compact the particles of a material are within a specific space. The density of tomato juice is typically around 1020 to 1060 kg/m³ at 25-30°C. The density of tomato juice decreases when the temperature increases **(Colle *et al*., 2010)**.

3.6.5 Rheological properties of tomato

3.6.5.1 Viscosity (μ)

Viscosity is a measure of a fluid's resistance to flow. Viscosity of tomato juice has been measured by rotational viscometer at different temperature. It describes how easily a fluid can be deformed or how much it resists being moved. The viscosity of tomato juice at this temperature might be in the range of approximately 2 to 10 centipoise (cP) **(Colle *et al*., 2010).**

3.6.6 Thermophysical properties of nanofluid

3.6.6.1 Thermal conductivity (k)

Many studies have attempted to predict variations in the thermal conductivity of nanofluids as temperature changes. Various factors, such as concentration, particle

morphology, size, and distribution, can potentially influence this property. The alterations in the thermal conductivity of nanofluids containing alumina and water as base components were computed following the methodology outlined by **(Nguyen *et al.*, 2005).**

$$K_{nf}=k_w\frac{(kp+2kw+2conc(kp-kw)}{(kp+2kw-con\ (kp-\quad))} \qquad \textbf{... (3.3)}$$

Where,

- k_{nf} is the thermal conductivity of nanofluid (W/m.K)
- k_W is the thermal conductivity of water (W/m.K)
- k_p is the thermal conductivity of nanoparticle (W/m.K)

3.6.6.2 Specific heat (C_p)

The specific heat capacity of alumina-water nanofluid can be influenced by factors such as the concentration of nanoparticles, particle size, and temperature. On average, the specific heat capacity of alumina-water nanofluids might range from approximately 2.2 to 2.7 J/g°C. Specific heat capacity$(C_P)_{nf}$ of alumina water nanofluid were calculated according to the empirical equations **(Pak & Cho, 1998).**

$$(C_p)_{nf} = \frac{(1-\varphi)P_f\,(C_p)_f+\varphi P_p\,(C_p)_p}{P_{nf}} \qquad \textbf{.... (3.4)}$$

Where,

- φ is the volume concentration of nanoparticle water mixture
- $(C_p)_{nf}$ is the specific heat of nanofluid
- $(C_p)_f$ is the specific heat of basefluid
- P_f is the density of base fluid

3.6.6.3 Density (ρ)

The density of alumina-water nanofluid can be influenced by factors such as nanoparticle concentration, particle size, and temperature. Generally, the density of alumina-water nanofluids might range from around 1000 to 1100 kg/m³. Density of alumina water nanofluid were calculated according to the empirical equations **(Pak & Cho, 1998).**

$$\rho_{nf} = (1 - \varphi)\rho_f + \varphi\rho_p \quad \text{.... (3.5)}$$

Where,

- P_f is the density of base fluid
- ρ_{nf} is the density of nanofluid
- ρ_p is the density of nanoparticle

3.6.7 Rheological properties of nanofluid

3.6.7.1 Viscosity (μ)

The viscosity of alumina-water nanofluids might range from approximately 2 to 10 centipoise (cP). Einstein equation for determining viscosity (μ_{nf}) of nanofluids was represented by **(Pak & Cho, 1998).**

$$\mu_{nf} = \mu_f(1 + 2.5\varphi) \quad \text{... (3.6)}$$

Where,

- μ_{nf} is the viscosity of nanofluid
- μ_f is the viscosity of base fluid

3.6.8 Quality analysis of treated tomato juice

3.6.8.1 Lycopene determination

Dark bottles were used to contain a mixture consisting of 5 mL of 95% ethanol, 5 mL of butylated hydroxytoluene in acetone (0.05% w/v), 10 mL of hexane, and approximately 0.6 g of tomato juice. The contents were stirred for 15 minutes using a magnetic stirrer at 1500 rpm. Subsequently, 3 mL of deionized water was added to each bottle, and the bottles were shaken for an additional 5 minutes. The upper hexane layer of each sample, along with a blank sample of hexane, was analyzed using a UV-Vis spectrophotometer with a double beam (LI- 2904, LASANY) at a wavelength of 503 nm. The lycopene content will be determined using the following equation **(Davis *et al*., 2003).**

$$\text{Lycopene (mg/kg juice)} = \frac{\mathbf{A503\ X\ 31{\cdot}2}}{\boldsymbol{gmjuice}} \quad \text{...(3.7)}$$

Lycopene retention will be calculated using the **Eq 3.8**

Lycopene Retention (%) = $\frac{\boldsymbol{mg\ lycopene/kg\ juice\ after\ treatment}}{\textbf{mg lycopene/ kg juice before treatment}}$ X100 …**(3.8)**

3.6.8.2 Ascorbic Acid determination

The vitamin C content (mg per 100 g) in the samples was determined using the indophenolmethod. The titrant solution was prepared by dissolving 50 mg of 2,6-dichloroindophenol Na salt and 42 mg of sodium bicarbonate in 50 mL of water, which was then diluted with 200 mL of distilled water. The extracting solution was prepared by mixing 15 g of metaphosphoric acid and 40 mL of acetic acid, which was also diluted with 500 mL of distilled water. Both solutions were stored in dark bottles at 4°C. Subsequently, 100 mL of watermelon juice was mixed with 100 mL of the extracting solution. The resulting mixture was titrated with the titrant solution until a bright pink color persisted for at least 5 seconds.

The retention of vitamin C was calculated using a **Eq (3.9) (Jafari *et al.*, 2017b)**.

Vitamin C Retention (%) = $\frac{\boldsymbol{mg\ ascorbic\ acid/kg\ juice\ after\ treatment}}{\textbf{mg }\boldsymbol{ascorbic\ acid}\textbf{/ kg juice before treatment}}$ X 100 …**(3.9)**

3.6.8.3 pH determination

At room temperature, pH measurements were conducted using a digital pH meter (Citizen ID50-01). Prior to the measurements, the pH meter was calibrated using pH=7 and pH=4 buffers. For each sample, three distinct points were chosen, and the average values obtained from these points were recorded **(Jafari *et al.*, 2017b).**

3.6.8.4 Color difference

The tomato juice samples were subjected to color analysis using the separation method in Photoshop CS5 version 12.0. The color parameters L* (brightness), a* (red-green), and b* (yellow-blue) were determined based on the photos taken using an Apple iPhone 14 with a 12-megapixel digital camera. To quantify the overall color difference between each sample and a reference sample, the total color difference (ΔE*) was computed using a **Eq (3.10) (Pathare *et al.*, 2013).**

$$\Delta E* = [(\Delta L*^2) - (\Delta a*^2) + (\Delta b*^2)]^{0.5} \quad \textbf{(3.10)}$$

$$\Delta L^* = (L_1^* - L_0^*) \quad \textbf{(3.11)}$$

$$\Delta a^* = (a_1^* - a_0^*) \quad \textbf{(3.12)}$$

$$\Delta b^* = (b_1^* - b_0^*) \quad \ldots \textbf{(3.13)}$$

where, subscripts '0' and '1' depicted color values for the raw and processed tomato juices, respectively.

Given that ΔL*, Δa*, and Δb* can exhibit both positive and negative values, it's important to note that the overall color difference (ΔE) is consistently positive. ΔL* represents variations in lightness, with positive values indicating increased lightness and negative values signifying darkness. Similarly, Δa* denotes shifts towards redness when positive and towards greenness when negative, while Δb* signifies changes towards yellowness when positive and towards blueness when negative.

3.6.8.5 Total Phenolic Content (TPC)

To begin the process, a 2 g sample of juice was crushed and combined with 10 ml of 80% ethanol. Following this, the resultant homogenate underwent centrifugation at 10000 rpm for 20 minutes at a temperature of 4°C. The supernatant obtained from this step was employed for the total phenols assay.

Next, a mixture was prepared by taking 2.8 ml of distilled water, 100 µl of the sample, and 0.5 ml of 2 N Folin-Ciocalteau reagent. After a 3-minute interval, 2 ml of 20% Na_2CO_3 solution was introduced into the mixture. This solution was left for a period of time until it assumed a blue-black coloration. Subsequently, the absorbance was gauged at 760 nm utilizing a 1 cm cuvette in a Perkin-Elmer UV-VIS Lambda 25 spectrophotometer. To establish a standard calibration curve, Gallic acid within a range of 0 to 800 mg/l was utilized. The quantification of total phenolic content was conveyed as micrograms of Gallic acid equivalent per gram of fresh weight (mg/100 g FW) **(Jafari *et al*., 2017b).**

$$\text{Total phenol content} = \frac{OD760 * Volume\ made\ up(wit\ \ 80\%\ ethan\ \ ) * 100}{Aliquot\ taken * weigh\ \ of\ sample * 1000} \quad \textbf{...(3.14)}$$

3.6.8.6 Total soluble solids (TSS)

TSS measures the concentration of all soluble solids, including sugars, organic acids, and other dissolved compounds.

Total Soluble Solids (TSS) index of tomato juice sample will measure by digital refractometer at 25℃ and expressed in terms of °brix.

3.6.9 Thermal analysis of the tomato juice

3.6.9.1 Logarithmic Mean Temperature Difference (LMTD)

The Log Mean Temperature Difference (LMTD) serves as a factor in the assessment

and planning of double pipe heat exchangers. It gauges the temperature gradient facilitating heat transfer between the hot and cold fluids. This metric considers the temperature variations at both the inlet and outlet points of the hot and cold fluids.

The formula to calculate the LMTD for a double pipe heat exchanger depends on the flow configuration:

$$(\Delta T)_{LMTD} = (\Delta T1 - \Delta T2) / \ln(\Delta T1 / \Delta T2) \text{ (Albadr } \textit{et al.}\text{, 2013)} \quad \text{…(3.15)}$$

For counter flow (both fluids flow in opposite directions):

$$\Delta T1 = Th_i - Tc_o$$

$$\Delta T2 = Th_o - Tc_i \text{ (Reddy } \textit{et al.}\text{, 2017)} \quad \text{…(3.16)}$$

Where,

- Th_i is the inlet temperature of hot fluid
- Th_o is the outlet temperature of hot fluid
- Tc_i is the inlet temperature of cold fluid
- Tc_o is the outlet temperature of cold fluid

3.6.9.2 Overall heat transfer coefficient

The overall heat transfer coefficient (U) in a dual-pipe heat exchanger gauges the efficiency of thermal exchange between the hot and cold fluids within the system. It measures the pace of heat transfer per unit surface area of the exchanger, considering the temperature contrast between the two fluids. The comprehensive heat transfer coefficient encompasses the distinct heat transfer coefficients of the fluids, the thermal resistance of the pipe wall, and any extra impediments stemming from fouling or other elements that could influence heat transfer effectiveness.

For inner pipe,

$$U_i = Q_c / A_i \times \Delta T_{lmtd} \text{ (Kumar } \textit{et al.}\text{, 2018)} \quad \text{… (3.17)}$$

For annulus pipe,

$$Uo = Qh / Ao \times \Delta T_{lmtd} \quad \text{… (3.18)}$$

3.6.9.3 Nusselt Number

The Nusselt number (Nu) is a dimensionless value utilized to describe the convective heat transfer in the movement of fluid. The Nu number can be derived through its conventional definition:

For inner pipe:- $Nu_i = (D_i \times h_i)/ k_i$ …**(3.19)**

For annulus pipe:- $Nu_o = (D_h \times h_o)/ k_o$; **(Mozafarie and Javaherdeh, 2019)**

Where:

- h is the convective heat transfer coefficient (in W/(m²·K))
- D is the characteristic length or hydraulic diameter of the pipe (in m)
- k is the thermal conductivity of the fluid (in W/(m·K))

3.6.9.4 Heat Transfer Coefficient

For Inner Pipe

The Dittus-Boelter equation is commonly used for turbulent flow conditions and is expressed as:

hi = 0.023 * (Rei^0.8) * (Pri^0.4) * (ki/ Di)**(Kumar *et al.*, 2018)** … **(3.20)**

where:

- h_i is the heat transfer coefficient (in W/m²·K)
- Re_i is the Reynolds number (dimensionless)
- Pr_i is the Prandtl number (dimensionless)
- k_i is the thermal conductivity of the fluid (in W/m·K)
- D_i is the diameter of the inner pipe (in meters)

For Outer Pipe

$h_o = 0.023 \times Re^{0.8} \times Pr^{0.4} \times (1 + 0.45f_o/D_h)$ **(Kumar *et al.*, 2018)** … **(3.21)**

where:

- h_o is the heat transfer coefficient of annulus (in W/m²·K)
- Re_o is the Reynolds number (dimensionless)
- Pr_o is the Prandtl number (dimensionless)
- f_o is the friction factor (dimensionless)
- D_h is the hydraulic diameter of the annulus pipe (in meters)

3.6.9.5 Effectiveness

The effectiveness of a dual-pipe heat exchanger is a metric that assesses its capability to facilitate heat transfer between the hot and cold fluids.

Number of transfer units, $NTU = (U \times A)/ C_{min}$

$NTU = Q/ ((\Delta T)_{LMTD} \times C_{min})$ …**(3.22)**

Heat capacity of tube side fluid, $C_c = \dot{m}h \times Cp_i$

Heat capacity of annulus side fluid, $C_h = \dot{m}c \times Cp_o$

where C_{min} is lesser than as compared to C_c and C_h.

The efficiency of a dual-pipe heat exchanger quantifies its ability to transfer heat between the hot and cold fluids.

$$\varepsilon = 1 - \exp(-NTU\,(1 - Z))/\,[1 - Z\exp(-NTU\,(1 - Z))]$$ **(Kumar *et al.*, 2018)**

…**(3.23)**

where, $Z = C_{min}/\,C_{max}$

The effectiveness of a double pipe heat exchanger varies between 0 and 1. A value of 1 signifies that the heat exchanger has the capacity to transfer all the accessible heat from the hot fluid to the cold fluid, achieving optimal efficiency in heat transfer.

3.7 Statistical Analysis of Model

3.7.1 Data modelling

The formulation of the model was achieved through the application of response surface methodology (RSM), facilitated by the utilization of design expert software version 13.1.0.1. The complete second-order model, as presented in **Eq (3.2)**, was incorporated to analyse the dataset. To assess the validity of the model, indicators such as the coefficient of determination (R-squared) and the F-test (Fisher's) were employed.

3.7.2 Adequacy of model

The solution for **Eq (3.2)** was achieved through a statistical method known as the method of least squares (MLS). This technique, a form of multiple regression, is employed to establish a mathematical model that best fits a collection of experimental data by minimizing residuals. The outcomes of the regression analysis encompassed various metrics, including ANOVA (analysis of variance), regression coefficients, associated statistical values, standard deviation, coefficient of determination (R-squared), and assessment of lack of fit. These outcomes collectively determined the suitability of the predictive model and elucidated the influence of independent parameters on the response. The utilization of the MLS technique facilitates the

identification of the model that aligns most closely with the observed data, enhancing the understanding of relationships between variables.

3.7.2.1 Test for significance of response regression model

The examination was conducted in the form of an analysis of variance (ANOVA), involving the computation of the F-value situated between the mean square of regression and the mean square error. Referred to as the variance ratio, the F-value depicts the proportion of variance attributed to the impact of a factor (in this scenario, the model) against the variance attributed to the error term. This ratio serves as a metric to evaluate the model's significance in relation to the variance encompassing all terms contained within the error term. This assessment is performed at the specified significance levels, notably the 1% and 5% thresholds.

3.7.2.2 Test for significance on individual model coefficient

Furthermore, thorough evaluations were conducted to establish the model's capability in representing the experimental data. These evaluations encompassed diverse coefficient of determination (R-squared) calculations. These R-squared coefficients lie within the range of 0 to 1, where 1 signifies an enhanced alignment of the model with the data. These coefficients were utilized to explore how differences in one variable could elucidate variations in another variable. A heightened coefficient indicated a more favorable degree of alignment in the observations.

In tandem with the above, an assessment of the model's adequacy was undertaken through the scrutiny of residuals. These residuals constitute the distinctions between the respective observed responses and the projected responses. This assessment involved the utilization of normal probability plots for the residuals and plots depicting the residuals vis-à-vis the anticipated responses. For a satisfactory model, the points on the normal probability plots of the residuals are expected to conform to a linear pattern, signifying a well-fitted model.

3.7.2.3 Test for lack of it

Since five measurements were conducted at the central point while analysing responses, an evaluation termed the lack of fit test appraises the significance of duplicate errors vis-à-vis errors associated with the model. This evaluation segregates

the sum of squares for residuals or errors into two components: one arising from pure error owing to repeated measurements and the other arising from lack of fit, which involves the ratio of the lack of fit mean square to the pure error mean square. Subsequently, the F-test is employed to ascertain whether the lack of fit holds statistical significance at the specified probability level.

3.7.3 Optimization of process parameters

Optimization pertains to enhancing the efficiency of a system, process, or product to achieve the utmost advantage from it. Among the pertinent multivariate techniques utilized in analytical optimization is response surface methodology (RSM). This methodology proves valuable when numerous responses of interest are influenced by a designated set of variables. In this current investigation, the focus of optimization centered on the process parameters of thermally treated tomato juice. To accomplish this, a comprehensive total of 12 responses were taken into account. These encompassed factors such as lycopene content, ascorbic acid levels, pH, color variation, Total Soluble Solids (TSS), Total Phenolic Content (TPC), Log Mean Temperature Difference (LMTD), overall heat transfer coefficient, heat transfer rate, Nusselt numbers for both the inner and outer pipes, as well as effectiveness.

3.7.4 Data interpretation

The impact of different parameters on various responses was assessed through the interpretation of the developed model. The significance probability of the predictor's coefficient indicates the degree of influence of the predictor on the response. The sign and magnitude of the coefficient elucidate the character of the effect, where a negative sign at the linear level signifies a decrease in response as the predictor's level rises. Conversely, a positive sign implies an elevation in the response.

Significant negative interactions imply that one predictor's level can increase while the other decreases while keeping response values constant. Positive interactions suggest that the response is minimized at the central point and increases when both variables deviate from this central point. A positive interaction involving a quadratic term indicates a response minimum at the parameter's central value, escalating with deviations from this point. Conversely, a negative coefficient of a

quadratic term indicates a response maximum at the central value, escalating with deviations from this central value.

To visualize this, response surface plots were generated both at the linear level and for interactions among the three independent variables, with the remaining variables' values held constant.

3.8 Validation of Regression Model

In the context of Response Surface Methodology (RSM), it's essential for the regression models formulated to offer a reliable approximation that can be applied to real-world systems. Validation of these models predominantly involves two approaches: graphical and numerical methods. The graphical method evaluates the residuals' characteristics (discrepancies between observed values and their fitted counterparts) within the model. On the other hand, the numerical method leverages metrics such as the coefficient of determination (R^2) as well as the (R^2_{adj}) to validate the model.

Results & Discussion

Chapter 4 RESULTS AND DISCUSSION

An extensive investigation was carried out to examine how the quality of tomato juice is influenced by thermal treatment. The objective behind subjecting tomato juice to thermal treatment was to preserve its quality more effectively. This treatment process was executed using a double pipe heat exchanger, wherein the conventional hot fluid was substituted with a nanofluid to enhance heat transfer efficiency. Consequently, in addition to assessing the juice's quality, we also investigated the impact of the nanofluid on the heat transfer process. The study was divided into three phases: initially, an assessment of the quality characteristics of the tomato juice was conducted, followed by an analysis of the thermal processes involved, and finally, an optimization of the process parameters to assess the impact of thermal treatment on the tomato juice's quality. Various levels for the independent variables were established based on preliminary experiments. During these trials, it was noted that the temperature of the hot fluid, the duration of treatment, and the concentration of nanofluid all played a significant role in affecting the quality of the tomato juice.

The initial stage focuses on evaluating the quality of tomato juice after undergoing thermal treatment. All three independent variables have a notable impact on the tomato juice's quality. The quality metrics under examination encompass lycopene retention, ascorbic acid retention, pH, total soluble solids, total phenolic content, and color difference. The outcomes are detailed in the subsequent section of this chapter.

The second stage involves analyzing the thermal aspects of the processed juice. Likewise, there is a significant influence from all three independent variables: the temperature of the hot fluid (75, 85, 95 degrees Celsius), the duration (20, 30, 40 seconds), and the concentration of nanofluid (0, 2.5, 5%) on the outcomes. The responses being investigated for the impact of these independent variables encompass the Log Mean Temperature Difference (LMTD), the overall heat transfer coefficient, the rate of heat transfer, Nusselt number of inner pipe, Nusselt number of outer pipe and effectiveness. The outcomes for these specific responses are presented in **Table 4.1**.

Table 4.1 Experimental results for retaining the better quality of thermally treated tomato juice

S. No.	Independent Variables			Dependent Variables											
	X_1	X_2	X_3	Lycopene (mg/kg)	Ascorbic Acid (mg/100ml)	pH	TSS	TPC	Δ E	LMTD	U	Q	Nu_i	Nu_o	E
	(°C)	(sec)	(%)				(°brix)	(µg/g)		(°C)	W/(m2•K)	(W)			
1	75	40	2.5	40	259.08	4.6	5.56	290.02	**4**	33	3500	22001	106	75	0.561
2	85	30	2.5	36	253.14	4.6	5.49	285.04	4.8	34	3200	21400	107	76	0.62
3	85	20	0	35	237.32	4.7	5.49	263.12	5.5	30	2500	19000	105	70	0.48
4	95	30	5	33	233.36	4.7	5.46	259.13	6	**42****	**3854.97****	**26900****	**111****	**77****	**0.656****
5	85	20	5	38	257.1	4.6	5.48	287.04	4.5	33	2400	23000*	106	77	0.6
6	75	30	0	36	247.09	4.5	5.68	271.09	5	**28***	**2250***	**18000***	**104***	**70***	**0.48***
7	85	40	5	37	255.1	4.6	**5.47***	286.24	4.8	37	3765.5	23000	107	75	0.63
8	85	30	2.5	36	253.146	4.6	5.55	281.11	4.8	34	3150.2	21300	107	76	0.57
9	75	20	2.5	41	261.057	4.6	**5.69****	291.02	4.8	32	2650	22000	106	74	0.61
10	85	30	2.5	36	251.16	4.6	5.51	281.11	4.9	34	3298	21100	107	76	0.59
11	95	20	2.5	35	244.44	4.6	5.54	267.11	5	39	3200	25121	109	77	0.61
12	85	30	2.5	36	249.19	4.6	5.52	279.06	4.7	34	3250	21500	107	76	0.57
13	85	30	2.5	36	249.19	4.6	5.53	275.08	4.8	34	2990.7	21000	107	76	0.58
14	95	30	0	**29***	**221.358***	**4.7****	5.53	**293.255****	**7.2****	37	3200	21500	107	72	0.41
15	95	40	2.5	32	227.43	4.7	5.57	255.14	7	41	3674	26502	108	77	0.43
16	75	30	5	**42****	**262.14****	**4.55***	5.45	**247.542***	**3.6***	35	3250	22000	106	74	0.58
17	85	40	0	30	225.06	4.7	5.67	251.16	6	29	3500	19200	106	73	0.56

*- Minimum, **- Maximum

The final phase involves optimizing the settings of the independent variables: the temperature of the hot fluid (75, 85, 95 degrees Celsius), the duration (20, 30, 40 seconds), and the nanofluid concentration (0, 2.5, 5%) to ensure the preservation of superior tomato juice quality, while also leveraging the nanofluid to improve heat transfer rate. Numerical optimization was conducted using the statistical software Design Expert 13.0.

4.1 Numerical analysis and effect of nanofluid aided thermal treatment on quality as well as thermal parameters of tomato juice

4.1.1 Lycopene retention of tomato juice

The outcomes from the experimentation concerning lycopene retention in tomato juice are detailed in **Table 4.1**, revealing a lycopene retention ranging between 29 and 42(mg/kg). The highest recorded value was in Experiment no. 16, characterized by a hot fluid temperature of 75°C, a duration of 30 seconds, and a nanofluid concentration of 5%. Conversely, the lowest value emerged from Experiment no. 14, involving the independent variables of 95°C hot fluid temperature, 30 seconds duration, and 0% nanofluid concentration. Interestingly, these results mirror those discovered by **Jafari *et al.*, (2017a),** who investigated the influence of nanofluid-aided thermal processing on tomato juice quality parameters.

An examination of the experimental data was performed to ascertain the influence of independent variables on lycopene retention. The model constructed for lycopene retention exhibited statistical significance at a significance level of 1%. As presented in **Table 4.2**, all three independent variables demonstrated a substantial impact ($p<0.01$) on lycopene content through linear terms, while interaction effects were discerned for all interaction parameters at the 1% significance level. Additionally, quadratic effects manifested significance at the 5% level for hot fluid temperature and at the 1% level for time. The statistical evaluation indicated the adequacy and significant fit of the proposed model. Regression analysis was conducted on the data to align with the response function, specifically the lycopene retention of tomato juice. Higher values for both R^2 and R^2_{adj} indicated a strong correlation between the experimental and predicted values, thus confirming the precision and consistency of the model detailed in **Table 4.2**. Subsequently, a second-order polynomial **Eq (4.1)** was established, presenting an empirical connection

between lycopene content and the input variables in their actual form. The anticipated regression equation for lycopene content is provided below as **Eq 4.1.**

Table 4.2: Numerical analysis of lycopene retention

Source	SS	df	MS	F-value	p-value
Model	156.90	9	17.43	137.12	< 0.0001**
X_1	0.9800	1	0.9800	7.71	0.0274*
X_2	1.80	1	1.80	14.20	0.0070**
X_3	6.48	1	6.48	50.97	0.0002**
X_1 X_2	10.56	1	10.56	83.08	< 0.0001**
X_1X_3	28.62	1	28.62	225.12	< 0.0001**
X_2X_3	36.60	1	36.60	287.88	< 0.0001**
X_1^2	1.33	1	1.33	10.48	0.0143*
X_2^2	70.35	1	70.35	553.30	< 0.0001**
X_3^2	0.3480	1	0.3480	2.74	0.1420
Residual	0.8900	7	0.1271		
Lack of Fit	0.7300	3	0.2433	6.08	0.0568
Pure Error	0.1600	4	0.0400		
Cor Total	157.79	16			
R^2	0.9944				
Adjusted R^2	0.9871				

**, * represents 1% and 5% level of significance respectively.

$$\text{Lycopene} = +33.40 - 0.3500X_1 + 0.4750X_2 + 0.9X_3 - 1.62X_1X_2 - 2.68\,X_2X_3 + 3.03\,X_1X_3 - 0.5625X_1^2 + 4.09\,X_2^2 + 0.2875\,X_3^2 \quad \ldots \textbf{(4.1)}$$

The equation encompasses terms that hold both significance and those that lack significance. Consequently, the nonsignificant terms were eliminated from the equation, resulting in its regeneration with only the significant terms retained. The resultant equation is as presented below:

$$\text{Lycopene} = +33.40 - 0.3500X_1 + 0.4750X_2 + 0.9X_3 - 1.62X_1X_2 + 2.68\,X_2X_3 - 3.03\,X_1X_3 - 0.5625X_1^2 + 4.09\,X_2^2 \quad \ldots \textbf{(4.2)}$$

The direction and magnitude of the coefficients in **Eq. 4.2** delineate the impact of the noteworthy independent parameters on lycopene retention. Positive effects are

observed for time (X_2) and nanofluid concentration (X_3) at the linear level, indicating that an increase in these parameters is associated with heightened lycopene retention. However, concerning the dependent parameter, hot fluid temperature (X_1), a negative effect is noted, implying that lycopene content diminishes as the hot fluid temperature rises. Negative coefficients for the combined effect of hot fluid temperature and time (X_1X_2) and the interaction between time and nanofluid concentration (X_2X_3) suggest a reduction in lycopene content when both these parameters are employed. Conversely, a positive impact is seen for the combined effect of time and nanofluid concentration (X_2X_3), suggesting lycopene content rises with elevated levels of both parameters. The negative influence of the squared term of hot fluid temperature ($X1^2$) at the quadratic level implies that lycopene content peaks at the midpoint of hot fluid temperature and declines as it deviates from this central value. Value of lycopene content in raw tomato is 44(mg/kg), and the maximum value obtained after thermal processing is 42(mg/kg), so we can say there is a retention of 95% of lycopene content at 75°C for 30 seconds at 5% of nanofluid concentration.

4.1.2 Ascorbic acid retention of tomato juice

Ascorbic acid, commonly recognized as vitamin C, is a vital water-soluble nutrient abundantly found in various fruits and vegetables, including tomato juice. This nutrient assumes a pivotal role in numerous biological processes and is renowned for its robust antioxidant attributes. Its presence in tomato juice imparts a range of health benefits to consumers. Beyond immune support, ascorbic acid plays an integral role in collagen synthesis—a fundamental protein vital for connective tissues, skin, blood vessels, and bones. The consumption of vitamin C-rich tomato juice consequently contributes to healthy skin, efficient wound healing, and overall tissue regeneration. Notably, vitamin C enhances the absorption of non-heme iron, prevalent in plant-based foods. By complementing iron-containing dietary components, it facilitates the body's more efficient iron uptake, aiding in maintaining optimal iron levels **(Jacob, 1990)**.

The outcomes obtained from the experiments regarding the ascorbic acid content in tomato juice are meticulously presented in **Table 4.1**, showcasing a variance spanning from 221.358 to 262.143(mg/100ml).

Table 4.3: Numerical analysis of ascorbic acid

Source	Sum of Squares	df	Mean Square	F-value	p-value
Model	1928.93	9	214.33	1612.54	< 0.0001**
X_1	50.14	1	50.14	377.24	< 0.0001**
X_2	61.05	1	61.05	459.34	< 0.0001**
X_3	1.29	1	1.29	9.73	0.0169*
$X_1 X_2$	219.04	1	219.04	1648.01	< 0.0001**
X_1X_3	716.85	1	716.85	5393.42	< 0.0001**
X_2X_3	150.06	1	150.06	1129.04	< 0.0001**
X_1^2	47.17	1	47.17	354.88	< 0.0001**
X_2^2	700.35	1	700.35	5269.28	< 0.0001**
X_3^2	1.90	1	1.90	14.31	0.1069
Residual	0.9304	7	0.1329		
Lack of Fit	0.1304	3	0.0435	0.2173	0.8799
Pure Error	0.8000	4	0.2000		
Cor Total	1929.86	16			
R^2	0.9995				
Adjusted R^2	0.9983				

**, * represents 1% and 5% level of significance respectively.

The highest recorded value emerged from Experiment no. 16, featuring specific conditions such as a hot fluid temperature of 75°C, a time duration of 30 seconds, and a nanofluid concentration of 5%. Conversely, the lowest recorded value was associated with Experiment no. 14, encompassing the combination of independent variables: 95°C hot fluid temperature, 30 seconds duration, and 0% nanofluid concentration. It is noteworthy that these findings parallel the conclusions drawn by **Jafari *et al.* (2017a)**, who investigated the influence of nanofluid-assisted thermal processing on various quality parameters of tomato juice, including ascorbic acid. Their results similarly indicated that the preservation of a higher quantity of ascorbic acid is achieved at a lower temperature of 75°C, a duration of 30 seconds, and a nanofluid concentration of 5%.

The analysis of the experimental data was systematically conducted to discern the impact of independent variables on the ascorbic acid content. The established model for ascorbic acid content exhibited noteworthy significance at a level of 1%. Upon scrutiny of **Table 4.3**, it is evident that both the hot fluid temperature (X_1) and time (X_2) independent variables significantly influenced ($p<0.01$) the ascorbic acid content in terms of linear factors. Meanwhile, the nanofluid concentration (X_3) exhibited a significant influence at a significance level of 5%. Moreover, interaction effects were apparent across all interaction parameters at the level of 1% significance. Notably, the quadratic effects surfaced with considerable significance at 1% for all independent parameters. The statistical assessment confirmed the suitability and significant alignment of the proposed model. Regression analysis was executed on the dataset to establish a correspondence with the response function, specifically the ascorbic acid content of tomato juice. Elevated values for both R^2 and R^2_{adj} underscored the proximity between the experimental and anticipated values, thus authenticating the precision and consistency of the model depicted in **Table 4.3**. Subsequently, a second-order polynomial **Eq (4.3)** was formulated, encapsulating an empirical correlation between the ascorbic acid content and the input variables in their factual representation. The projected regression equation for the ascorbic acid content is provided below as **Eq 4.3.**

$$\text{Ascorbic Acid} = +241.80 - 2.5X_1 + 2.76X_2 + 0.402X_3 - 7.4X_1X_2 - 13.39X_1X_3 + 6.12X_2X_3 - 3.35X_1^2 + 12.9X_2^2 - 0.672X_3^2 \quad \ldots \textbf{(4.3)}$$

The equation encompasses both terms of significance and those lacking significance. Hence, non-significant terms were eliminated, resulting in the reformation of the equation to encompass only the significant terms. The reconfigured equation is as presented below:

$$\text{Ascorbic Acid} = +241.80 - 2.5X_1 + 2.76X_2 + 0.402X_3 - 7.4X_1X_2 - 13.39X_1X_3 + 6.12X_2X_3 - 3.35X_1^2 + 12.9X_2^2 - 0.672X_3^2 \quad \ldots \textbf{(4.4)}$$

The direction and magnitude of the coefficients in **Eq 4.4** illustrate the influence of the significant independent parameters on ascorbic acid. Positive impacts are evident for time (X_2) and nanofluid concentration (X_3) at the linear level, indicating that heightened levels of these factors correlate with increased ascorbic

acid. Conversely, in the case of the dependent parameter, hot fluid temperature (X_1), a negative effect emerges, suggesting that as the hot fluid temperature increases, ascorbic acid decreases. Negative coefficients for the joint effect of hot fluid temperature and time (X_1X_2) and the interaction between temperature and nanofluid concentration (X_2X_3) imply a reduction in ascorbic acid content when both these factors are simultaneously adjusted. However, a favorable impact arises for the combined effect of time and nanofluid concentration (X_2X_3), indicating that higher levels of both parameters coincide with increased ascorbic acid content. The adverse effect of the squared term of hot fluid temperature (X_1^2) and nanofluid concentration (X_2^3) at the quadratic level signifies that ascorbic acid content reaches a maximum at the midpoint of hot fluid temperature and diminishes as it deviates from this central value. Moreover, the positive impact of the squared term of time (X_2^2) at the quadratic level suggests that ascorbic acid content attains its minimum at the midpoint of time and escalates as it deviates from this central point.

4.1.3 pH of tomato juice

The pH of tomato juice signifies its degree of acidity or alkalinity on the pH scale, which spans from 0 to 14. This scale quantifies the concentration of hydrogen ions within a solution, with lower values indicating higher acidity, higher values representing greater alkalinity, and a pH of 7 indicating neutrality. In the context of tomato juice, pH plays a multifaceted role. It significantly contributes to the flavor and taste of the juice, as the natural acids present in tomatoes, like citric and malic acids, determine its characteristic tanginess. The pH level influences how these acids are perceived by our taste receptors, shaping the overall taste experience **(Makroo *et al.*, 2017).**

The outcomes of the experiments pertaining to pH in tomato juice are presented in **Table 4.1**, showcasing a pH range from 4.55 to 4.7. The highest value was recorded in Experiment no. 14, characterized by conditions including a hot fluid temperature of 95°C, a duration of 30 seconds, and a nanofluid concentration of 0%. Conversely, the lowest value emerged from Experiment no. 16, featuring the combination of independent variables: 75°C hot fluid temperature, 30 seconds duration, and 5% nanofluid concentration.

Table 4.4: Numerical analysis for pH

Source	Sum of Squares	df	Mean Square	F-value	p-value
Model	0.0331	9	0.0037	245.50	< 0.0001**
X_1	0.0001	1	0.0001	3.33	0.1106
X_2	0.0003	1	0.0003	20.83	0.0026**
X_3	0.0015	1	0.0015	100.83	< 0.0001**
X_1 X_2	0.0030	1	0.0030	201.67	0.1451
X_1X_3	0.0110	1	0.0110	735.00	0.1501
X_2X_3	0.0000	1	0.0000	0.0000	1.0000
X_1^2	0.0047	1	0.0047	315.02	0.1401
X_2^2	0.0123	1	0.0123	818.53	< 0.0001**
X_3^2	0.0008	1	0.0008	55.02	0.0001**
Residual	0.0001	7	0.0002		
Lack of Fit	0.0000	3	8.333E-06	0.4167	0.7510
Pure Error	0.0001	4	0.0001		
Cor Total	0.0332	16			
R^2	0.9968				
Adjusted R^2	0.9928				

**, * represents 1% and 5% level of significance respectively.

These findings closely resemble the conclusions drawn by **Jafari *et al.* (2017a)**, who investigated the effects of nanofluid-assisted thermal processing on quality parameters of tomato juice. It is noteworthy that the impact of thermal processing on the pH of tomato juice is minimal, resulting in only slight changes. The outcomes indicate that the least pH value is attained at lower temperature conditions of 75°C, a duration of 30 seconds, and a nanofluid concentration of 5%. An analysis of the experimental data was executed to discern the influence of independent variables on pH. The established model for pH exhibited notable significance at a significance level of 1%. As depicted in **Table 4.4**, it is evident that both time (X_2) and nanofluid concentration (X_3) independent variables significantly impacted pH

through linear terms ($p<0.01$). The quadratic effect was notably observed for time (X_2) and nanofluid concentration (X_3) at the 1% significance level.

The statistical evaluation indicated that the proposed model was suitable and significantly aligned. Regression analysis was carried out on the dataset to effectively align with the response function, which in this case is the pH of tomato juice. Enhanced values of R^2 and R^2_{adj} underscored the proximity between the experimental and predicted outcomes, thereby confirming the precision and reliability of the model illustrated in **Table 4.4**. Subsequently, a second-order polynomial **Eq (4.5)** was formulated, encapsulating an empirical relationship that establishes a connection between lycopene content and the input variables in their real-world representation. The anticipated regression equation for pH is provided below as **Eq 4.5**.

$$pH= +4.62-0.35X_1- 0.0063X_2 -0.0137X_3+ 0.0275X_1X_2+ 0.0525X_1X_3+ 3.03X_2X_3- 0.0335X_1^2-0.054X_2^2-0.014X_3^2 \quad \ldots \textbf{(4.5)}$$

The equation encompasses terms of both significance and insignificance. Hence, non-significant terms were eliminated from the equation, resulting in its reformation to solely encompass the significant terms. The resulting equation is presented as follows:

$$pH= +4.62- 0.0063X_2- 0.0137X_3 - 0.054X_2^2 -0.014X_3^2 \quad \ldots \textbf{(4.6)}$$

The implications of both the sign and the magnitude of the coefficients in **Eq 4.6** shed light on the impact of the noteworthy independent variables on pH. The adverse influence on time (X_2) and nanofluid concentration (X_3) at the linear level indicates that pH exhibits a decline as these variables increase. On the other hand, there is no effect of interaction of independent variables on pH. The negative influence stemming from the squared terms of hot fluid temperature (X_1^2) and nanofluid concentration (X_3^2) at the quadratic level highlights that the pH reaches its pinnacle at the midpoint of hot fluid temperature and time. However, it decreases when diverging from this central value in either direction.

4.1.4 Total soluble solids (TSS)

Total Soluble Solids (TSS) in tomato juice denote the collective concentration of dissolved solids present within the juice, excluding any insoluble particles. This measurement encompasses sugars, organic acids, minerals, and other soluble constituents suspended in the liquid matrix. TSS plays a pivotal role in determining its

sweetness and overall flavor characteristics. The inclusion of sugars among the soluble components directly influences the perceived sweetness, contributing to the juice's overall taste profile **(Makroo *et al*., 2017).**

The outcomes obtained from the experiments pertaining to TSS content in tomato juice are displayed in **Table 4.1**, revealing a range of total soluble solids (TSS) content spanning from 5.47 to 5.69. The highest recorded TSS value emerged from Experiment no. 9, characterized by conditions including a hot fluid temperature of 75°C, a time duration of 20 seconds, and a nanofluid concentration of 2.5%. In contrast, the lowest value was associated with Experiment no. 7, featuring the amalgamation of independent variables: 85°C hot fluid temperature, 40 seconds duration, and a 5% nanofluid concentration. These observations underscore that optimal TSS content is preserved through lower temperature conditions of 75°C, a duration of 20 seconds, and a nanofluid concentration of 2.5%. Interestingly, it is evident that the impact of thermal processing on TSS values is relatively minor, with insignificant fluctuations noted.

An examination of the experimental data was conducted to ascertain the influence of independent variables on Total Soluble Solids (TSS). The formulated model for TSS demonstrated a noteworthy significance, reaching the 1% level of significance. As detailed in **Table 4.5**, it is evident that both the hot fluid temperature (X_1) and time (X_2) independent variables significantly affected TSS through linear terms ($p<0.01$). Furthermore, an interactive effect was observed for the combined influence of hot fluid temperature and time (X_1X_2), attaining significance at the 1% level. The statistical assessment indicated that the proposed model was suitable and exhibited significant alignment. A regression analysis was conducted on the dataset to effectively conform to the response function, specifically the Total Soluble Solids (TSS) of tomato juice. Elevated values of R^2 and adjusted R_{adj}^2 illustrated the close concordance between experimental and predicted values, thereby validating the precision and stability of the model presented in **Table 4.5**.

Table 4.5: Numerical analysis for TSS of tomato juice

Source	Sum of Squares	df	Mean Square	F-value	p-value
Model	0.0772	9	0.0086	58.89	< 0.0001**
X_1	0.0162	1	0.0162	111.18	< 0.0001**

X_2	0.0221	1	0.0221	151.32	< 0.0001**
X_3	0.0002	1	0.0002	1.37	0.2797
X_1 X_2	0.0156	1	0.0156	107.23	< 0.0001**
X_1X_3	0.0156	1	0.0156	107.23	0.0801
X_2X_3	0.0072	1	0.0072	49.58	0.2102
X_1^2	0.0001	1	0.0001	0.9554	0.3609
X_2^2	0.0001	1	0.0001	0.9554	0.3609
X_3^2	2.368E-06	1	2.368E-06	0.0163	0.9021
Residual	0.0010	7	0.0001		
Lack of Fit	0.0007	3	0.0002	2.92	0.1639
Pure Error	0.0003	4	0.0001		
Cor Total	0.0782	16			
R^2	0.9870				
Adj R^2	0.9702				

**, * represents 1% and 5% level of significance respectively.

Subsequently, a second-order polynomial **Eq (4.7)** was formulated, encapsulating an empirical association that outlines the connection between TSS and the input variables in their authentic representation. The anticipated regression equation for TSS is presented below as **Eq 4.**7**.**

$$TSS= 5.53- 0.045X_1- 0.0525X_2- 0.005X_3 + 0.0625X_1X_2+ 0.0625X_1X_3- 0.0425X_2X_3+ 0.0058X_1^2+ 0.0058X_2^2- 0.0007X_3^2 \quad ...(4.7)$$

The equation encompasses terms of both significance and insignificance. Consequently, non-significant terms were eliminated from the equation, resulting in its reconfiguration to solely encompass the significant components. The revised equation is presented as follows:

$$TSS= 5.53 -0.045 * A -0.0525 * B + 0.0625 * AB \quad ...(4.8)$$

The implications of the sign and magnitude of the coefficients in **Eq 4.8** elucidate the impact of the pertinent independent variables on Total Soluble Solids (TSS). The adverse influence of hot fluid temperature (X_1) and time (X_2) at the linear

level signifies that TSS declines with an augmentation in these parameters. Conversely, the positive coefficient associated with the combined effect (X_1X_2) of both hot fluid temperature and time indicates that TSS experiences an increase when both of these parameters are employed simultaneously. There is a slight change in TSS, when temperature increases TSS gets decreased because of its heat sensitive nature, and there is no significant effect of nanofluid aided thermal processing on the retention of TSS.

4.1.5 Total phenolic content (TPC)

Total Phenolic Content (TPC) in tomato juice pertains to the collective concentration of diverse phenolic compounds within the juice matrix. These phenolic compounds, including phenolic acids, flavonoids, and tannins, hold notable significance owing to their inherent antioxidant attributes and diverse biological activities. The influence of phenolic compounds extends beyond health attributes, impacting sensory aspects of tomato juice. These compounds influence flavor, color, and overall sensory perceptions, albeit sometimes introducing subtle bitterness or astringency **(Colle *et al*., 2010).**

The findings derived from the experimental endeavours concerning total phenolic content in tomato juice are meticulously outlined in **Table 4.1**. The total phenolic content exhibited a range, oscillating between 247.542 and 293.255. The apex value materialized in Experiment no. 14, characterized by experimental conditions involving a hot fluid temperature of 95°C, a 30-second time frame, and a nanofluid concentration of 0%. In stark contrast, the nadir value emerged from Experiment no. 16, wherein the amalgamation of independent variables entailed a 75°C hot fluid temperature, a 30-second duration, and a 5% nanofluid concentration. This analysis emphasizes the optimal retention of total phenolic content under elevated conditions of 95°C temperature, a 30-second interval, and the absence of nanofluid concentration. An examination of the experimental data was conducted to discern the influence of independent variables on Total Phenolic Content (TPC). The established model for TPC demonstrated remarkable significance, achieving a significance level of 1%. As outlined in **Table 4.6**, it is evident that both the hot fluid temperature (X_1) and time (X_2) independent variables significantly impacted TPC through linear terms ($p<0.01$). Moreover, an interactive effect was noted for the

combined influence of hot fluid temperature and time (X_1X_2), bearing significance at the 1% level.

Table 4.6: Numerical analysis for TPC

Source	Sum of Squares	df	Mean Square	F-value	p-value
Model	2982.62	9	331.40	2147.98	< 0.0001**
X_1	84.50	1	84.50	547.69	< 0.0001**
X_2	109.52	1	109.52	709.85	< 0.0001**
X_3	0.0800	1	0.0800	0.5185	0.4948
X_1 X_2	338.56	1	338.56	2194.37	< 0.0001**
X_1X_3	876.16	1	876.16	5678.81	0.1501
X_2X_3	327.61	1	327.61	2123.40	0.17081
X_1^2	0.0658	1	0.0658	0.4264	0.5346
X_2^2	1177.79	1	1177.79	7633.84	< 0.0001**
X_3^2	38.53	1	38.53	249.72	0.3282
Residual	1.08	7	0.1543		
Lack of Fit	0.2800	3	0.0933	0.4667	0.7213
Pure Error	0.8000	4	0.2000		
Cor Total	2983.70	16			
R^2	0.9996				
Adjusted R^2	0.9992				

**, * represents 1% and 5% level of significance respectively.

The statistical evaluation confirmed the appropriateness and significant alignment of the proposed model. A regression analysis was performed on the dataset to effectively tailor it to the response function, specifically the Total Phenolic Content (TPC) of tomato juice. Elevated values of R^2 and R^2adj illustrated the close correspondence between experimental and predicted values, thus substantiating the accuracy and stability of the model showcased in **Table 4.6.** Subsequently, a second-order polynomial **Eq (4.9)** was derived, encapsulating an empirical relationship that outlines the connection between TPC and the input variables in their real-world

representation. The anticipated regression equation for TPC is provided below as **Eq 4.9**.

$$TPC= 262.80+ 3.25X_1+ 3.70X_2- 0.1X_3 – 9.20X_1X_2- 14.80X_1X_3+ 9.05X_2X_3- 0.125X_1^2+16.72X_2^2+ 3.03X_3^2 \quad \text{... (4.9)}$$

The equation comprises both terms of significance and insignificance. Consequently, non-significant terms were eliminated from the equation, leading to its reformation with only the significant components included. The resultant equation is presented as follows:

$$TPC= 262.80+ 3.25X_1+ 3.70X_2– 9.20X_1X_2 + 16.72X_2^2 \quad \text{... (4.10)}$$

The implications of the sign and magnitude of the coefficients within **Eq 4.10** delineate the impact of the pertinent independent parameters on Total Phenolic Content (TPC). The affirmative impact of hot fluid temperature (X_1) and time (X_2) at the linear level underscores that TPC ascends in correspondence with the elevation of these parameters. In contrast, the presence of a negative coefficient associated with the combined effect (X_1X_2) of both hot fluid temperature and time indicates that TPC experiences a reduction when both these parameters are concurrently applied. Moreover, the constructive effect of the squared term of time (X_2^2) at the quadratic level illustrates that TPC achieves a nadir at the central point of time while registering an increment when deviating on either side of this midpoint.

4.1.6 Color Difference

The experimental findings regarding the color difference within tomato juice are presented comprehensively in **Table 4.1**. The color difference exhibited a range, spanning from 3.6 to 7.2. Experiment no. 14 emerged with the highest value, encompassing experimental parameters of 95°C hot fluid temperature, a 30-second duration, and a 0% nanofluid concentration. Conversely, Experiment no. 16 demonstrated the lowest value, involving the confluence of independent variables comprising a 75°C hot fluid temperature, a 30-second time interval, and a 5% nanofluid concentration. These results accentuate the preservation of tomato juice color under the conditions of 75°C temperature, a 30-second duration, and a 5% nanofluid concentration. An in-depth examination of the experimental data was conducted to investigate the influence of independent variables on the color difference phenomenon. The established model for color difference demonstrated notable

significance, attaining a significance level of 1%. As outlined in **Table 4.7**, it is apparent that both hot fluid temperature (X_1) and nanofluid concentration (X_3) independent variables exhibited a pronounced impact ($p<0.01$) on color difference through their linear terms. Moreover, an interactive effect was observed concerning the combined influence of hot fluid temperature and nanofluid concentration (X_1X_3), attaining significance at the 1% level.

Table 4.7: Numerical analysis for color difference

Source	Sum of Squares	df	Mean Square	F-value	p-value
Model	36.03	9	4.00	339.19	< 0.0001**
X_1	3.13	1	3.13	264.75	< 0.0001**
X_2	2.59	1	2.59	219.24	0.2010
X_3	1.49	1	1.49	126.05	< 0.0001**
X_1 X_2	5.76	1	5.76	487.99	0.3101
X_1X_3	17.64	1	17.64	1494.46	< 0.0001**
X_2X_3	5.41	1	5.41	457.97	0.1901
X_1^2	0.0008	1	0.0008	0.0674	0.8026
X_2^2	0.0024	1	0.0024	0.2012	0.6673
X_3^2	0.0229	1	0.0229	1.94	0.2063
Residual	0.0826	7	0.0118		
Lack of Fit	0.0106	3	0.0035	0.1968	0.8936
Pure Error	0.0720	4	0.0180		
Cor Total	36.12	16			
R^2	0.9977				
Adjusted R^2	0.9948				

**, * represents 1% and 5% level of significance respectively.

The statistical assessment confirmed that the proposed model aligns well and bears significance. A regression analysis was executed on the dataset to tailor it to the response function, specifically the Color Difference of tomato juice. Elevated values of R^2 and R^2_{adj} underscored the proximity between experimental and predicted values, thus validating the precision and stability of the model featured in **Table 4.7**. Subsequently, a second-order polynomial **Eq (4.11)** was formulated, encapsulating an empirical relationship that elucidates the connection between color difference and the

input variables in their factual representation. The anticipated regression equation for color difference is furnished below as **Eq 4.11.**

Color difference = $+4.79+ 0.975X_1+ 0.2X_2- 0.55X_3 + 0.8X_1X_2- 0.055X_1X_3- 0.055X_2X_3+ 0.33X_1^2- 0.02X_2^2+ 0.043X_3^2$ ... **(4.11)**

The equation encompasses both noteworthy and inconsequential terms. Consequently, non-significant elements were excised from the equation, leading to its recalibration with only

the substantial components retained. The resultant equation is presented as follows:

Color difference = $+4.79+ 0.975X_1- 0.55X_3 + 0.8X_1X_2$ ... **(4.12)**

The implications of the coefficients' sign and magnitude in **Eq 4.12** elucidate the impact of the significant independent variables on color difference. The constructive influence of hot fluid temperature (X_1) at the linear level indicates that color difference rises in tandem with the elevation of this parameter. On the other hand, there is a negative effect at the linear level associated with nanofluid concentration (X_3), leading to a decrease in color difference with an increase in nanofluid concentration. Moreover, the presence of a negative coefficient for the combined effect (X_1X_3) involving hot fluid temperature and nanofluid concentration underscores the prediction that color difference would diminish when both these parameters are concurrently engaged.

4.1.7 Log Mean Temperature Difference (LMTD)

The log mean temperature difference (LMTD) is a fundamental parameter utilized in the design and analysis of heat exchangers. It serves as an indicator of the driving force for heat transfer between two fluids within a heat exchanger. The LMTD considers the temperature variations at the inlet and outlet of both the hot and cold fluids involved in the heat exchange process. This parameter is crucial for determining the efficiency and effectiveness of heat transfer in various types of heat exchangers **(Han *et al*., 2017).**

The experimental outcomes regarding the Log Mean Temperature Difference (LMTD) in the context of nanofluid-assisted thermal processing of tomato juice are presented in detail in **Table 4.1**.

Table 4.8: Numerical analysis for LMTD

Source	Sum of Squares	df	Mean Square	F-value	p-value
Model	379.68	9	42.19	254.69	< 0.0001**
X_1	30.03	1	30.03	181.30	< 0.0001**
X_2	23.81	1	23.81	143.71	< 0.0001**
X_3	13.78	1	13.78	83.20	< 0.0001**
X_1 X_2	37.21	1	37.21	224.64	< 0.0001**
X_1X_3	87.42	1	87.42	527.78	< 0.0001**
X_2X_3	28.09	1	28.09	169.58	0.1501
X_1^2	25.43	1	25.43	153.51	< 0.0001**
X_2^2	135.24	1	135.24	816.48	< 0.0001**
X_3^2	2.99	1	2.99	18.04	0.0038**
Residual	1.16	7	0.1656		
Lack of Fit	0.0075	3	0.0025	0.0087	0.9987
Pure Error	1.15	4	0.2880		
Cor Total	380.84	16			
R^2	0.9970				
Adjusted R^2	0.9930				

**, * represents 1% and 5% level of significance respectively.

The LMTD values encompassed a range spanning from 28 to 42. Experiment no. 4 showcased the highest value, featuring experimental conditions involving a hot fluid temperature of 95°C, a 30-second duration, and a 5% nanofluid concentration. Conversely, Experiment no. 6 registered the lowest value, characterized by a combination of independent variables including a 75°C hot fluid temperature, a 30-second time interval, and a 0% nanofluid concentration. These findings correspond closely to the research conducted by **Jafari *et al.*, (2017a)**, which explored the impact of nanofluid-assisted thermal processing on tomato juice. Consequently, it is evident

that optimal LMTD values are achieved at elevated temperatures of 95°C, with a duration of 30 seconds and a nanofluid concentration of 5%.

An extensive examination of the experimental data was conducted to discern the impact of independent variables on the Log Mean Temperature Difference (LMTD). The established model for LMTD exhibited substantial significance, attaining a significance level of 1%. As delineated in Table 4.8, it becomes evident that each of the three independent variables exerted a significant influence ($p<0.01$) on LMTD through their respective linear terms. Furthermore, the interactive effect was evident across all interaction parameters, achieving significance at the 1% level. Additionally, the quadratic effect was observed for all independent parameters, signifying significance at the 1% level as well.

The statistical assessment indicated that the proposed model was not only appropriate but also significantly congruent. Regression analysis was conducted to align the data with the response function, which in this case pertains to the Log Mean Temperature Difference (LMTD). Higher values of R^2 and R_{adj}^2 were indicative of the close correspondence between experimental and predicted values, thus validating the precision and stability of the model showcased in **Table 4.8**. Subsequently, a second-order polynomial **Eq (4.13)** was formulated, serving as a representation of the empirical relationship between LMTD and the input variables in their actual configuration. The projected regression equation for LMTD is detailed below as **Eq 4.13.**

$$LMTD = +33.76+ 3.75X_1+ 0.75X_2+ 2.75X_3 + 0.25X_1X_2- 0.75X_1X_3+ 1.25X_2X_3+ 2.75X_1^2- 0.255X_2^2- 1.26X_3^2 \quad \dots \textbf{(4.13)}$$

The equation encompasses both relevant and non-relevant components. Consequently, the irrelevant components were eliminated from the equation, leading to its revision, which now solely comprises significant terms. The resultant equation is presented as follows:

$$LMTD = +33.76+ 3.75X_1+ 0.75X_2+ 2.75X_3 + 0.25X_1X_2- 0.75X_1X_3+ 2.75X_1^2- 0.255X_2^2- 1.26X_3^2 \quad \dots \textbf{(4.14)}$$

The coefficients' signs and magnitudes within **Eq. 4.14** illustrate the impact of significant independent parameters on the Log Mean Temperature Difference

(LMTD). At the linear level, a positive influence of hot fluid temperature (X_1), time (X_2), and nanofluid concentration (X_3) is apparent, indicating that LMTD rises in correspondence with the elevation of these parameters. Furthermore, the positive coefficient for the joint effect of hot fluid temperature and time (X_1X_2) suggests an increase in LMTD when both parameters are concurrently adjusted. Conversely, the negative coefficient of the combined effect of hot fluid temperature and nanofluid concentration (X_1X_3) suggests a decrease in LMTD under similar circumstances. Additionally, the positive effect of the squared term of hot fluid temperature (X_1^2) at the quadratic level signifies that the LMTD is minimized at the central point of hot fluid temperature, subsequently increasing as the temperature deviates from this midpoint. On the other hand, the negative effect of the squared terms of time (X_2^2) and nanofluid concentration (X_3^2) at the quadratic level indicates that the LMTD reaches its maximum at the central point of these variables, declining as they vary away from this central point.

4.1.8 Overall heat transfer coefficient (U)

The overall heat transfer coefficient, often denoted as U, represents a critical parameter in heat exchanger analysis. It characterizes the efficiency of heat exchange between two fluids within the heat exchanger. This coefficient quantifies the rate of heat transfer per unit area of the heat exchanger's surface, considering the temperature difference between the two fluids involved. The overall heat transfer coefficient incorporates various factors, including the individual heat transfer coefficients of the fluids, the thermal resistance of the pipe or boundary separating them, and any additional resistances due to fouling or other influences that can affect the efficiency of heat transfer **(Han *et al*., 2017).**

The outcomes of the experimental trials concerning the overall heat transfer coefficient (U) within the context of nanofluid-assisted thermal processing of tomato juice are documented in **Table 4.1**. The range of variation for the overall heat transfer coefficient (U) extended from 2250 to 3854.97. The highest recorded value was documented in Experiment no. 4, characterized by the experimental conditions of a hot fluid temperature of 95°C, a processing time of 30 seconds, and a nanofluid concentration of 5%. In contrast, the lowest value was noted in Experiment no. 6, featuring an independent variable combination of 75°C hot fluid temperature, 30

seconds processing time, and a nanofluid concentration of 0%. These findings underscore that optimal levels of the overall heat transfer coefficient (U) were achieved at elevated conditions, encompassing a high hot fluid temperature of 95°C, a processing time of 30 seconds, and a nanofluid concentration of 5%.

The examination of the collected experimental data was conducted with the purpose of assessing the influence of independent variables on the overall heat transfer coefficient (U). The statistical analysis confirmed that the model governing the overall heat transfer coefficient (U) was statistically significant at a significance level of 1%. As indicated in **Table 4.9**, all three independent variables exhibited a substantial impact ($p<0.01$) on the overall heat transfer coefficient (U) in terms of linear effects. Additionally, an interactive effect emerged between the hot fluid temperature and processing time (X_1X_2) at a significance level of 1%. However, no quadratic effects of the independent variables on the overall heat transfer coefficient (U) were observed.

The conducted statistical analysis validated the suitability and significant appropriateness of the proposed model. Regression analysis was carried out to conform the response function, namely the overall heat transfer coefficient (U). Higher values of R^2 and R^2_{adj} adjusted were indicative of the proximity between the actual experimental outcomes and the anticipated predictions. This validation process assured the precision and reliability of the model illustrated in **Table 4.9**. A second-degree polynomial **Eq (4.15)** was formulated to encapsulate the empirical relationship between the overall heat transfer coefficient (U) and the respective input variables. The anticipated regression equation for the overall heat transfer coefficient (U) is provided below as **Eq 4.15**.

Table 4.9: Numerical analysis for Overall heat transfer coefficient

Source	Sum of Squares	df	Mean Square	F-value	p-value
Model	3.900E+06	9	4.333E+05	26.33	0.0001**
X_1	9.487E+05	1	9.487E+05	57.64	0.0001**
X_2	2.498E+06	1	2.498E+06	151.76	< 0.0001**
X_3	1.048E+05	1	1.048E+05	6.36	0.0397*
X_1 X_2	1.580E+05	1	1.580E+05	9.60	0.0174*

X_1X_3	75625.00	1	75625.00	4.59	0.0693
X_2X_3	33392.40	1	33392.40	2.03	0.1974
X_1^2	30274.88	1	30274.88	1.84	0.2172
X_2^2	52192.93	1	52192.93	3.17	0.1182
X_3^2	2648.35	1	2648.35	0.1609	0.7003
Residual	1.152E+05	7	16460.86		
Lack of Fit	59318.02	3	19772.67	1.41	0.3618
Pure Error	55908.03	4	13977.01		
Cor Total	4.015E+06	16			
R^2	0.9713				
Adjusted R^2	0.9344				

**, * represents 1% and 5% level of significance respectively.

$$U = +3177.78+ 344.37X_1+ 558.81X_2+ 114.43X_3 – 198.76X_1X_2- 137.5X_1X_3+ 91.37X_2X_3+84.80X_1^2-111.34X_2^2-25.08X_3^2 \quad \text{… (4.15)}$$

The equation encompasses both substantial and insignificant components. Hence, the non-significant elements were omitted from the equation, leading to its reformation, incorporating solely the significant factors. The resultant equation is presented as follows:

$$U = +3177.78+ 344.37X_1+ 558.81X_2+ 114.43X_3 – 198.76X_1X_2 \quad \textbf{… (4.16)}$$

The coefficients' direction and magnitude in **Eq. 4.16** reveal the impact of the significant independent variables on the overall heat transfer coefficient (U). The linear increase in hot fluid temperature (X_1), time (X_2), and nanofluid concentration (X_3) indicates a corresponding rise in the overall heat transfer coefficient (U). Conversely, the combined influence of hot fluid temperature and time (X_1X_2) has a negative coefficient, implying that the overall heat transfer coefficient (U) decreases when both parameters are simultaneously altered. No quadratic effect was observed.

4.1.9 Heat transfer rate (Q)

The heat transfer rate (Q) refers to the amount of heat energy transferred per unit of time. It signifies the rate at which heat is exchanged between two substances or systems due to a temperature difference. The heat transfer rate is a fundamental

concept in thermodynamics and plays a crucial role in various engineering and scientific applications **(Han *et al*., 2017)**.

The outcomes from the experiments on heat transfer rate (Q) in nanofluid-assisted thermal processing of tomato juice are presented in **Table 4.1**. The values of the heat transfer rate varied between 18000 and 26900 Watts. Experiment number 4 exhibited the highest heat transfer rate under the conditions of a hot fluid temperature of 95°C, a processing time of 30 seconds, and a nanofluid concentration of 5%. Conversely, the lowest heat transfer rate was recorded in Experiment number 6, where the independent variables were set to a hot fluid temperature of 75°C, a processing time of 30 seconds, and a nanofluid concentration of 0%. These results indicate that optimal heat transfer rates are achieved at elevated temperatures of 95°C, processing times of 30 seconds, and nanofluid concentrations of 5%.

An examination of the experimental data was conducted to understand the influence of independent variables on the rate of heat transfer (Q). The model representing the rate of heat transfer (Q) was determined to be statistically significant at a significance level of 1%. As indicated in **Table 4.10**, all three independent variables exhibited a substantial impact ($p<0.01$) on the rate of heat transfer (Q) with regards to linear terms. Notably, there were no observed interactive effects. Furthermore, quadratic effects were noted for the independent parameters of hot fluid temperature (X_1) and time (X_2), both significant at a 1% significance level.

The statistical analysis demonstrated that the proposed model was both suitable and significantly accurate. A regression analysis was conducted to align the data with the response function, namely the rate of heat transfer (Q). The higher values of R^2 and R_{adj}^2 indicated the proximity between the experimental and predicted outcomes, thereby affirming the precision and consistency of the model, as indicated in **Table 4.10**. Consequently, a second-order polynomial **Eq (4.17)** was formulated to establish an empirical connection between the rate of heat transfer (Q) and the input variables, as they exist. The projected regression equation for the rate of heat transfer (Q) is presented below as **Eq 4.17**.

Table 4.10: Numerical analysis of heat transfer rate (Q)

Source	Sum of Squares	df	Mean Square	F-value	p-value
Model	8.964E+07	9	9.960E+06	16.15	0.0007**
X_1	5.007E+07	1	5.007E+07	81.21	< 0.0001**
X_2	1.189E+07	1	1.189E+07	19.28	0.0032**
X_3	8.044E+06	1	8.044E+06	13.05	0.0086**
X_1 X_2	1.114E+06	1	1.114E+06	1.81	0.2209
X_1X_3	2.025E+05	1	2.025E+05	0.3284	0.5845
X_2X_3	1.587E+06	1	1.587E+06	2.57	0.1526
X_1^2	5.066E+06	1	5.066E+06	8.22	0.0241*
X_2^2	9.451E+06	1	9.451E+06	15.33	0.0058**
X_3^2	2.737E+06	1	2.737E+06	4.44	0.0731
Residual	4.316E+06	7	6.166E+05		
Lack of Fit	1.230E+06	3	4.100E+05	0.5315	0.6847
Pure Error	3.086E+06	4	7.715E+05		
Cor Total	9.396E+07	16			
R^2	0.9541				
Adjusted R^2	0.895				

**, * represents 1% and 5% level of significance respectively.

$$U = +21260+ 2002.86X_1+ 197.74X_2+ 2150X_3 +345.22\ X_1X_2+ 350X_1X_3- 50X_2X_3+ 1847.99X_1^2+ 797.99X_2^2- 1007.99X_3^2 \quad \ldots \textbf{(4.17)}$$

The equation comprises both impactful and inconsequential components. Consequently, the insignificant factors were eliminated from the equation, leading to its regeneration that solely incorporates the significant elements. The resulting equation is presented as follows:

$$U = +21260+ 2002.86X_1+ 197.74X_2+ 2150X_3+ 1847.99X_1^2+ 797.99X_2^2 \quad \ldots \textbf{(4.18)}$$

The direction and magnitude of the coefficients in **Eq. 4.18** reflect the impact of the significant independent parameters on the rate of heat transfer (Q). The linear coefficients indicate a positive relationship between the rate of heat transfer and hot

fluid temperature (X_1), time (X_2), and nanofluid concentration (X_3), implying that an increase in these factors corresponds to an increase in the rate of heat transfer. Additionally, the positive quadratic coefficients for hot fluid temperature (X_1^2) and time (X_2^2) at the quadratic level suggest that the rate of heat transfer reaches a minimum at the central point of hot fluid temperature and time but increases when deviating from this midpoint in either direction.

4.1.10 Nusselt number of inner pipe (Nu_i)

The Nusselt number in a double pipe heat exchanger refers to a dimensionless parameter that characterizes the convective heat transfer performance within the exchanger. It represents the ratio of convective heat transfer to conductive heat transfer across the fluid boundary layers. In the context of a double pipe heat exchanger, the Nusselt number is a crucial factor in assessing the efficiency of heat transfer between the two fluids, usually a hot fluid flowing through the inner pipe and a cold fluid through the annular space between the pipes. The Nusselt number is influenced by various factors such as fluid properties, flow rates, pipe geometry, and the Reynolds number. A higher Nusselt number indicates improved heat transfer efficiency and enhanced convective heat exchange, which are key considerations in designing and optimizing heat exchanger systems **(Han *et al.*, 2017).**

The outcomes obtained from the experimental trials of Nusselt number of inner pipe (Nu_i) in the context of nanofluid-enhanced thermal processing of tomato juice are documented in **Table 4.1**. The Nusselt number pertaining to the inner pipe (Nu_i) exhibited a range between 104.2 and 110.5. The highest value was recorded during Experiment No. 4, which entailed conditions involving a hot fluid temperature of 95°C, a processing time of 30 seconds, and a nanofluid concentration of 5%. In contrast, the lowest value was noted in Experiment No. 6, where the independent variables were set to 75°C for the hot fluid temperature, 30 seconds for the processing time, and 0% for the nanofluid concentration. These findings align with the research conducted by **Jafari *et al.*, (2017a),** who explored the impact of employing nanofluid-enhanced thermal processing on tomato juice. The results consistently highlight that the optimal Nusselt number for the inner pipe (Nu_i) is attained at elevated conditions, specifically a high hot fluid temperature of 95°C, a processing time of 30 seconds, and a nanofluid concentration of 5%.

An analysis of the experimental data was performed to examine the impact of independent variables on the Nusselt number of the inner pipe (Nu_i). The model governing the Nusselt number of the inner pipe (Nu_i) demonstrated a noteworthy level of significance at a 1% confidence level. As outlined in **Table 4.11**, all three independent variables exhibited a substantial effect ($p<0.01$) on the Nusselt number of the inner pipe (Nu_i) in terms of linear terms.

Table 4.11: Numerical analysis for Nusselt number of inner pipe

Source	Sum of Squares	df	Mean Square	F-value	p-value
Model	39.17	9	4.35	46.00	< 0.0001**
X_1	27.57	1	27.57	291.34	< 0.0001**
X_2	0.9453	1	0.9453	9.99	0.0159*
X_3	3.43	1	3.43	36.28	0.0005**
$X_1 X_2$	0.8742	1	0.8742	9.24	0.0189*
X_1X_3	2.16	1	2.16	22.84	0.0020*
X_2X_3	0.0225	1	0.0225	0.2378	0.6407
X_1^2	0.5092	1	0.5092	5.38	0.0534
X_2^2	2.99	1	2.99	31.57	0.0008**
X_3^2	0.6898	1	0.6898	7.29	0.0306*
Residual	0.6623	7	0.0946		
Lack of Fit	0.5426	3	0.1809	6.05	0.0574
Pure Error	0.1197	4	0.0299		
Cor Total	39.83	16			
R^2	0.9834				
Adjusted R^2	0.9620				

**, * represents 1% and 5% level of significance respectively.

Furthermore, interactive effects were observed for specific cases such as the combination of hot fluid temperature and time (X_1X_2), as well as hot fluid temperature

and nanofluid concentration (X_1X_3), both demonstrating significance at a 5% confidence level. Additionally, quadratic effects were evident for the time (X_2) independent variable at a 1% confidence level and for the nanofluid concentration (X_3) independent variable at a 5% confidence level. The adequacy of the proposed model and its significant fit were confirmed through statistical analysis. Regression analysis was conducted to establish the response function for the Nusselt number of the inner pipe (Nu_i). The high values of R_2 and R^2_{adj} adjusted indicated the close agreement between the experimental and predicted values, thus validating the precision and consistency of the model detailed in **Table 4.11**. A second-degree polynomial **Eq (4.19)** was formulated, presenting an empirical connection between the Nusselt number of the inner pipe (Nu_i) and the input test variables in practical terms. The anticipated regression equation for the Nusselt number of the inner pipe (Nu_i) is provided as **Eq 4.19**.

$$Nu\_i = +107.17+ 1.86X_1+ 0.3438X_2+0.655X_3 -0.4655 X_1X_2+ 0.7350X_1X_3- 0.075X_2X_3+0.3477X_1^2-0.8423X_2^2-0.4047X_3^2 \quad \ldots \textbf{(4.19)}$$

Given that the equation encompassed both significant and non-significant terms, the non-significant elements were excluded from the equation. The equation was then reconfigured to solely encompass the significant terms. The resulting equation is presented below:

$$Nu\_i = +107.17+ 1.86X_1+ 0.3438X_2+0.655X_3 -0.4655X_1X_2+ 0.7350X_1X_3- 0.8423X_2^2- 0.4047X_3^2 \quad \textbf{\ldots (4.20)}$$

The coefficients' signs and magnitudes in **Eq 4.20** reveal how the significant independent variables impact the Nusselt number of the inner pipe (Nu_i). The linear level positive impact of hot fluid temperature (X_1), time (X_2), and nanofluid concentration (X_3) suggests that increasing these parameters leads to an increase in the Nusselt number of the inner pipe (Nu_i). Additionally, the positive coefficient of the combined effect (X_1X_3) of hot fluid temperature and nanofluid concentration (X3) implies that the Nusselt number of the inner pipe (Nu_i) will rise when both parameters are concurrently employed. Conversely, the negative coefficient of the combined effect (X_1) of hot fluid temperature and time (X_2) suggests that the Nusselt number of the inner pipe (Nu_i) will decrease when both parameters are simultaneously altered. The quadratic negative effects of the squared time term (X_2^2)

and squared nanofluid concentration term (X_3^2) suggest that the Nusselt number of the inner pipe (Nu_i) peaks at the center point and diminishes as these parameters diverge from that central value.

4.1.11 Nusselt number of outer pipe (Nu_o)

The experimental findings of Nusselt number of the outer pipe (Nu_o) in nanofluid-enhanced thermal processing of tomato juice are detailed in **Table 4.1**. The Nusselt number of the outer pipe (Nu_o) exhibited a range from 70 to 77.2. The highest recorded value was observed in Experiment No. 4, characterized by experimental conditions of a hot fluid temperature of 95°C, a processing time of 30 seconds, and a nanofluid concentration of 5%. On the other hand, the lowest value was identified in Experiment No. 6, which involved an independent variable combination of 75°C hot fluid temperature, 30 seconds processing time, and 0% nanofluid concentration. The outcomes underscore that optimal Nusselt number of the outer pipe (Nu_o) is attained under higher temperature conditions of 95°C, along with a processing time of 30 seconds and a nanofluid concentration of 5%. The statistical examination was conducted to explore the influence of the independent variables on the Nusselt number of the outer pipe (Nu_o).

The statistical model representing the Nusselt number of the outer pipe (Nu_o) demonstrated significance at a confidence level of 1%. According to **Table 4.12**, all three independent variables exhibited a substantial impact ($p<0.01$) on the Nusselt number of the outer pipe (Nu_o) in terms of linear relationships. Furthermore, interactions were identified between the hot fluid temperature and the processing time (X_1X_2), as well as between the hot fluid temperature and nanofluid concentration (X_1X_3), with significance observed at a 5% confidence level. The quadratic effect was also found to be significant at a 1% confidence level for the processing time (X_2) independent parameter. The statistical examination confirmed the suitability and significance of the proposed model. A regression analysis was conducted to align the collected data with the response function, specifically the Nusselt number of the outer pipe (Nu_o). The higher values of R^2 and adjusted R_{adj}^2 indicated a close alignment between the experimental outcomes and the predicted values, thus affirming the precision and stability of the model outlined in **Table 4.12**.

Table 4.12: Numerical analysis for Nusselt number of outer pipe (Nu_o)

Source	Sum of Squares	df	Mean Square	F-value	p-value
Model	91.94	9	10.22	6.69	0.010**
X_1	0.7692	1	0.7692	0.5034	0.5010
X_2	8.55	1	8.55	5.59	0.0500*
X_3	2.19	1	2.19	1.43	0.2702
X_1 X_2	9.41	1	9.41	6.16	0.0421*
X_1X_3	10.81	1	10.81	7.07	0.0325*
X_2X_3	15.61	1	15.61	10.22	0.1151
X_1^2	7.56	1	7.56	4.95	0.0615
X_2^2	33.10	1	33.10	21.66	0.0023**
X_3^2	4.71	1	4.71	3.08	0.1225
Residual	10.70	7	1.53		
Lack of Fit	1.27	3	0.4231	0.1795	0.9051
Pure Error	9.43	4	2.36		
Cor Total	102.64	16			
R^2	0.8958				
Adjusted R^2	0.7618				

**, * represents 1% and 5% level of significance respectively.

By developing a second-order polynomial **Eq (4.21)**, a practical relationship was established between the Nusselt number of the outer pipe (Nu_o) and the input test variables. The anticipated regression equation for the Nusselt number of the outer pipe (Nu_o), labeled as **Eq 4.21**, is provided below.

$$Nu\_o = +75.82+ 1.34X_1+ 0.2250X_2 +2.26X_3 -0.1500X_1X_2+ 0.2750X_1X_3- 1.05X_2X_3- 0.3735X_1^2+ 0.2515X_2^2- 2.12X_3^2 \quad \ldots \textbf{(4.21)}$$

The equation encompasses both meaningful and irrelevant terms. Hence, the insignificant elements were excluded from the equation, leading to its regeneration with solely relevant factors. The resultant equation is as follows:

$$Nu\_o = +75.82+ 0.2250X_2 -0.1500X_1X_2+ 0.2750X_1X_3+ 0.2515X_2^2 \quad \ldots \textbf{(4.22)}$$

The coefficients' signs and magnitudes in **Eq. 4.22** denote the impact of significant independent variables on the Nusselt number of the outer pipe (Nu_o). The favourable impact of increased hot fluid and time (X_2) at the linear level indicates an increase in the Nusselt number of the outer pipe (Nu_o) with these factors. The positive coefficient of the combined effect (X_1X_3) of hot fluid temperature and nanofluid concentration suggests that the Nusselt number of the outer pipe (Nu_o) will rise when both parameters are employed. Conversely, the negative coefficient of the combined effect (X_1X_2) of hot fluid temperature and time indicates that the Nusselt number of the outer pipe (Nu_o) will decrease when both these parameters are simultaneously adjusted. The positive impact of the square of time (X_2^2) at the quadratic level signifies that the Nusselt number of the outer pipe (Nu_o) reaches a minimum at the center point of hot fluid temperature and then increases when deviating from this central value.

4.1.12 Effectiveness

The effectiveness of a double pipe heat exchanger refers to its efficiency in transferring heat between two fluids with different temperatures. It is a crucial performance parameter that quantifies the actual heat transfer achieved compared to the maximum possible heat transfer. In other words, it measures how effectively the heat exchanger can exchange heat energy between the two fluids **(Han *et al.*, 2017).**

The effectiveness of nanofluid aided thermal processing of tomato juice was examined through experimental data presented in **Table 4.1**. The effectiveness values ranged from 0.487 to 0.656. Experiment number 4, conducted at a hot fluid temperature of 95°C, a processing time of 30 seconds, and a nanofluid concentration of 5%, yielded the highest effectiveness value. Conversely, the lowest effectiveness value was observed in Experiment number 6, which employed the conditions of 75°C hot fluid temperature, 30 seconds processing time, and 0% nanofluid concentration. These results highlight that optimal effectiveness was achieved at elevated conditions of 95°C hot fluid temperature, 30 seconds processing time, and a nanofluid concentration of 5%.

Statistical analysis was conducted to examine the influence of independent variables on the Effectiveness. The model for Effectiveness demonstrated significance at a 1% level of confidence. As depicted in **Table 4.13**, solely the nanofluid concentration (X_3) as an independent variable exhibited a notable impact ($p<0.01$) on

the effectiveness in terms of linear terms. No interactive effects were observed among the variables, while a quadratic effect surfaced at a 5% level of significance exclusively for the nanofluid concentration (X_3) independent parameter.

Table 4.13: Numerical analysis for Effectiveness

Source	Sum of Squares	df	Mean Square	F-value	p-value
Model	0.0619	9	0.0069	9.90	0.0032**
X_1	0.0030	1	0.0030	4.30	0.0768
X_2	0.0015	1	0.0015	2.15	0.1858
X_3	0.0433	1	0.0433	62.21	< 0.0001**
$X_1 X_2$	0.0012	1	0.0012	1.76	0.2260
X_1X_3	0.0001	1	0.0001	0.1516	0.7086
X_2X_3	0.0007	1	0.0007	1.06	0.3374
X_1^2	0.0001	1	0.0001	0.1908	0.6754
X_2^2	0.0033	1	0.0033	4.73	0.0661
X_3^2	0.0079	1	0.0079	11.34	0.0120*
Residual	0.0049	7	0.0007		
Lack of Fit	0.0005	3	0.0002	0.1680	0.9127
Pure Error	0.0043	4	0.0011		
Cor Total	0.0668	16			
R^2	0.9271				
Adjusted R^2	0.8335				

**, * represents 1% and 5% level of significance respectively.

The statistical examination confirmed the appropriateness and significant fitting of the proposed model. The data underwent regression analysis to tailor the response function, specifically, the Effectiveness. Elevated values of R^2 and R^2_{adj}

underscored the proximity between the experimental and predicted outcomes, thus corroborating the precision and steadfastness of the model delineated in **Table 4.13**. A second-order polynomial **Eq (4.21)** was devised to encapsulate the empirical relationship between the Effectiveness and the respective input test variables in their actual form. The anticipated regression equation for the Effectiveness is presented below as **Eq 4.23.**

$$E = +0.6261+ 0.0193X_1+ 0.0137X_2 +0.0735X_3 -0.0051X_1X_2+ 0.0136X_1X_3-0.0175X_2X_3-0.0056X_1^2-0.0028X_2^2-0.0433X_3^2 \quad \ldots \textbf{(4.23)}$$

The equation comprises both noteworthy and inconsequential elements. Consequently, the insignificant factors were excluded from the equation, leading to its regeneration that now encompasses solely the significant variables. The resultant equation is provided as follows:

$$E = +0.626 +0.0735X_3 - 0.0433X_3^2 \quad \ldots \textbf{(4.24)}$$

The coefficients' signs and values in **Eq. 4.24** depict how the significant independent factors impact the Effectiveness. The increase in nanofluid concentration (X_3) at the linear level suggests a positive influence on Effectiveness. On the other hand, the quadratic effect of (X_3^2) nanofluid concentration indicates that Effectiveness reaches its peak at the center temperature point and decreases when varying away from that point.

4.2 Graphical analysis and Effect of process parameters on Different Dependent parameters

Following the numerical and statistical examination of diverse independent variables' influence on the outcome parameters of thermally processed tomato juice, graphical assessment was conducted to comprehend how responses alter with the levels of crucial procedural factors. Graphs depicting response surfaces were generated, illustrating the effect of two independent variables on the response, while keeping other variables consistent at their midpoint.

4.2.1 Effect of independent variable on lycopene retention

The impact of elevated hot fluid temperatures on the retention of lycopene content is depicted in **Fig 4.1 (a)**, where the central values of time and nanofluid concentration are considered. The graph unmistakably illustrates a linear relationship between the hot fluid temperature and lycopene content retention. Notably, as the

temperature of the hot fluid rises from 75°C to 95°C, there is a marked and rapid decline in lycopene content retention. This decline in retention can be attributed to the heightened sensitivity of lycopene to elevated temperatures; as the temperature increases, the lycopene content substantially decreases. This phenomenon aligns with the findings of a prior study conducted by **Jafari *et al.* (2017a),** where a similar pattern was observed. In their research, they investigated the influence of thermal processing involving nanofluids on the overall quality of tomato juice. As observed in **Fig 4.1 (b)**, the graph demonstrates an initial decrease in the retention of lycopene content as the time increases from 20 to 30 seconds. However, beyond the 30-second mark, there is a subsequent increase in lycopene retention, reaching up to 40 seconds. This observed trend can be attributed to heat transfer dynamics. Initially, during the brief time span, the rate of heat transfer is relatively slow. Subsequently, after the 30-second threshold, there is a notable enhancement in the transfer of heat to the juice. Research conducted by **Jafari *et al.* (2017a)** arrived at a similar conclusion, highlighting this particular pattern.

The impact of varying nanofluid concentrations on the retention of lycopene content, under constant values of hot fluid temperature and time, is illustrated in **Fig 4.1 (c)**. Evidently, a linear correlation is observed between the hot fluid temperature and the retention of lycopene content.

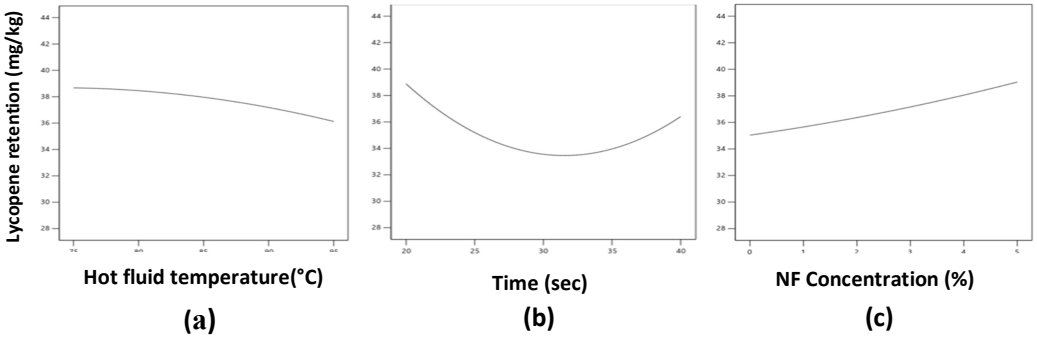

Fig 4.1: Effect of (a) Hot fluid temperature (°C), (b) Time(sec), (c) Nanofluid concentration on Lycopene content retention by keeping other parameters at centre point

Furthermore, the graph illustrates a pronounced surge in lycopene content retention with the escalation of nanofluid concentration from 0 to 5%. This observed increase in lycopene content retention as nanofluid concentration rises can be

attributed to the accelerated thermal processing resulting from higher nanofluid concentrations. This, in turn, expedites heat transfer processes, consequently leading to heightened lycopene content retention. Notably, a similar pattern was deduced by **Jafari *et al.* (2017a)** in their investigation of nanofluid thermal processing's influence on the quality of tomato juice.

Illustrated in **Fig 4.2** is the notable impact of both hot fluid temperature and time, centered around a constant nanofluid concentration, on the retention of lycopene content. The lycopene retention demonstrates a decline with elevated temperatures, whereas an increase is observed as the processing time extends. This indicates that, at lower hot fluid temperatures, there is higher lycopene retention compared to situations with higher temperatures. Similarly, longer processing times yield greater lycopene retention than shorter durations. This phenomenon could be attributed to the inherent sensitivity of lycopene to heat. Lycopene is a heat sensitive nutritional compound, and it gets decreased with the increase in temperature concluded by **Odriozola-Serrano *et al.* (2009).**

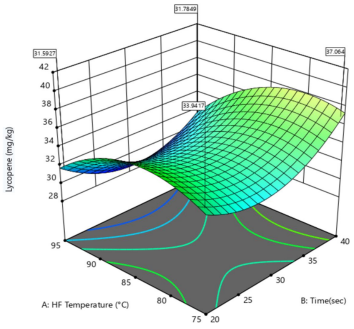

Fig 4.2: Effect of hot fluid temperature and time on lycopene content retention by keeping the nanofluid concentration at centre point

Displayed in **Fig 4.3** is the notable influence of hot fluid temperature and nanofluid concentration, centered around a constant time point, on lycopene content retention. A decline in lycopene retention is observed as temperatures rise, while a modest increase is noted with higher nanofluid concentrations. This indicates that, at lower hot fluid temperatures, lycopene retention surpasses that at higher temperatures. Similarly, greater retention is achieved at elevated nanofluid concentrations compared to lower concentrations. The underlying cause of this phenomenon could be attributed to the sensitivity of lycopene to heat.

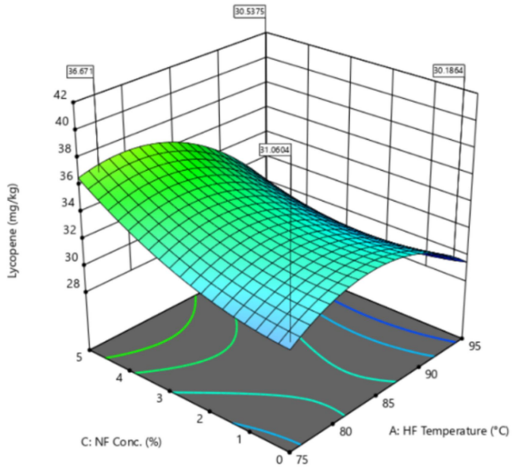

Fig 4.3: Effect of hot fluid temperature and nanofluid concentration on lycopene content retention by keeping the time at centre point

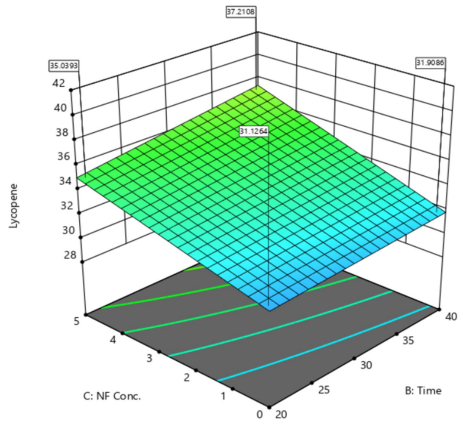

Fig 4.4: Effect of time and nanofluid concentration on lycopene content retention by keeping the hot fluid temperature at centre point

Presented in **Fig 4.4** is the notable impact of time and nanofluid concentration, centered around a constant hot fluid temperature, on lycopene content retention. A rise in nanofluid concentration corresponds to an increase in lycopene retention, while a slight upward trend is observed with extended processing time. This suggests that higher nanofluid concentrations lead to greater lycopene retention compared to lower concentrations. Similarly, extended processing times result in higher retention compared to shorter durations. This phenomenon could be attributed to the augmented heat transfer enhancement facilitated by the presence of nanofluid.

4.2.2 Effect of independent variable on ascorbic acid retention

The impact of varying hot fluid temperatures on the retention of ascorbic acid, while keeping time and nanofluid concentration constant, is illustrated in **Fig 4.5 (a)**. The graph exhibits a clear linear relationship between hot fluid temperature and ascorbic acid retention. Notably, as the hot fluid temperature increases from 75°C to 95°C, there is a pronounced decline in ascorbic acid retention. This reduction in ascorbic acid retention at elevated temperatures is attributed to its sensitivity to heat—higher temperatures lead to a decrease in ascorbic acid content. This pattern aligns with findings by **Jafari *et al.*, (2017a)**, who explored the influence of nanofluid thermal processing on the quality of tomato juice and arrived at a similar conclusion.

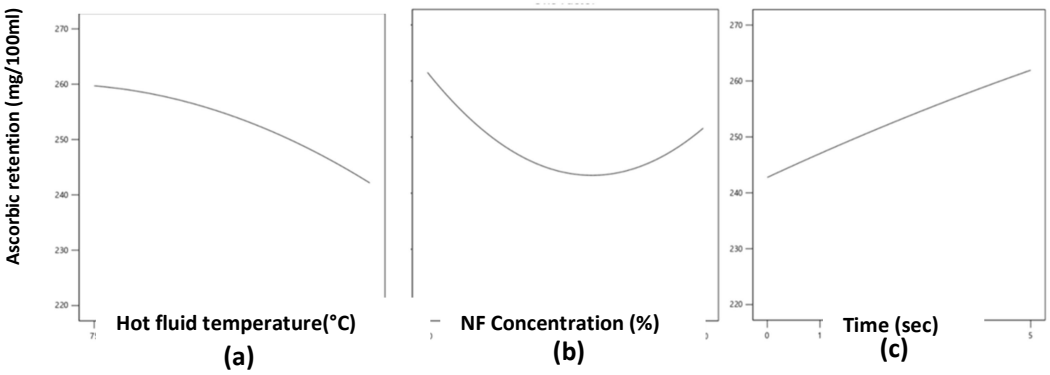

Fig 4.5: Effect of (a) Hot fluid temperature (°C), (b) Time(sec), (c) Nanofluid concentration on Ascorbic acid retention by keeping other parameters at centre point

The graph in **Fig 4.5 (b)** demonstrates an initial decrease in ascorbic acid retention as time increases from 20 to 30 seconds. However, beyond the 30-second mark, there is a subsequent increase in ascorbic acid retention, up to 40 seconds. This trend is attributed to heat transfer dynamics: initially, within a short time frame, the heat transfer rate is slow. Subsequently, after the 30-second threshold, there is a notable enhancement in heat transfer to the juice. A study conducted by **Jafari *et al.*, (2017a)** arrived at the same conclusion, highlighting this particular pattern. The influence of nanofluid concentration on ascorbic acid retention, while maintaining constant values for hot fluid temperature and time, is depicted in **Fig 4.5 (c)**. The graph distinctly portrays a linear relationship between nanofluid concentration and the retention of ascorbic acid. Notably, as the nanofluid concentration increases from 0 to

5%, there is a marked enhancement in ascorbic acid retention. This substantial increase in retention can be attributed to the heightened nanofluid concentration facilitating faster thermal processing rates. This acceleration in thermal processing results in improved heat transfer, leading to greater retention of ascorbic acid.

Illustrated in **Fig 4.6** is the noteworthy impact of both hot fluid temperature and time, centered around a constant nanofluid concentration, on ascorbic acid retention. The retention of ascorbic acid exhibits a decline with elevated temperatures, while an increase is noted with longer processing times. This pattern indicates that higher retention of ascorbic acid occurs at lower hot fluid temperatures compared to higher temperatures. Similarly, greater retention is achieved with extended processing times compared to shorter durations. This phenomenon can be attributed to the susceptibility of ascorbic acid to heat.

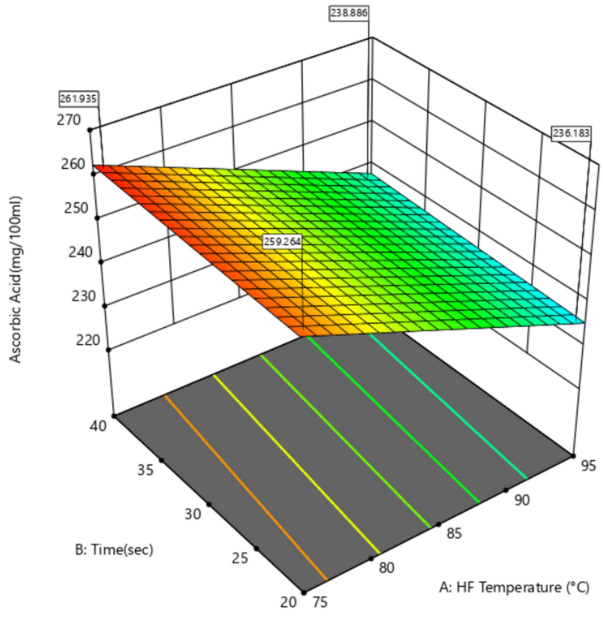

Fig 4.6: Effect of hot fluid temperature and time on ascorbic acid retention by keeping the nanofluid concentration at centre point

Displayed in **Fig 4.7** is the notable influence of both hot fluid temperature and nanofluid concentration, centered around a constant time point, on ascorbic acid retention. An increase in hot fluid temperature corresponds to a decline in ascorbic acid retention, while an increase is observed with higher nanofluid concentrations.

This suggests that at lower hot fluid temperatures, there is higher retention of ascorbic acid in comparison to situations with higher temperatures. Similarly, elevated retention occurs with higher nanofluid concentrations as opposed to lower concentrations. The underlying reason for this phenomenon could be attributed to the heat-sensitive nature of ascorbic acid.

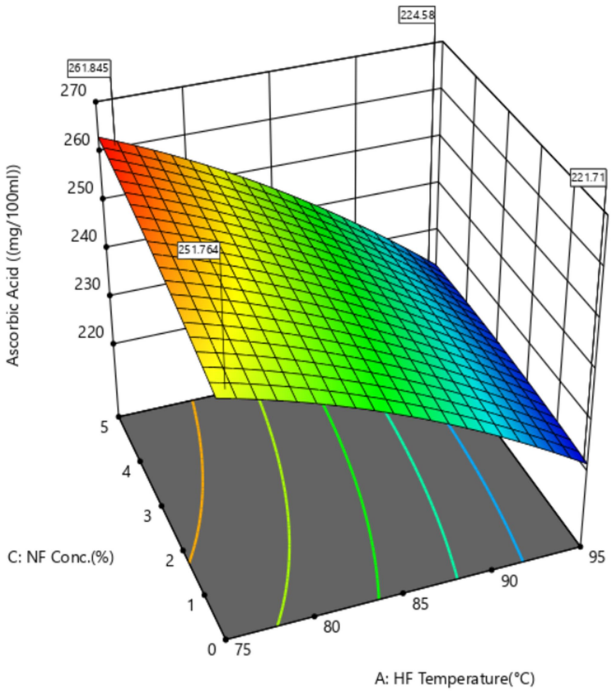

Fig 4.7: Effect of hot fluid temperature and nanofluid concentration on ascorbic acid retention by keeping the time at centre point

Fig 4.8 illustrates the significant impact of time and nanofluid concentration, centered around a fixed hot fluid temperature, on the retention of ascorbic acid content. An increase in nanofluid concentration corresponds to an increase in the retention of ascorbic acid, with a modest upward trend observed as processing time extends. This implies that higher nanofluid concentrations lead to greater retention of ascorbic acid compared to lower concentrations. Similarly, extended processing times result in higher retention compared to shorter durations. This phenomenon can be attributed to the intensified enhancement of heat transfer facilitated by the presence of nanofluid.

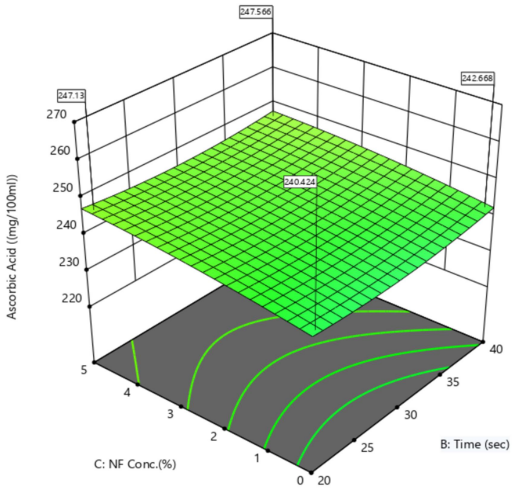

Fig 4.8: Effect of time and nanofluid concentration on ascorbic acid retention by keeping the hot fluid temperature at centre point

4.2.3 Effect of independent variable on pH

Observed in **Fig 4.9(a)**, the graph demonstrates an initial decrease in pH as time increases from 20 to 30 seconds. However, beyond the 30-second mark, there is a subsequent increase in pH, peaking at 40 seconds. This pattern is attributed to the initial rise being linked to the accelerated heat transfer rate up to the 30-second point, after which the process stabilizes. This observation aligns with the findings of a study conducted by **Jafari *et al.* (2017b)**, where a similar conclusion was drawn, highlighting the limited impact of time on the pH of tomato juice.

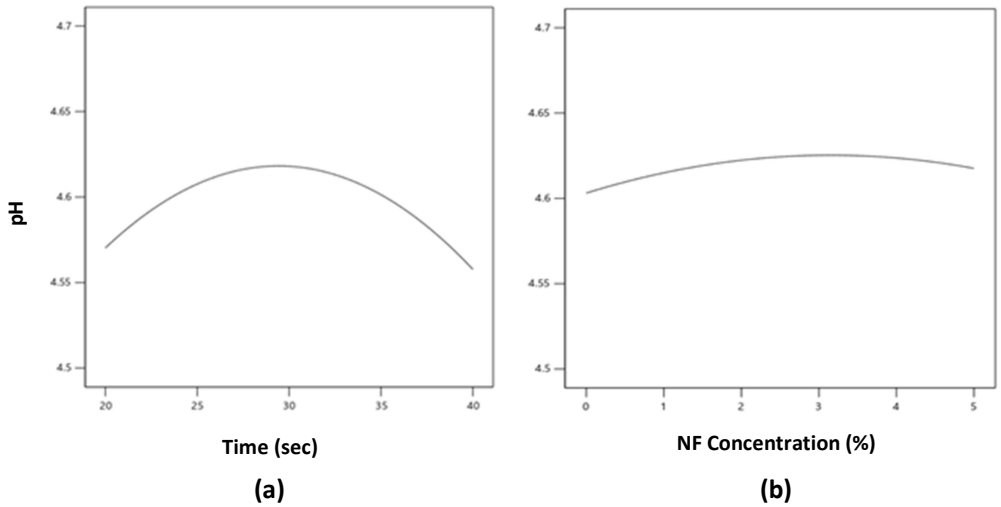

Fig 4.9: Effect of (a) Time (sec), (b) Nanofluid concentration (%) on pH by keeping other parameters at centre point

The influence of nanofluid concentration on pH, while maintaining constant values for hot fluid temperature and time, is depicted in **Fig 4.9 (b)**. The graph distinctly portrays a linear relationship between hot fluid temperature and pH. Notably, as the nanofluid concentration increases from 0 to 5%, there is a marked decrease in pH. This substantial reduction in pH with higher nanofluid concentrations can be attributed to the accelerated thermal processing rates resulting from increased nanofluid concentrations. This augmentation in thermal processing facilitates heightened heat transfer, thereby leading to values of pH. A similar trend was observed in a study by **Jafari *et al.*, (2017b)** in which explored the effects of nanofluid thermal processing on the quality of tomato juice. They also concluded that with the increament of nanofluid concentration, pH level decreases.

4.2.4 Effect of independent variable on TSS

The impact of varying hot fluid temperatures on Total Soluble Solids (TSS), while keeping time and nanofluid concentration constant, is depicted in **Fig 4.10 (a)**. The graph illustrates a distinct linear correlation between hot fluid temperature and TSS. Notably, as the hot fluid temperature increases from 75°C to 95°C, there is a significant decline in TSS. This reduction in TSS at elevated temperatures is due to its sensitivity to heat at higher temperatures lead to a decrease in TSS content. As depicted in **Fig 4.10(b)**, the graph indicates a consistent decrease in Total Soluble Solids (TSS) as time progresses. This decline in TSS values is attributed to the rapid rates of heat transfer. These findings align with the outcomes of **Makroo *et al.*, (2017)**, whose research centered around the TSS content in tomato juice.

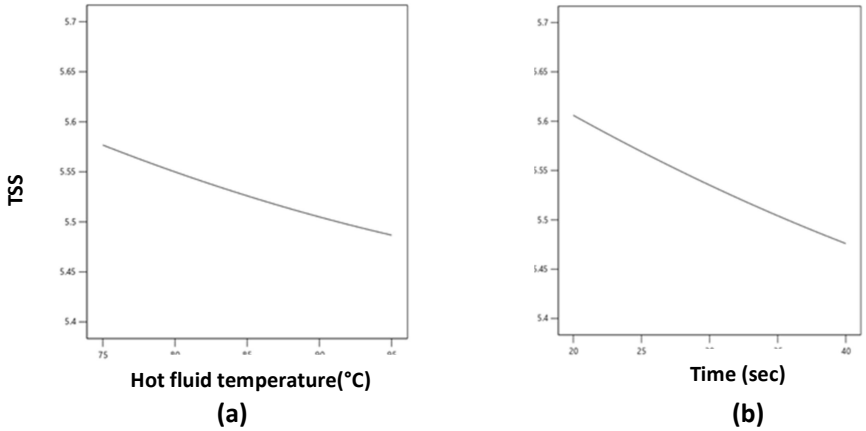

Fig 4.10: Effect of (a) Hot fluid temperature (b) Time(sec), on TSS by keeping other parameters at centre point

Fig 4.11 demonstrates the notable impact of both hot fluid temperature and time, centered around a constant nanofluid concentration, on Total Soluble Solids (TSS). There is a decrease in TSS with rising temperatures, and a similar trend is observed with increasing time. This pattern indicates that lower hot fluid temperatures and shorter time durations result in higher TSS values compared to situations with higher temperatures and longer times. This phenomenon could be attributed to the sensitivity of tomato juice to heat.

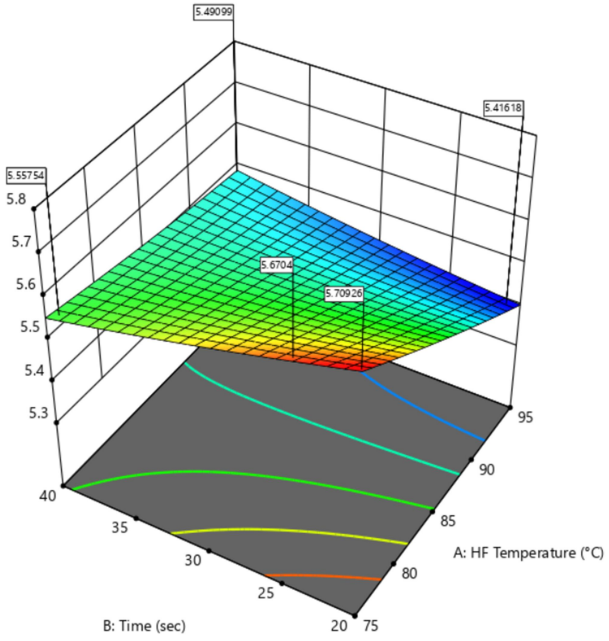

Fig 4.11: Effect of hot fluid temperature and time on TSS by keeping the nanofluid concentration at centre point

4.2.5 Effect of independent variable on TPC

The impact of varying hot fluid temperatures on Total Phenolic Content (TPC), while maintaining constant values for time and nanofluid concentration, is depicted in **Fig 4.12 (a)**. The graph distinctly illustrates a linear relationship between hot fluid temperature and TPC. Notably, as the hot fluid temperature increases from 75°C to 95°C, there is a notable reduction in TPC. This decline in TPC in response to elevated hot fluid temperatures can be attributed to the diminished availability of phenolic compounds at higher temperatures. **Colle *et al.* (2010)**, in their research, also concluded that the TPC of tomatoes decreases with increasing temperatures due to its sensitivity to heat.

As observed in **Fig 4.12(b)**, the graph illustrates a decline in Total Phenolic Content (TPC) as time progresses. This decrease in TPC values is attributed to the swift rates of heat transfer. These findings align with the conclusions of Colle et al. in 2010, whose study focused on the TPC content in tomato juice.

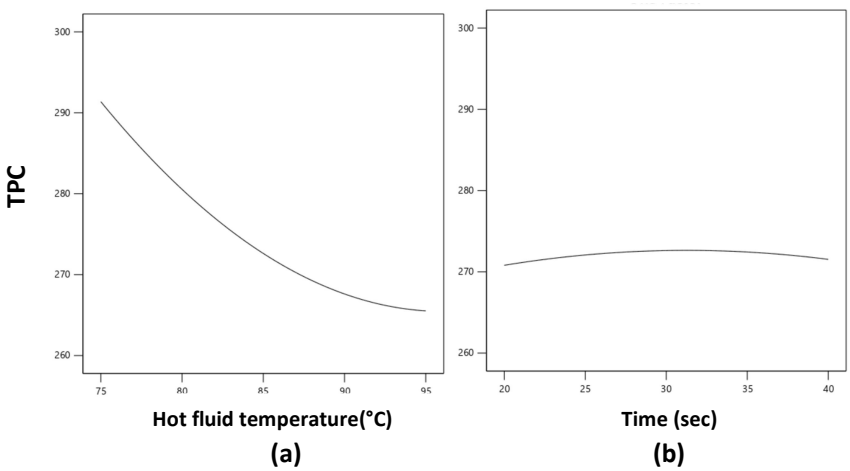

Fig 4.12: Effect of (a) Hot fluid temperature (b) Time(sec), on TPC by keeping other parameters at centre point

Fig 4.13 illustrates the noteworthy influence of both hot fluid temperature and time, centered around a constant nanofluid concentration, on Total Phenolic Content (TPC). There is a decrease in TPC with rising temperatures, and a similar trend is observed with increasing time. This pattern indicates that lower hot fluid temperatures and shorter time durations result in higher TPC values compared to situations with higher temperatures and longer times. This phenomenon could be attributed to the sensitivity of tomato juice to heat.

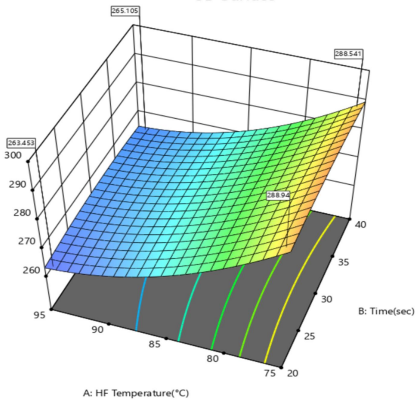

Fig 4.13: Effect of hot fluid temperature and time on TPC by keeping the nanofluid concentration at centre point

4.2.6 Effect of independent variable on Color Difference (ΔE)

The impact of varying hot fluid temperatures on Color Difference (ΔE), while maintaining constant values for time and nanofluid concentration, is depicted in **Fig 4.14 (a)**. The graph distinctly shows a linear relationship between hot fluid temperature and Color Difference (ΔE). Notably, as the hot fluid temperature increases from 75°C to 95°C, there is a marked increase in Color Difference (ΔE). This significant rise in Color Difference (ΔE) with higher hot fluid temperatures is attributed to the loss of color in tomatoes at elevated temperatures. **Gupta *et al.*, (2010)** also concluded that the color of tomatoes decreases as the temperature rises, mainly due to their sensitivity to heat. The impact of various nanofluid concentrations on Color Difference (ΔE), while maintaining constant values for hot fluid temperature and time, is depicted in **Fig 4.14 (b)**. The graph clearly displays a linear correlation between nanofluid concentration and Color Difference (ΔE). Notably, as the nanofluid concentration increases from 0 to 5%, there is a pronounced decrease in Color Difference (ΔE). This significant reduction in Color Difference (ΔE) with higher nanofluid concentrations can be attributed to the accelerated thermal processing resulting from elevated nanofluid concentrations. This acceleration in thermal processing leads to enhanced heat transfer, resulting in a lesser degree of color change in tomatoes.

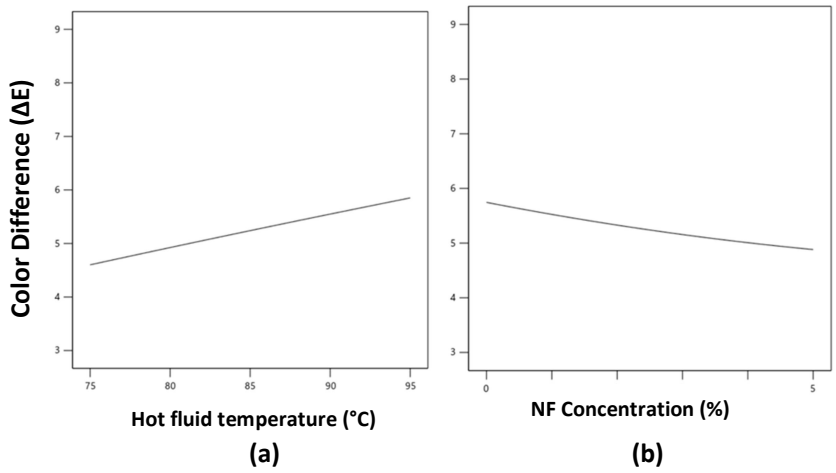

Fig 4.14: Effect of (a) Hot fluid temperature (b) Nanofluid concentration (%) on Color Difference (ΔE) by keeping other parameters at centre point

Illustrated in **Fig 4.15** is the significant impact of both hot fluid temperature and nanofluid concentration, centered around a constant time point, on Color Difference (ΔE). There is an increase in Color Difference (ΔE) with higher temperatures, while a decrease is observed with elevated nanofluid concentrations. This pattern suggests that lower hot fluid temperatures result in lower Color Difference (ΔE) compared to higher temperatures, and higher nanofluid concentrations lead to reduced Color Difference (ΔE) compared to lower concentrations. This trend could be attributed to the possibility that higher concentrations of nanofluid facilitate more rapid heat transfer.

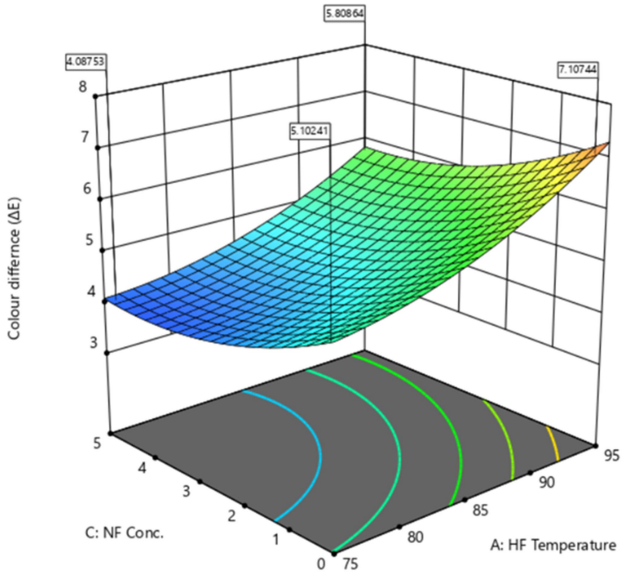

Fig 4.15: Effect of hot fluid temperature and nanofluid concentration on Color Difference (ΔE) by keeping the time at centre point

4.2.7 Effect of independent variable on Log Mean Temperature Difference (LMTD)

The impact of varying hot fluid temperatures on the Log Mean Temperature Difference (LMTD), while maintaining constant values for time and nanofluid concentration, is depicted in **Fig 4.16 (a)**. The graph clearly illustrates a linear correlation between hot fluid temperature and the Log Mean Temperature Difference (LMTD). Notably, as the hot fluid temperature increases from 75°C to 95°C, there is a marked increase in the Log Mean Temperature Difference (LMTD). This significant rise in Log Mean Temperature Difference (LMTD) with higher hot fluid temperatures

is attributed to the larger temperature difference between the hot and cold fluids. Displayed in **Fig 4.16(b)**, the graph illustrates a noticeable increase in the Log Mean Temperature Difference (LMTD) as time progresses. This rise in Log Mean Temperature Difference (LMTD) values is attributed to the accelerated rates of heat transfer when a longer period of time is provided. A similar results was revelead by **Reddy *et al.*, (2017).**

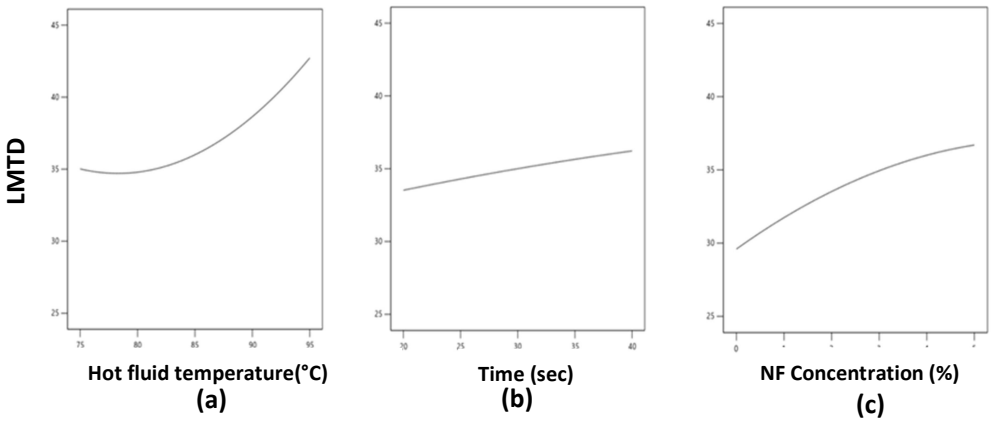

Fig 4.16: Effect of (a) Hot fluid temperature (°C), (b) Time (sec), (c) Nanofluid concentration on Log Mean Temperature Difference (LMTD) by keeping other parameters at centre point

The influence of various nanofluid concentrations on the Log Mean Temperature Difference (LMTD), while maintaining constant values for hot fluid temperature and time, is depicted in **Fig 4.16 (c)**. The graph distinctly illustrates a linear correlation between nanofluid concentration and the Log Mean Temperature Difference (LMTD). Notably, as the nanofluid concentration increases from 0 to 5%, there is a marked increase in the Log Mean Temperature Difference (LMTD). This significant rise in the Log Mean Temperature Difference (LMTD) with higher nanofluid concentrations can be attributed to the accelerated thermal processing facilitated by elevated nanofluid concentrations. This acceleration in thermal processing results in enhanced heat transfer, leading to a higher value of the Log Mean Temperature Difference (LMTD). Illustrated in **Fig 4.17** is the substantial impact of both hot fluid temperature and time, centered around a constant nanofluid concentration, on the Log Mean Temperature Difference (LMTD). There is an elevation in LMTD as temperature increases, and a corresponding increase in LMTD is observed as time progresses. This trend signifies that lower hot fluid temperatures

yield lower LMTD values compared to higher temperatures, and an analogous pattern is seen for time: higher time values result in greater LMTD compared to shorter time durations. Ilustrated in **Fig 4.18** is the notable influence of both hot fluid temperature and nanofluid concentration, centered around a constant time point, on the Log Mean Temperature Difference (LMTD). With increasing temperature, there is an increase in the Log Mean Temperature Difference (LMTD), and a similar trend is observed with elevated nanofluid concentrations. This pattern indicates that lower hot fluid temperatures result in lower Log Mean Temperature Difference (LMTD) compared to higher temperatures, and higher nanofluid concentrations lead to increased Log Mean Temperature Difference (LMTD) compared to lower concentrations. This could be attributed to the possibility that higher nanofluid concentrations facilitate more rapid heat transfer, consequently increasing the difference in temperature between the hot and cold fluids.

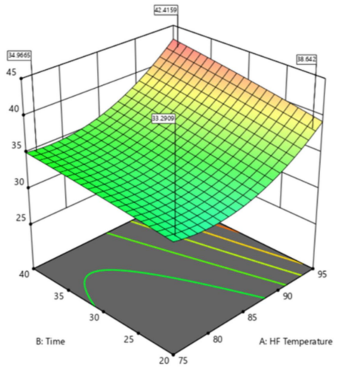

Fig 4.17: Effect of hot fluid temperature and time on LMTD by keeping the nanofluid concentration at centre point

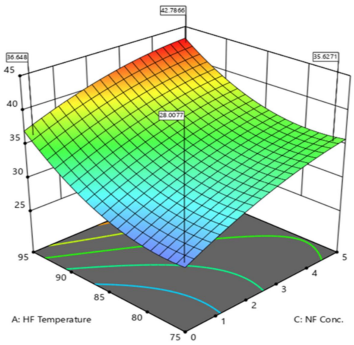

Fig 4.18: Effect of hot fluid temperature and nanofluid concentration on LMTD by keeping the time at centre point

4.2.8 Effect of independent variable on Overall Heat Transfer Coefficient (U)

The impact of varying hot fluid temperatures on the Overall Heat Transfer Coefficient (U), while maintaining constant values for time and nanofluid concentration, is illustrated in **Fig 4.19 (a)**. The graph distinctly portrays a linear relationship between hot fluid temperature and the Overall Heat Transfer Coefficient (U). Notably, as the hot fluid temperature increases from 75°C to 95°C, there is a substantial increase in the Overall Heat Transfer Coefficient (U). This marked rise in the Overall Heat Transfer Coefficient (U) with higher hot fluid temperatures is attributed to the larger value of the heat transfer rate (Q). Similar result was obtained by **Jafari *et al*., (2017b).** As depicted in **Fig 4.19(b)**, the graph reveals a clear increase in the Overall Heat Transfer Coefficient (U) as time progresses. This pattern is attributed to the swift rates of heat transfer, which become more pronounced with an extended duration of time.

The impact of varying nanofluid concentrations on the Overall Heat Transfer Coefficient (U), while maintaining constant values for hot fluid temperature and time, is illustrated in **Fig 4.19 (c)**. The graph distinctly portrays a linear relationship between nanofluid concentration and the Overall Heat Transfer Coefficient (U). Notably, as the nanofluid concentration increases from 0 to 5%, there is a clear increase in the Overall Heat Transfer Coefficient (U). This marked rise in the Overall Heat Transfer Coefficient (U) with higher nanofluid concentrations can be attributed to the heightened thermal processing rates facilitated by increased nanofluid concentrations. This acceleration in thermal processing leads to improved heat transfer, resulting in a higher value for the Overall Heat Transfer Coefficient (U).

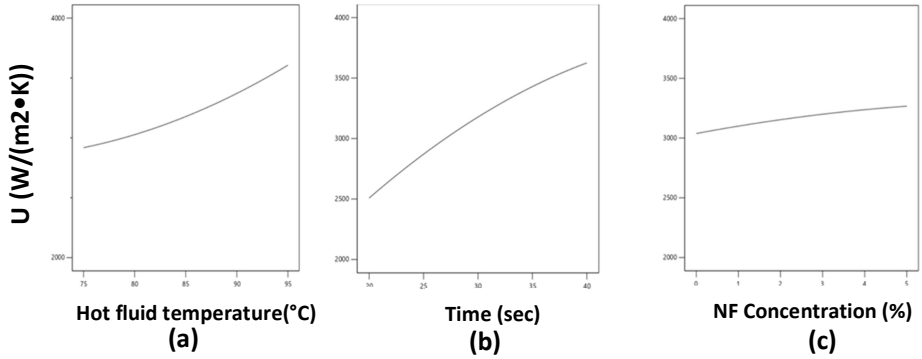

Fig 4.19: Effect of (a) Hot fluid temperature (°C), (b) Time (sec), (c) Nanofluid concentration on Overall Heat Transfer Coefficient (U) by keeping other parameters at centre point

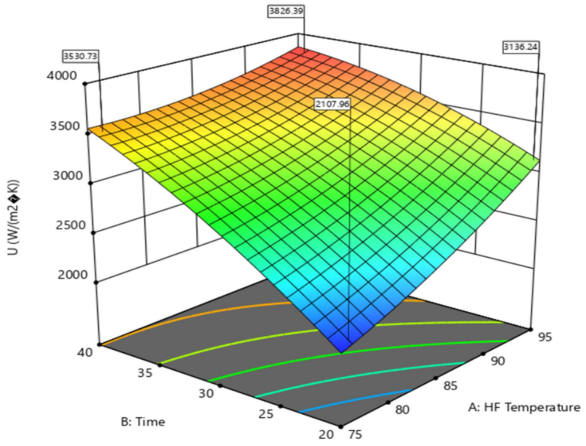

Fig 4.20: Effect of hot fluid temperature and time on U by keeping the nanofluid concentration at centre point

Illustrated in **Fig 4.20** is the notable influence of both hot fluid temperature and time, centered around a constant nanofluid concentration, on the Overall Heat Transfer Coefficient (U). There is an elevation in the Overall Heat Transfer Coefficient (U) as temperature increases, and a corresponding increase is observed as time progresses. This pattern signifies that lower hot fluid temperatures correspond to lower Overall Heat Transfer Coefficient (U) values in comparison to higher temperatures. Similarly, higher time values result in a higher Overall Heat Transfer Coefficient (U) compared to shorter time durations.

4.2.9 Effect of independent variable on Heat transfer Rate (Q)

The impact of varying hot fluid temperatures on Heat Transfer Rate (Q), while maintaining constant values for time and nanofluid concentration, is illustrated in **Fig 4.21 (a)**. The graph distinctly portrays a linear relationship between hot fluid temperature and Heat Transfer Rate (Q). Notably, as the hot fluid temperature increases from 75°C to 95°C, there is a notable increase in Heat Transfer Rate (Q). This significant rise in Heat Transfer Rate (Q) with higher hot fluid temperatures is attributed to the larger value of the Log Mean Temperature Difference (LMTD) that comes with the increasing temperature. Depicted in **Fig 4.21(b)**, the graph demonstrates an evident increase in Heat Transfer Rate (Q) as time advances. This pattern is attributed to the swift rates of heat transfer that become more pronounced with an extended duration of time.

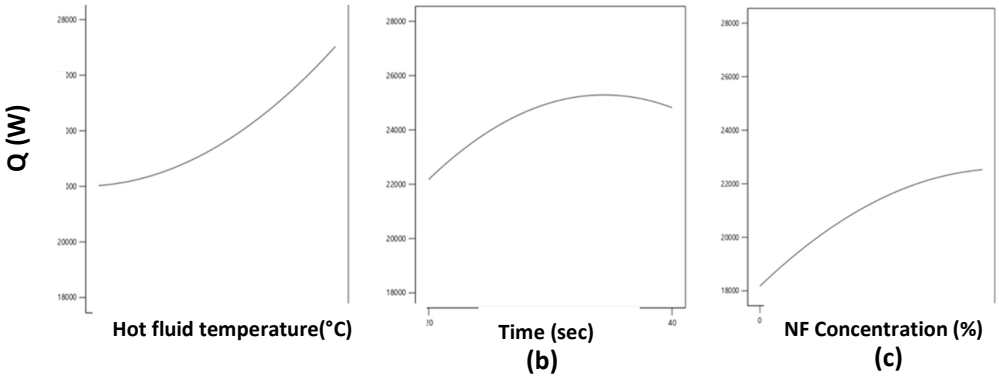

Fig 4.21: Effect of (a) Hot fluid temperature (°C), (b) Time (sec), (c) Nanofluid concentration on Hear transfer rate(Q) by keeping other parameters at centre point

The impact of various nanofluid concentrations on Heat Transfer Rate (Q), while maintaining constant values for hot fluid temperature and time, is depicted in **Fig 4.21 (c)**. The graph distinctly illustrates a linear correlation between nanofluid concentration and Heat Transfer Rate (Q). Notably, as the nanofluid concentration increases from 0 to 5%, there is a clear increase in Heat Transfer Rate (Q). This significant rise in Heat Transfer Rate (Q) with higher nanofluid concentrations can be attributed to the accelerated thermal processing facilitated by elevated nanofluid concentrations. This acceleration in thermal processing leads to enhanced heat transfer, resulting in a higher value for Heat Transfer Rate (Q).

4.2.10 Effect of independent variable on Nusselt number of inner pipe (Nu_i)

The impact of varying hot fluid temperatures on the Nusselt number of the inner pipe (Nu_i), while maintaining constant values for time and nanofluid concentration, is depicted in **Fig 4.22 (a)**. The graph distinctly illustrates a linear relationship between hot fluid temperature and the Nusselt number of the inner pipe (Nu_i). Notably, as the hot fluid temperature increases from 75°C to 95°C, there is a notable increase in the Nusselt number of the inner pipe (Nu_i). This significant rise in the Nusselt number of the inner pipe (Nu_i) with higher hot fluid temperatures is attributed to the larger value of the Log Mean Temperature Difference (LMTD) associated with the increasing temperature.

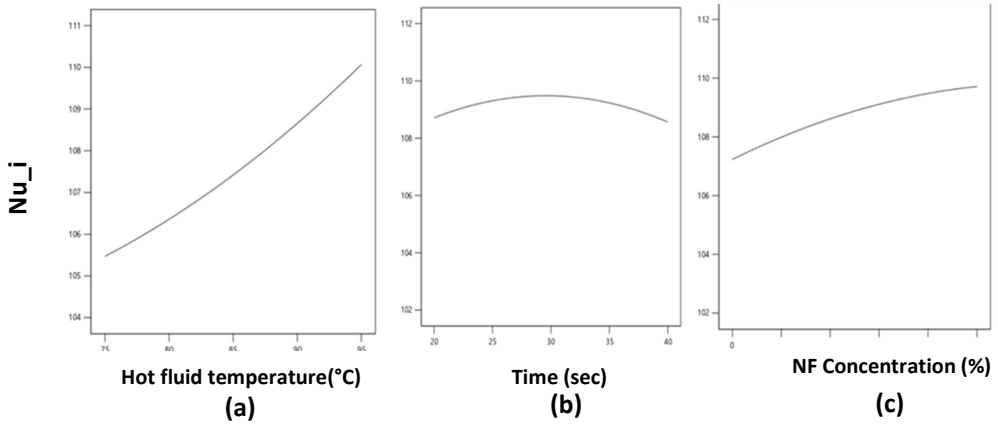

Fig 4.22: Effect of (a) Hot fluid temperature (°C), (b) Time (sec), (c) Nanofluid concentration on Nusselt number of inner pipe (Nu_i) by keeping other parameters at centre point

Depicted in **Fig 4.22(b)**, the graph demonstrates a clear increase in the Nusselt number of the inner pipe (Nu_i) as time progresses. This trend signifies that with the passage of time, there is an evident rise in the Nusselt number of the inner pipe (Nu_i). It's worth noting that the effect of time on the value of Nu_i is relatively modest. The impact of various nanofluid concentrations on the Nusselt number of the inner pipe (Nu_i), while maintaining constant values for hot fluid temperature and time, is illustrated in **Fig 4.22 (c)**. The graph distinctly illustrates a linear correlation between nanofluid concentration and the Nusselt number of the inner pipe (Nu_i). Notably, as the nanofluid concentration increases from 0 to 5%, there is a clear increase in the Nusselt number of the inner pipe (Nu_i). This marked rise in the Nusselt number of the inner pipe (Nu_i) with higher nanofluid concentrations can be attributed to the accelerated thermal processing facilitated by elevated nanofluid concentrations. This acceleration in thermal processing leads to enhanced heat transfer, resulting in a higher value for the Nusselt number of the inner pipe (Nu_i).

Illustrated in **Fig 4.23** is the notable influence of both hot fluid temperature and time, centered around a constant nanofluid concentration, on the Nusselt number of the inner pipe (Nu_i). There is an elevation in the Nusselt number of the inner pipe (Nu_i) as temperature increases, and a corresponding increase is observed as time progresses. This pattern signifies that lower hot fluid temperatures correspond to lower values of the Nusselt number of the inner pipe (Nu_i) in comparison to higher

temperatures. Similarly, higher time values result in a higher Nusselt number of the inner pipe (Nu_i) compared to shorter time durations.

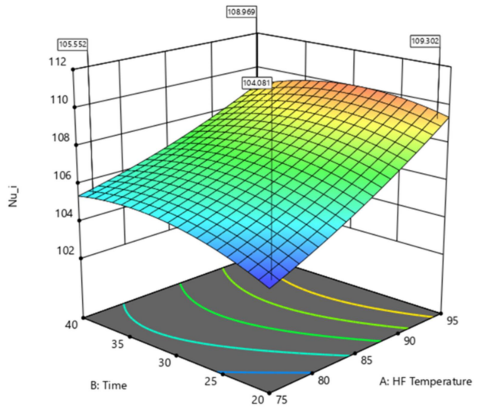

Fig 4.23: Effect of hot fluid temperature and time on Nusselt number of inner pipe (Nu_i) by keeping the nanofluid concentration at centre point

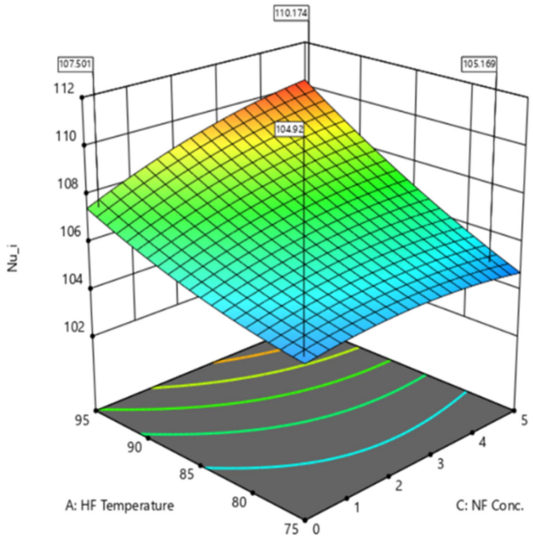

Fig 4.24: Effect of hot fluid temperature and nanofluid concentration on Nusselt number of inner pipe (Nu_i) by keeping the time at centre point

Depicted in **Fig 4.24** is the significant impact of varying hot fluid temperature and nanofluid concentration, while maintaining a constant time point, on the Nusselt number of the inner pipe (Nu_i). With an increase in temperature, there is a corresponding rise in the Nusselt number of the inner pipe (Nu_i), and this trend holds true for higher nanofluid concentrations as well. This pattern signifies that lower hot fluid temperatures yield lower Nusselt number of the inner pipe (Nu_i) values in

comparison to higher temperatures, and similarly, higher nanofluid concentrations lead to an increase in Nusselt number of the inner pipe (Nu_i) compared to lower concentrations.

4.2.11 Effect of independent variable on Nusselt number of outer pipe (Nu_o)

The graph depicted in **Fig 4.25** demonstrates an evident increase in the Nusselt number of the outer pipe (Nu_o) as time progresses. This trend indicates that the Nusselt number of the outer pipe (Nu_o) experiences a noticeable rise with the passage of time. It's noteworthy that the effect of time on the value of Nu_o is relatively modest.

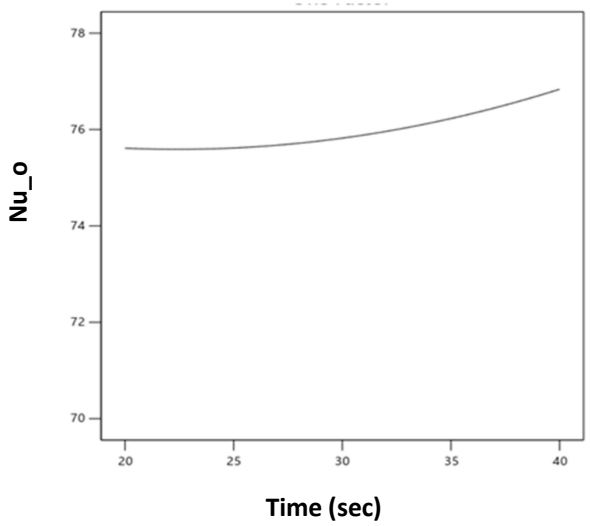

Fig 4.25: Effect of Time (sec) on Nusselt number of outer pipe (Nu_o) by keeping other parameters at centre point

Displayed in **Fig 4.26** is the prominent impact of both hot fluid temperature and time, centered on a consistent nanofluid concentration, on the Nusselt number of the outer pipe (Nu_o). With escalating temperature, there is an augmentation in the Nusselt number of the outer pipe (Nu_o), and a similar trend is observed with the passage of time. Consequently, at lower hot fluid temperatures, the value of the Nusselt number of the outer pipe (Nu_o) is relatively lower compared to higher temperatures. Similarly, at longer time intervals, the Nusselt number of the outer pipe (Nu_o) assumes a higher value compared to shorter durations.

Depicted in **Fig 4.27** is the significant impact of varying hot fluid temperature and nanofluid concentration, while maintaining a constant time point, on the Nusselt number of the outer pipe (Nu_o). An increase in temperature is associated with a

corresponding rise in the Nusselt number of the outer pipe (Nu_o), and a similar pattern emerges with higher nanofluid concentrations. This trend indicates that lower hot fluid temperatures yield lower Nusselt number of the outer pipe (Nu_o) values compared to higher temperatures. Similarly, enhanced nanofluid concentrations lead to an increase in the Nusselt number of the outer pipe (Nu_o) when compared to lower concentrations.

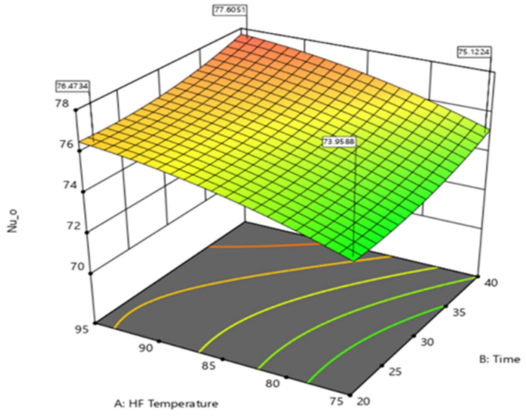

Fig 4.26: Effect of hot fluid temperature and time on Nusselt number of outer pipe (Nu_o) by keeping the nanofluid concentration at centre point

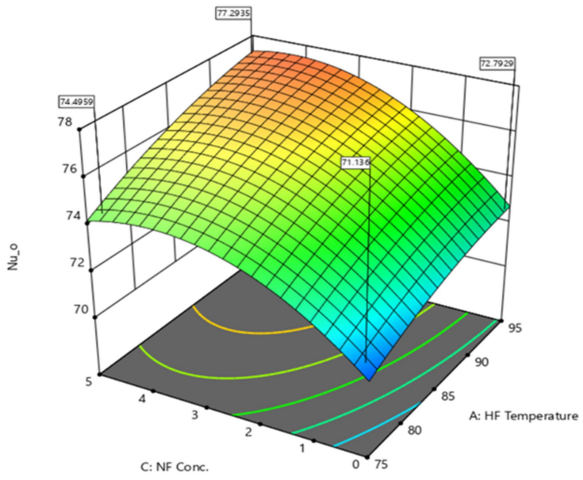

Fig 4.27: Effect of hot fluid temperature and nanofluid concentration on Nusselt number of outer pipe (Nu_o) by keeping the time at centre point

4.2.12 Effect of independent variable on Effectiveness (E)

The impact of varying nanofluid concentrations on the effectiveness (E), while maintaining constant values for hot fluid temperature and time, is depicted in **Fig 4.28**. The graph clearly illustrates a linear relationship between nanofluid concentration and effectiveness (E), revealing that as the nanofluid concentration increases from 0 to 5%, there is a marked enhancement in effectiveness (E). This notable increase in effectiveness (E) with higher nanofluid concentrations is attributed to the accelerated thermal processing facilitated by elevated rates of nanofluid concentration. This acceleration in thermal processing results in improved heat transfer and consequently leads to a higher value of effectiveness (E).

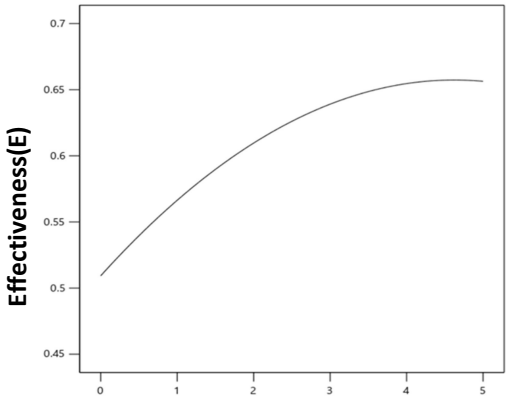

Fig 4.28: Effect of Nanofluid cc iveness(E) by keeping other parameters at centre point

4.3 Optimization of Independent Parameters for quality and thermal analysis of tomato juice

The aim of this study was to find the optimal levels of independent variables, namely hot fluid temperature (°C), time (sec), and nanofluid concentration (%), to enhance the quality of tomato juice. To achieve this, numerical optimization was conducted using Design Expert 13.0.1 statistical software. Several responses, including lycopene content retention, ascorbic acid retention, pH, TSS, TPC, color difference, LMTD, overall heat transfer coefficient, heat transfer rate, Nusselt number of the inner pipe, Nusselt number of the outer pipe, and effectiveness, were taken into account for optimization. The primary objective was to optimize these parameters to maximize the retention of quality, as outlined in **Table 4.14**. The final optimized solution was selected based on these criteria.

Table 4.14: Constraints for optimization and optimum value for better quality retention of tomato juice

	Name	Goal	Optimum Values
Independent Parameters	Hot fluid temperature temperature (°C)	is in range	89.7
	Time(sec)	minimize	30
	Nanoparticle concentration (%)	minimize	3.543
Dependent Parameters	Lycopene content (mg/kg)	maximize	38.395
	Ascorbic acid (mg/100ml)	maximize	254.367
	pH	is in range	4.582
	TSS(°brix)	is in range	5.481
	TPC(µg/g)	maximize	281.813
	Colour difference	minimize	5.967
	LMTD (°C)	maximize	38.060
	Overall heat transfer coefficient (U) (W/(m^2K))	maximize	3767.362
	Rate of heat transfer (Q)(W)	maximize	24547.195
	Nusselt number (Inner pipe Nu_i)	maximize	107.724
	Nusselt number (Outer pipe Nu_o)	maximize	76.967
	Effectiveness (E)	maximize	0.656

4.3.1 Validation of optimized results for the better-quality retention of tomato juice

To ensure the accuracy of the model, a regression analysis was performed to compare actual values with predicted model values. **Table 4.15** provides the actual and predicted values of the responses, along with their respective F values.

Table 4.15: Validation of optimized sample (Hot fluid temperature 89.7 °C, time (30sec) and Nanofluid concentration (3.54 %))

Parameters	Predicted values	Actual values	F value
Lycopene content (mg/kg)	**38.395**	**38.1**	**0.76 N.S**
Ascorbic acid (mg/100ml)	**254.367**	**253.2**	**0.45 N.S**
pH	**4.582**	**4.647**	**1.41 N.S**
TSS (brix)	**5.481**	**5.518**	**0.67 N.S**
TPC (brix)	**281.813**	**280.54**	**0.45 N.S**
Colour difference (Δ E)	**5.967**	**5.89**	**1.29 N.S**
LMTD (**°C**)	**38.060**	**37.97**	**0.23 N.S**
Overall heat transfer coefficient (U) W/(m2•K)	**3767.372**	**3757.57**	**0.25 N.S**
Rate of heat transfer (Q) (W)	**24547.195**	**24664.55**	**0.47 N.S**
Nusselt number (Inner pipe Nu_i)	**107.724**	**106.8**	**0.85 N.S**
Nusselt number (Outer pipe Nu_o)	**76.967**	**75.98**	**1.28 N.S**
Effectiveness (E)	**0.656**	**0.647**	**1.37 N.S**

N.S: non-significant

Plate 4.1 Treated Juice sample

Summary & Conclusion

Chapter 5 SUMMARY AND CONCLUSIONS

Tomatoes, scientifically known as *Lycopersicon esculentum*, hold significant global importance as a crop, ranking just behind potatoes in terms of production. They are cultivated worldwide and are unique in that, despite their botanical classification as fruits, they are predominantly consumed and prepared as vegetables. While ripe tomatoes are commonly red, they can exhibit a range of hues, including yellow, orange, green, and even purple. Tomatoes also come in various subspecies, each with distinct shapes and flavours.

In terms of nutritional composition, carbohydrates constitute approximately 4% of the content in raw tomatoes, equivalent to less than 5 grams of carbs per medium-sized tomato (123 grams). These fruits are notably rich in vitamins, with a medium-sized tomato providing around 28% of the Recommended Daily Intake (RDI) for essential nutrients. Lycopene, a potent antioxidant, is among the most abundant plant compounds found in tomatoes. Its concentration is highest in tomato-based products like ketchup, juice, paste, and sauce.

Research has shown that the consumption of tomatoes and tomato products may be associated with a reduced risk of heart disease and various types of cancer. Additionally, tomatoes offer benefits for skin health, potentially offering protection against sunburn.

The utilization of nanofluid in the thermal processing of tomatoes represents a promising advancement for achieving higher quality tomato products and satisfying consumer preferences. Consequently, this study unfolded in three sequential phases: the initial phase involved the thermal processing of tomato juice, followed by the quality assessment of the processed tomato juice, and concluded with the analysis of thermal parameters.

To investigate the means of retaining superior quality in tomato juice and enhancing heat transfer through nanofluids, we employed the Box-Behnken design within the framework of Response Surface Methodology. This approach incorporated three key independent variables: Hot fluid temperature (set at 75, 85, and 95 °C), processing time (varying between 20, 30, and 40 seconds), and nanofluid concentration (ranging from 0 to 2.5 and 5%). A total of 17 distinct experiments were

meticulously conducted to elucidate the influence of these independent variables on a range of responses, encompassing Lycopene content retention (mg/kg), ascorbic acid retention (mg/100ml), pH levels, TSS (brix), TPC (µg/100gm), Color Difference (Δ E), Log Mean Temperature Difference (LMTD) expressed in °C, Overall Heat Transfer Coefficient (U) in W/(m2•K), Heat Transfer Rate (Q) in W, Nusselt number of the Outer pipe (Nu_o), and Effectiveness (E).

The data collected from various experimental runs underwent statistical analysis, facilitated by Design Expert 13.0.1 software. This analysis encompassed multiple regression assessments, and for each response, we established second-order models. Subsequently, the data gleaned from this statistical scrutiny guided us in deriving optimized values for all the independent variables. To achieve this optimization, we imposed constraints on both the responses and independent variables before undertaking numerical optimization.

Following the experimental trials, there was a range of outcomes: Lycopene content fluctuated between 29 to 42 (mg/kg), ascorbic acid exhibited variations from 221.358 to 262.64 (mg/100ml), pH levels ranged from 4.55 to 4.7, TSS had fluctuations between 5.47 to 5.69 (brix), TPC displayed a range of values from 247.542 to 293.255 (µg/100gm), Color difference (Δ E) spanned from 3.6 to 7.2, LMTD had a spectrum from 28 to 42 (°C), U covered a range of 2250 to 3854.97 W/(m2•K), Q had variations between 18000 to 26900 (W), Nu_i oscillated between 104 to 111, Nu_o exhibited a range from 70 to 77, and effectiveness demonstrated variations from 0.48 to 0.656.

From the outcomes of the experiments and the analysis of the data, we can derive the following conclusions:

- 95% of the lycopene content was preserved. The raw tomatoes initially contained 44 mg/kg of lycopene. When the juice was treated at 75°C for 30 seconds with a 5% nanofluid concentration, it resulted in a lycopene content of 42 mg/kg. Therefore, the highest lycopene retention was achieved at lower temperatures and higher nanofluid concentrations. The temperature tomato juice is attaining at 75°C hot fluid temperature is 55°C, So the best quality is retaining at this temperature.

- 66.4% of the ascorbic acid content was preserved. The raw tomatoes initially contained 395.324 mg/100ml of ascorbic acid. When the juice was treated at 75°C for 30 seconds with a 5% nanofluid concentration, it resulted in an ascorbic acid content of 262.64 mg/100ml. Therefore, the highest ascorbic acid retention was achieved at lower temperatures and higher nanofluid concentrations. The optimal temperature for retaining the best quality of tomato juice is 55°C, where the temperature of the hot fluid reaches 75°C.
- The pH of tomato juice was 4.55 specifically at 75°C for 30 seconds with a 5% nanofluid concentration and it is increasing at higher temperature.
- TSS of the tomato juice was found maximum at 75°C for 30 seconds with a 5% nanofluid concentration affected by thermal processing.
- There was a substantial retention of 73.5% in the TPC compared to the raw juice. This retention occurred at lower temperature settings and higher nanofluid concentrations, specifically at 75°C for 30 seconds with a 5% nanofluid concentration. The juice temperature reached 55°C during this process.
- The lowest color difference (Δ E) recorded was 3.6, and this was achieved at a lower temperature setting, specifically 75°C for 30 seconds, with a 5% nanofluid concentration. It's worth noting that as the temperature increased, the color difference also increased.
- The presence of nanofluid had a substantial effect on the overall heat transfer coefficient. Specifically, at a temperature of 95°C for 30 seconds with no nanofluid concentration (0%), the overall heat transfer coefficient (U) measured 2700 W/(m²•K). However, when the nanofluid concentration increased from 0% to 5% at the same temperature and duration, the value of U significantly rose to 3854.97 W/(m²•K). This represents a notable improvement of 42.7% in the overall heat transfer coefficient.

Based on the findings of this study, it can be inferred that nanofluid holds significant promise in the field of food processing and can play a vital role in preserving the quality of food products during heat treatment. The application of nanofluid-assisted thermal processing notably improved the retention of quality in the treated tomato juice.

Literature Cited

LITERATURE CITED

Adekunte, A. O., Tiwari, B. K., Cullen, P. J., Scannell, A. G. M. and O'Donnell, C. P. 2010. Effect of sonication on colour, ascorbic acid and yeast inactivation in Tomato Juice. *Food Chem*, 122(3): 500–507.

Ahmadi, M. H., Mirlohi, A., Alhuyi Nazari, M. and Ghasempour, R. 2018. A review of thermal conductivity of various nanofluids. *J. Mol. Liq,* 265: 181–188.

Akanbi, C. T., and Oludemi, F. O. 2004. Effect of processing and packaging on the lycopene content of tomato products. *Int. J. Food Prop.*, 7(1): 139–152.

Akhtari, M., Haghshenasfard, M., and Talaie, M. R. 2013. Numerical and experimental investigation of heat transfer of α-Al 2O3/water nanofluid in double pipe and shell and tube heat exchangers. *Numer Heat Ta A-Appl.*, 63(12): 941–958.

Akyürek, E. F., Geliş, K., Şahin, B., and Manay, E. 2018. Experimental analysis for heat transfer of nanofluid with wire coil turbulators in a concentric tube heat exchanger. *Results Phys.*, 9(6): 376–389.

Albadr, J., Tayal, S., and Alasadi, M. 2013. Heat transfer through heat exchanger using Al2O3 nanofluid at different concentrations. *Case Stud. Therm. Eng.*, 1(1): 38–44.

Ali, H., Babar, H., Shah, T., Sajid, M., Qasim, M. and Javed, S. 2018. Preparation techniques of TIO2 nanofluids and challenges: A Review. *Appl Sci*, 8(4): 587.

Ali, M.Y., Sina, A.A.I., Khandker, S.S., Neesa, L., Tanvir, E.M., Kabir, A., Khalil, M.I. and Gan, S.H., 2020. Nutritional composition and bioactive compounds in tomatoes and their impact on human health and disease: *A review. Foods*, 10(1): 45.

Allahyar, H. R., Hormozi, F., and Zare Nezhad, B. 2016. Experimental investigation on the thermal performance of a coiled heat exchanger using a new hybrid nanofluid. *Exp. Therm. Fluid Sci.*, 76(9): 324–329.

Anguelova, T. and Warthesen, J. 2000. Lycopene stability in tomato powders. *J. Food Sci*, 65(1): 67–70.

Anoop, K., Cox, J., & Sadr, R. 2013. Thermal evaluation of nanofluids in heat exchangers.

Int. Commun. Heat Mass Transf., 49(12): 5–9.

Arya, H., Sarafraz, M. M., Pourmehran, O., and Arjomandi, M. 2019. Heat transfer and pressure drop characteristics of MgO nanofluid in a double pipe heat exchanger. *Heat Mass Transf.*, 55(6): 1769–1781.

Babita, Sharma, S. K. and Gupta, S. M. 2016. Preparation and evaluation of stable nanofluids for Heat Transfer Application: A Review. *Exp. Therm. Fluid Sci,* 79: 202–212.

Badin, E. E., Mercatante, M. M., Mascheroni, R. H., Quevedo-Leon, R., Ibarz, A., Ribotta, P. D. and Lespinard, A. R. 2023. Effect of pasteurization on color, ascorbic acid and lycopene of Crushed Tomato: A computational study with experimental validation. *J. Food Eng,* 337:111218.

Barreiro, J. A., Milano, M. and Sandoval, A. J. 1997. Kinetics of colour change of double concentrated tomato paste during thermal treatment. *J. Food Eng*, 33(3–4): 359–371.

Barzegarian, R., Moraveji, M. K., and Aloueyan, A. 2016. Experimental investigation on heat transfer characteristics and pressure drop of BPHE (brazed plate heat exchanger) using TiO2-water nanofluid. *Exp. Therm. Fluid Sci.*, 74(6): 11–18.

Bergougnoux, V. 2014. The history of Tomato: From domestication to biopharming. *Biotechnol. Adv*., 32(1): 170–189.

Bhattacharyya, M. K., Nandpuri, K. S. and Singh, S. 1979. Genetic divergence in tomato. *Acta Hortic*, (93): 289–300.

Bramley, P. M. 2000. Is lycopene beneficial to human health? *Phytochem,* 54(3): 233–236.

Cadoni, E., Rita De Giorgi, M., Medda, E. and Poma, G. 1999. Supercritical CO2 extraction of lycopene and β-carotene from ripe tomatoes. *Dyes Pigm*, 44(1): 27–32.

Calligaris, S., Falcone, P., & Anese, M. 2002. Color changes of tomato purees during storage at freezing temperatures. *J. Food Sci.*, 67(6): 2432–2435.

Calvo, M. M., García, M. L. and Selgas, M. D. 2008. Dry fermented sausages enriched with lycopene from Tomato Peel. *Meat Sci*, 80(2): 167–172.

Charles N. I. 2014. Effect of thermal processing on lycopene, beta-carotene and vitamin C content of tomato. *Food Sci. Nutr,* 2(3): 87.

Chavda, N. K., Patel, J. R., Patel, H. H., and Parmar, A. P. 2014. Effect of nanofluid on heat transfer characteristics of Double Pipe Heat Exchanger: Part-I: Effect of aluminum oxide nanofluid. *Int. j. res. eng. technol.*, 12(03): 42-52.

Chintamani, L. B. and Ghuge, N. C. 2015. A review paper on experimental heat transfer enhancement using nanofluids. *IJIRAE,* 2(2): 64–67.

Colle, I., Lemmens, L., Van Buggenhout, S., Van Loey, A. and Hendrickx, M. 2010. Effect of thermal processing on the degradation, isomerization, and bioaccessibility of lycopene in tomato pulp. *J. Food Sci*, 75(9).

Coruh, S., Elevli, S. and Geyikçi, F. 2012. Statistical evaluation and optimization of factors affecting the leaching performance of copper flotation waste. *Sci. World J.*, 2012(5): 1-8.

Davis, A.R., Fish, W.W. and Perkins-Veazie, P. 2003. A rapid spectrophotometric method for analyzing lycopene content in tomato and tomato products. *Postharvest Biol. Technol.*, 28(3): 425-430.

Fan, J. and Wang, L. 2011. Review of heat conduction in nanofluids. *Journal of Heat Transfer*, 133(4).

Ghanbarpour, M., Bitaraf Haghigi, E. and Khodabandeh, R. 2014. Thermal properties and rheological behavior of water based al2o3 nanofluid as a heat transfer fluid. *Exp. Therm. Fluid Sci,* 53: 227–235.

Goula, A. M. and Adamopoulos, K. G. 2005. Stability of lycopene during spray drying of Tomato Pulp. *LWT*, 38(5): 479–487.

Gould, W. A. 1992. Total acidity and ph. *Tomato Production, Processing and Technology*, 345–352.

Gupta, R., Balasubramaniam, V. M., Schwartz, S. J. and Francis, D. M. 2010. Storage stability of lycopene in tomato juice subjected to combined pressure−heat treatments. *J. Agric. Food Chem*, *58*(14): 8305–8313

Han, D., He, W.F. and Asif, F.Z. 2017. Experimental study of heat transfer enhancement using nanofluid in double tube heat exchanger. *Energy Procedia*, 142(12): 2547- 2553.

Hobson, G.E. and Davies, J.N., 1976. Protein and enzyme changes in tomato fruit in relation to blotchy ripening and potassium nutrition. *J. Sci. Food Agric*, 27(1): 15-22.

Hsu, K.C., Tan, F.J. and Chi, H.Y. 2008. Evaluation of microbial inactivation and physicochemical properties of pressurized tomato juice during refrigerated storage. *LWT - Food Sci. Technol.*, 41(3): 367-375.

Huang, W., Li, Z., Niu, H., Li, D. and Zhang, J. 2008. Optimization of operating parameters for supercritical carbon dioxide extraction of lycopene by response surface methodology. *J. Food Eng*, *89*(3): 298–302.

Jabbari, S.S., Jafari, S.M., Dehnad, D. and Shahidi, S.A. 2018. Changes in lycopene content and quality of tomato juice during thermal processing by a nanofluid heating medium. *J. Food Eng.*, 230(8): 1-7

Jacob, R. A. 1990. Assessment of human vitamin C status. *The Journal of Nutrition*, 120: 1480–1485.

Jafari, S. M., Ganje, M., Dehnad, D., Ghanbari, V., and Hajitabar, J. 2017. Arrhenius equation modeling for the shelf-life prediction of tomato paste containing a natural preservative. *J. Sci. Food Agric.*, 97(15): 5216–5222.

Jafari, S. M., Jabari, S. S., Dehnad, D., and Shahidi, S. A. 2017a. Effects of thermal processing by nanofluids on vitamin C, total phenolics and total soluble solids of tomato juice. *J. Food Sci. Technol.*, 54(3): 679–686.

Jafari, S. M., Jabari, S. S., Dehnad, D., and Shahidi, S. A. 2017b. Heat Transfer Enhancement in Thermal Processing of Tomato Juice by Application of Nanofluids. *Food Bioproc. Tech.*, 10(2): 307–316.

Kaur, D., Wani, A. A., Oberoi, D. P. S. and Sogi, D. S. 2008. Effect of extraction conditions on lycopene extractions from tomato processing waste skin using response surface methodology. *Food Chem.*, 108(2): 711–718.

Khachik, F., Beecher, G. R. and Smith, J. C. 1995. Lutein, lycopene, and their oxidative metabolites in chemoprevention of cancer. *J. Cell. Biochem*, 59(S22): 236–246.

Khan, A. I. and Arasu, A. V. 2019. A review of influence of nanoparticle synthesis and geometrical parameters on thermophysical properties and stability of nanofluids. *TSEP.*

Koltun, S. J., MacIntosh, A. J., Goodrich-Schneider, R. M., Klee, H. J., Hutton, S. F., Junoy, L. J. and Sarnoski, P. J. 2021. Effects of thermal processing on flavor and consumer perception using tomato juice produced from Florida grown fresh market cultivars. *J. Food Process. Preserv,* 46(1).

Kong, K.-W., Khoo, H.-E., Prasad, K. N., Ismail, A., Tan, C.-P. and Rajab, N. F. 2010. Revealing the power of the natural red pigment lycopene. *Molecules*, 15(2): 959–987.

Kumar, N., Sonawane, S. S., and Sonawane, S. H. 2018. Experimental study of thermal conductivity, heat transfer and friction factor of Al2O3 based nanofluid. *Int. Commun. Heat Mass Transf.*, 9(1): 1–10.

Kumar, P., Tanwar, R., Gupta, V., Upadhyay, A., Kumar, A. and Gaikwad, K.K., 2021. Pineapple peel extract incorporated poly (vinyl alcohol)-corn starch film for active food packaging: Preparation, characterization antioxidant activity. *Int. J. Biol. Macromol.*, 187(9): 223-231.

Ladi, O., Awod, Y., Obogeh, K. and Alfa, I. 2017. Effect of drying methods and storage conditions on nutritional value and sensory properties of dehydrated tomato powder (lycopersicon esculentum). *Int. j. biochem. res. Rev,* 19(1): 1–7.

Leela Vinodhan, V., Suganthi, K. S. and Rajan, K. S. 2016. Convective heat transfer performance of CuO-water nanofluids in U-shaped minitube: Potential for improved energy recovery. *Energy Convers. Manag.*, 118(6): 415–425.

Li, C. H. and Peterson, G. P. 2006. Experimental investigation of temperature and volume fraction variations on the effective thermal conductivity of nanoparticle suspensions (nanofluids). *J. Appl. Phys,* 99(8).

Liu, F., Cao, X., Wang, H. and Liao, X. 2010. Changes of tomato powder qualities during storage. *J. Powder Technol.,* 204(1): 159–166.

Lovrić, T., Sablek, Z. and Bošković, M. 1970. Cis-trans isomerisation of lycopene and colour stability of foam—mat dried tomato powder during storage. *J. Sci. Food Agric,* 21(12): 641–647.

Lugasi, A., Bíró, L., Hóvárie, J., Sági, K. V., Brandt, S. and Barna, É. 2003. Lycopene content of foods and lycopene intake in two groups of the Hungarian population. *Nutr Res*, 23(8): 1035–1044.

Makroo, H. A., Saxena, J., Rastogi, N. K. and Srivastava, B. 2017. Ohmic heating assisted polyphenol oxidase inactivation of watermelon juice: Effects of the treatment on ph, lycopene, total phenolic content, and color of the juice. *J. Food Process. Preserv.* , 41(6).

Mishra, P. C., Mukherjee, S., Nayak, S. K., and Panda, A. 2014. A brief review on viscosity of nanofluids. *Int. Nano Lett.,* 4(4):109–120.

Mozafarie, S. S. and Javaherdeh, K. 2019. Numerical design and heat transfer analysis of a non-Newtonian fluid flow for annulus with helical fins. *Eng. Sci. Technol.*,*22*(4): 1107–1115.

Murshed, S. M. S., Leong, K. C. and Yang, C. 2005. Enhanced thermal conductivity of tio2—water based nanofluids. *Int. J. Therm. Sci,* 44(4): 367–373.

Namburu, P. K., Kulkarni, D. P., Dandekar, A. and Das, D. K. 2007. Experimental investigation of viscosity and specific heat of silicon dioxide nanofluids. *Micro Nano Lett.*, 2(3), 67.

Nasiri, A., Shariaty-Niasar, M., Rashidi, A., Amrollahi, A., and Khodafarin, R. 2011.

Effect of dispersion method on thermal conductivity and stability of nanofluid. *Exp. Therm. Fluid Sci.*, 35(4): 717–723.

Nguyen, C.T., Roy, G. and Lajoie, P.R. 2005. May. Refroidissement des microprocesseurs à haute performance en utilisant des nano fluides. In *Congres Français de Thermique, SFT, Reims* (Vol. 30).

Nikkhah, V. 2015. Application of spherical copper oxide (ii) water nano-fluid as a potential coolant in a boiling annular heat exchanger. *Chem Biochem Eng Q*, 29(3): 405–415.

Odriozola-Serrano, I., Soliva-Fortuny, R., Hernández-Jover, T. and Martín-Belloso, O. 2009. Carotenoid and phenolic profile of tomato juices processed by high intensity pulsed electric fields compared with conventional thermal treatments. *Food Chem*, 112(1):258–266.

Ordóñez-Santos, L. E. and Martínez-Girón, J. 2019. Thermal degradation kinetics of carotenoids, vitamin C and provitamin A in tree tomato juice. *JFST*, 55(1): 201–210.

Østerlie, M. and Lerfall, J. 2005. Lycopene from tomato products added minced meat: Effect on storage quality and colour. *Food Res. Int,* 38(8–9): 925–929.

Pak, B. C. and Cho, Y. I. 1998. Hydrodynamic and heat transfer study of dispersed fluids with submicron metallic oxide particles. *Exp. Heat Transf,* 11(2): 151–170.

Pastoriza-Gallego, M. J., Casanova, C., Páramo, R., Barbés, B., Legido, J. L. and Piñeiro, M. M. 2009. A study on stability and thermophysical properties (density and viscosity) of Al2O3 in water nanofluid. *J. Appl. Phys*, 106(6).

Pathare, P.B., Opara, U.L. and Al-Said, F.A.J. 2013. Colour measurement and analysis in fresh and processed foods: a review. *Food Bioproc Tech.*, 6(5): 36-60.

Perincek, O. and Colak, M. 2013. Use of experimental Box-Behnken design for the estimation of interactions between harmonic currents produced by single phase loads. *Int. j. eng. res. Appl.*, 3(2): 158-165.

Qazi, S. 2017. Solar thermal electricity and solar insolation. In: Standalone Photovoltaic (PV) Systems for Disaster Relief and Remote Areas, 203–237.

Raei, B., Shahraki, F., Jamialahmadi, M. and Peyghambarzadeh, S.M., 2017.

Experimental study on the heat transfer and flow properties of γ-Al 2 O 3/water nanofluid in a double-tube heat exchanger. *J. Therm. Anal. Calorim.*, 127(9): 2561- 2575.

Raiola, A., Tenore, G., Barone, A., Frusciante, L. and Rigano, M. 2015. Vitamin E content and composition in tomato fruits: Beneficial roles and bio-fortification. *Int. J. Mol. Sci.* 16(12): 29250–29264.

Ranjith, and Shaji, K. 2016. Numerical Analysis on a Double Pipe Heat Exchanger with Twisted Tape Induced Swirl Flow on Both Sides. *Proc. Technol.*, 24(10): 436–443.

Reddy, N. S., Rajagopal, K. and Veena, P. H. 2017. Experimental Investigation of Heat Transfer Enhancement of a Double Pipe Heat Exchanger with Helical Fins in theAnnulus Side. *Int J Dyn Fluid*, 13(2): 285–293.

Said, Z., Rahman, S.M.A., Assad, M.E.H. and Alami, A.H. 2019. Heat transfer enhancement and life cycle analysis of a Shell-and-Tube Heat Exchanger using stable CuO/water nanofluid. Sustain. *Energy Technol. Assess.*, 31(2): 306–317.

Sadri, R., Ahmadi, G., Togun, H., Dahari, M., Kazi, S. N., Sadeghinezhad, E. and Zubir, N. 2014. An experimental study on thermal conductivity and viscosity of nanofluids containing carbon nanotubes. Nanoscale Res. Lett, *9*(1).

Salari, S. and Jafari, S.M. 2020. Application of nanofluids for thermal processing of food products. *Trends Food Sci Technol.,* 97(3): 100-113.

Sánchez-Moreno, C., Plaza, L., de Ancos, B. and Cano, M. P. 2006. Nutritional characterisation of commercial traditional pasteurised tomato juices:

Carotenoids, vitamin C and radical-scavenging capacity. *Food Chem*, *98*(4): 749–756.

Saremnejad Namini, F., Jafari, M., Ziaiifar, M. and Rashidi, M. 2015. Evaluation of Nutritional and Physical Properties of Watermelon Juice during the Thermal Processing by Using Alumina Nano-fluid in a Shell and Tube Heat Exchanger. *Nutr. Food Sci.*, 2(4): 47-54.

Sen Gupta, S., Manoj Siva, V., Krishnan, S., Sreeprasad, T. S., Singh, P. K., Pradeep, T. and Das, S. K. 2011. Thermal conductivity enhancement of nanofluids containing graphene nanosheets. *J. Appl. Phys*. 110(8).

Shahrul, I.M., Mahbubul, I.M., Saidur, R. and Sabri, M.F.M. 2016. Experimental investigation on Al2O3–W, SiO2–W and ZnO–W nanofluids and their application in a shell and tube heat exchanger. *Int. J. Heat Mass Transf.*, 97(6): 547-558.

Shi, J., Le Maguer, M., Kakuda, Y., Liptay, A. and Niekamp, F. 1999. Lycopene degradation and isomerization in tomato dehydration. *Food Res. Int.*, 32(1): 15-21.

Shi, J. and Maguer, M. L. 2000. Lycopene in tomatoes: Chemical and physical properties affected by food processing. *Crit Rev Food Sci Nutr,* 40(1): 1–42.

Sogi, D. S., Shivhare, U. S., Garg, S. K. and Bawa, A. S. 2003. Water sorption isotherm and drying characteristics of tomato seeds. *Biosyst. Eng,* 84(3): 297–301.

Sözen, A., Variyenli, H. İ., Özdemir, M. B., Gürü, M., and Aytaç, İ. 2016. Heat transfer enhancement using alumina and fly ash nanofluids in parallel and cross flow concentric tube heat exchangers. *J. Energy Inst.*, 89(3): 414–424.

Stahl, W. and Sies, H. 1996. Lycopene: A biologically important carotenoid for humans? *Arch. Biochem. Biophys.* 336(1): 1–9.

Taghizadeh-Tabari, Z., Zeinali Heris, S., Moradi, M. and Kahani, M. 2016. The study on application of tio 2 /water nanofluid in plate heat exchanger of milk pasteurization industries. *Renew. Sust. Energ. Rev.* 58: 1318–1326

Tarafdar, A., Sirohi, R., Negi, T., Singh, S., Badgujar, P. C., Chandra Shahi, N., Kumar, S., Jun Sim, S. and Pandey, A. 2021. Nanofluid research advances: Preparation, characteristics and applications in food processing. *Food Res. Int,* 150: 110751.

Thakur, R., Saberi, B., Pristijono, P., Stathopoulos, C. E., Golding, J. B., Scarlett, C. J., Bowyer, M., and Vuong, Q. V. 2017. Use of response surface methodology (RSM) to optimize pea starch–chitosan novel edible film formulation. *J. Food Sci. Technol.*, 54(8): 2270–2278.

Tiwari, A. K., Ghosh, P., and Sarkar, J. 2013. Performance comparison of the plate heat exchanger using different nanofluids. *Exp. Therm. Fluid Sci.*, 49(9): 141–151.

Viuda-Martos, M., Sanchez-Zapata, E., Sayas-Barberá, E., Sendra, E., Pérez-Álvarez, J. A. and Fernández-López, J. 2014. Tomato and tomato byproducts. human health benefits of lycopene and its application to meat products: A Review. *Crit Rev Food Sci Nutr,* 54(8): 1032–1049.

Wang, G., Qi, C., Liu, M., Li, C., Yan, Y. and Liang, L. 2019. Effect of corrugation pitch on thermo-hydraulic performance of nanofluids in corrugated tubes of heat exchanger system based on exergy efficiency. *Energy Convers. Manag,* 186: 51–65.

Wen, D., and Ding, Y. 2004. Experimental investigation into convective heat transfer of nanofluids at the entrance region under laminar flow conditions. *Int. J. Heat Mass Transf.*, 47(24): 5181–5188.

WINSTON, J. R. and MILLER, E. V. 2006. Vitamin C content and juice quality of exposed and shaded citrus fruits. *J. Food Sci*, 13(6): 456–460.

Xuan, Y., and Li, Q. 2003. Investigation on convective heat transfer and flow features of nanofluids. *J. Heat Transf.*, 125(1): 151–155.

Yildiz, H. and Baysal, T. 2007. Color and lycopene content of tomato puree affected by electroplasmolysis. *Int. J. Food Prop,* 10(3): 489–495.

Yu, W. and Xie, H. 2012. A review on nanofluids: Preparation, stability mechanisms, and applications. *J. Nanomater*, 1–17.

ZHAO, X., XIE, D. and PAN, K. 2013. Color image quality assessment algorithm based on color structural similarity. *J. Comput. Appl,* 33(6): 1715–1718.

Appendices

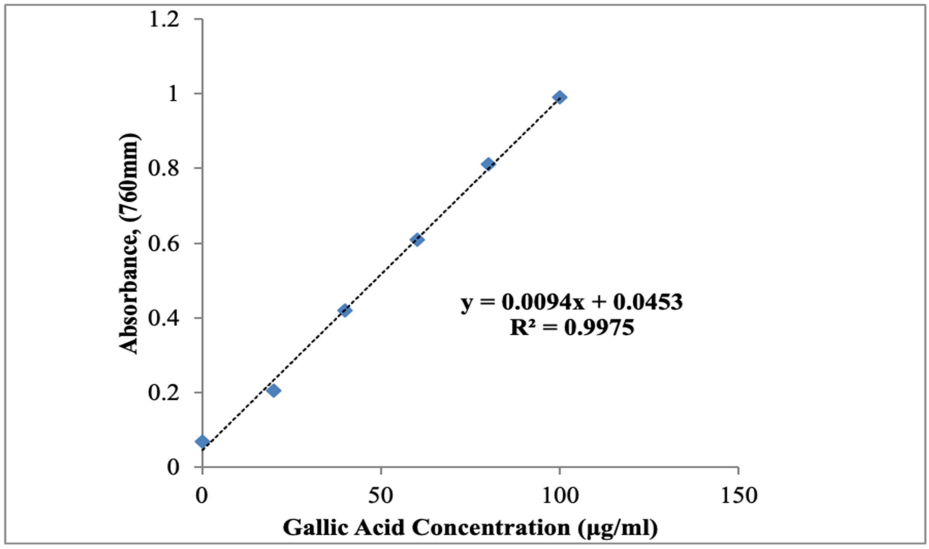

Fig A: Gallic acid curve for total phenolic content

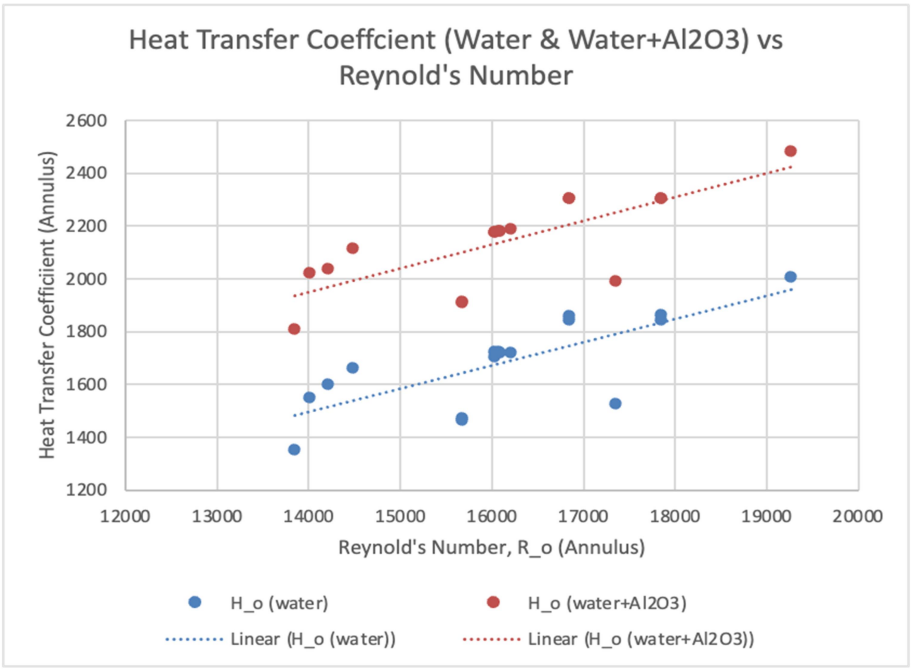

Fig B: Heat Transfer Coefficient (Water and Water + Al_2O_3) vs Reynold's Number

CURRICULUM VITAE

Name : Eshant Chaudhary

Phone Number : 7060277921

Mailing Address : New Hospital Road, Near Shivdan Singh Degree College, Iglas, Aligarh, Uttar Pradesh 202124

Permanent Address : New Hospital Road, Near Shivdan Singh Degree College, Iglas, Aligarh, Uttar Pradesh 202124

E-mail : chaudharyeshant8@gmail.com

Career Objective : To pursue career in Process and Food Engineering and utilize my knowledge and experience in accomplishing challenging assignments. To be a valuable member in an organization where competitive environment encourages innovation, learning & creativity.

Educational Qualification

S. No.	Examination Passed	Institution	Year	Percentage/ CGPA
1.	M.Tech.	G.B.P.U.A&T, Pantnagar	2023	Pursuing
2.	B.Tech.	A.K.T.U, Lucknow	2021	86.1
3.	Intermediate	S.B.H.S Inter College, Iglas	2017	70.80
4.	High school	Jagran Public School, Aligarh	2015	78

Specialization : Agricultural Engineering

Major : Process and Food Engineering

Minor : Nil

Thesis Title : **"OPTIMIZATION THE PROCESS PARAMETERS AND THERMAL PROCESSING FOR TOMATO JUICE WITH NANOFLUID IN DOUBLE PIPE HEAT EXCHANGER AND EVALUATING ITS QUALITATIVE PROPERTIES"**

Conferences/ Seminars/Workshops/Trainings Attended: NIL

List of papers presented in conference/seminar during degree programme: NIL

Software Skills : MS Office, AutoCAD, ANSYS

Place : Pantnagar
Date : September, 2023

(Eshant Chaudhary)

Name	:	Eshant Chaudhary	**Id No.**	:	57968
Sem. and year of admission	:	1st Sem., 2021-22	**Degree**	:	M. Tech (Agricultural Engineering)
Major	:	Process and Food Engineering	**Department**	:	Post Harvest Process and Food Engineering
Thesis title	:	**"OPTIMIZATION THE PROCESS PARAMETERS AND THERMAL PROCESSING FOR TOMATO JUICE WITH NANOFLUID IN DOUBLE PIPE HEAT EXCHANGER AND EVALUATING ITS QUALITATIVE PROPERTIES"**			
Page No.	:	**1-115**	**Advisor**	:	**Er. Sachin Kumar**

ABSTRACT

Tomatoes (Lycopersicon esculentum) rank among the world's significant crops, following only potatoes, and they thrive in various regions worldwide. Among the numerous plant compounds found in tomatoes, lycopene stands out as one of the most plentiful. Research indicates that incorporating tomatoes and tomato-based products into your diet might lower the risk of heart disease and various types of cancer. Furthermore, this fruit offers skin health benefits by potentially shielding against sunburn.

The primary goal of this research was to retain the quality of tomato juice and improve heat transfer by employing nanofluid-assisted thermal processing. To achieve this, we considered three independent variables: Hot fluid temperature (75, 85, 95 °C), time (20, 30, 40 seconds), and nanofluid concentration (0, 2.5, 5%). We evaluated various parameters, including lycopene content (mg/kg), ascorbic acid (mg/100ml), pH levels, TSS (brix), TPC (µg/100gm), Color difference (Δ E), LMTD (°C), U (W/(m2•K)), Q (W), Nu_i, Nu_o, and effectiveness. The data obtained from 17 experiments were statistically analyzed using Design Expert 13.1.0.1 software.

Lycopene retention of 95%, Ascorbic acid retention reached 66.4%, with the best results obtained at lower temperatures and higher nanofluid concentrations, specifically at 75°C for 30 seconds with a 5% nanofluid concentration. The pH and TSS of the tomato juice remained relatively less unchanged during thermal processing. However, there was a notable 73.5% retention in TPC, primarily at 75°C for 30 seconds with a 5% nanofluid concentration. The lowest color difference (Δ E) was 3.6, achieved at a lower temperature setting of 75°C for 30 seconds with a 5% nanofluid concentration. Higher temperatures led to increased color differences. The introduction of nanofluid significantly improved the overall heat transfer coefficient (U), with a remarkable 42.7% enhancement observed when the nanofluid concentration increased from 0% to 5% at a temperature of 95°C for 30 seconds.

In essence, these findings highlight the potential of nanofluid-assisted thermal processing for preserving the quality of tomato juice and enhancing heat transfer efficiency.

(Sachin Kumar)
Advisor

(Eshant Chaudhary)
Author

नाम	: ईशांत चौधरी	**परिचयांक संख्या**	: 57968
सत्र एवं प्रवेश वर्ष	: प्रथम, 2021–22	**उपाधि**	: एम.टेक. (कृषि अभियंत्रण)
प्रमुख विषय	: प्रोसेस और फूड इंजीनियरिंग	**मुख्य**	: पोस्ट हार्वेस्ट प्रोसेस और फूड इंजीनियरिंग
शोध शीर्षक	**: "डबल पाइप हीट एक्सचेंजर में नैनोफ्लूइड के साथ टमाटर के रस की प्रक्रिया पैरामीटर और थर्मल प्रसंस्करण का अनुकूलन और इसके गुणात्मक गुणों का मूल्यांकन"**		
पृष्ठ संख्या	**:1–114**	**सलाहकार**	**: इंजी0 सचिन कुमार**

सारांश

टमाटर (*लाईकोपरिसिकन एसकेलेनटम*) दुनिया के सबसे महत्वपूर्ण फसलों में से एक हैं, केवल आलू के बाद, और वे दुनिया भर में विभिन्न क्षेत्रों में पनपते हैं। टमाटर में पाए जाने वाले कई पौधों के यौगिकों में, लाइकोपीन सबसे प्रचुर मात्रा में है। शोध से पता चलता है कि आपके आहार में टमाटर और टमाटर से बने उत्पादों को शामिल करने से हृदय रोग और विभिन्न प्रकार के कैंसर के जोखिम को कम किया जा सकता है। इसके अलावा, यह फल त्वचा के स्वास्थ्य लाभ प्रदान करता है क्योंकि यह संभावित रूप से सनबर्न से बचाता है।

इस शोध का प्राथमिक उद्देश्य नैनोफ्लुइड–सहायता प्राप्त तापीय प्रसंस्करण का उपयोग करके टमाटर के रस की गुणवत्ता को बनाए रखना और गर्मी हस्तांतरण में सुधार करना था। इसे प्राप्त करने के लिए, हमने तीन स्वतंत्र चर पर विचार कियाः गर्म तरल तापमान (75, 85, 95 डिग्री सेल्सियस), समय (20, 30, 40 सेकंड) और नैनोफ्लुइड सांद्रता (0, 2.5, 5%)। हमने विभिन्न मापदंडों का मूल्यांकन किया, जिसमें लाइकोपीन सामग्री (मिलीग्रामधकिलोग्राम), एस्कॉर्बिक एसिड (मिलीग्राम/100 मिली), पीएच स्तर, टीएसएस (ब्रिक्स), टीपीसी (माइक्रोग्राम/100 ग्राम), रंग अंतर (Δ ई), एलएमटीडी (डिग्री सेल्सियस), यू (डब्ल्यू/(एम 2 • के)), क्यू (डब्ल्यू), नु _ आई, नु _ ओ, और प्रभावकारिता। 17 प्रयोगों से प्राप्त डेटा को डिजाइन एक्सपर्ट 13.1.0.1 सॉफ्टवेयर का उपयोग करके सांख्यिकीय रूप से विश्लेषित किया गया था।

95% लाइकोपीन प्रतिधारण, एस्कॉर्बिक एसिड प्रतिधारण 66.4% तक पहुंच गया, और सर्वोत्तम परिणाम कम तापमान और उच्च नैनोफ्लुइड सांद्रता पर प्राप्त हुए, विशेष रूप से 75^{o}C पर 30 सेकंड के लिए 5% नैनोफ्लुइड सांद्रता के साथ। टमाटर के रस का पीएच और टीएसएस तापीय प्रसंस्करण के दौरान अपेक्षाकृत अपरिवर्तित रहा। हालांकि, टीपीसी में उल्लेखनीय 73.5% प्रतिधारण हुआ, मुख्य रूप से 75^{o}C पर 30 सेकंड के लिए 5% नैनोफ्लुइड सांद्रता के साथ। सबसे कम रंग अंतर (Δ ई) 3.6 था, जो 75^{o}C पर 30 सेकंड के लिए 5% नैनोफ्लुइड सांद्रता के साथ एक निचले तापमान सेटिंग पर प्राप्त किया गया था। उच्च तापमान से रंग अंतर बढ़ जाता है। नैनोफ्लुइड के परिचय ने समग्र ताप हस्तांतरण गुणांक (यू) में उल्लेखनीय सुधार किया, जिसमें 95^{o}C पर 30 सेकंड के लिए नैनोफ्लुइड सांद्रता 0% से 5% बढ़ने पर उल्लेखनीय 42.7% वृद्धि देखी गई।

संक्षेप में, ये निष्कर्ष नैनोफ्लुइड–सहायता प्राप्त तापीय प्रसंस्करण की क्षमता को उजागर करते हैं जो टमाटर के रस की गुणवत्ता को संरक्षित करने और गर्मी हस्तांतरण दक्षता को बढ़ाने के लिए है।

(सचिन कुमार)
सलाहकार

(ईशांत चौधरी)
लेखक